

2007

An evolutionary model of parabolic dune development: blowout to mature parabolic, Padre Island National Seashore, Texas

Winston McKenna

Louisiana State University and Agricultural and Mechanical College, win.a.mckenna@gmail.com

Follow this and additional works at: https://digitalcommons.lsu.edu/gradschool_theses



Part of the [Social and Behavioral Sciences Commons](#)

Recommended Citation

McKenna, Winston, "An evolutionary model of parabolic dune development: blowout to mature parabolic, Padre Island National Seashore, Texas" (2007). *LSU Master's Theses*. 4153.

https://digitalcommons.lsu.edu/gradschool_theses/4153

This Thesis is brought to you for free and open access by the Graduate School at LSU Digital Commons. It has been accepted for inclusion in LSU Master's Theses by an authorized graduate school editor of LSU Digital Commons. For more information, please contact gradetd@lsu.edu.

AN EVOLUTIONARY MODEL OF PARABOLIC DUNE
DEVELOPMENT: FROM BLOWOUT TO MATURE PARABOLIC,
PADRE ISLAND NATIONAL SEASHORE, TEXAS

A Thesis

Submitted to the Graduate Faculty of the
Louisiana State University and
Agricultural and Mechanical College
in partial fulfillment of the
requirements for the degree of
Master of Science

In

The Department of Geography and Anthropology

By
Winston McKenna
B.A. University of Hawai'i at Manoa, 1999
December, 2007

Acknowledgements

I would like to offer my gratitude to my committee members: Patrick Hesp, Steve Namikas, and Gregory Stone, for taking the time to help provide insight into the coastal process, and for being excellent teachers. A special debt of gratitude is owed to my advisor, Dr. Patrick Hesp who has pushed, pulled, and prodded to help me complete this thesis and improve my scientific writing skills. The faculty, staff, and students in the department of Geography and Anthropology have been extremely supportive, encouraging, helpful, and patient with me and they are the reason why I have enjoyed LSU so very much.

This research would not have been possible without the help of a great group of field assistants. These individuals have endured extreme heat, extreme cold, extreme wind, a car breaking down, and working with me. The field assistants for this research were: Philip Schmutz, Graziella Miot de Silva, Ricardo Noriega, Gerardo Boquin, Harry Brignac, and Patricia Lustosa. Also, two individuals who helped me with equipment needs are Rob Mann and Walker Winas, who allowed me the use of a total station (Rob) and a rod and prism (Walker). My gratitude is extended to the board of the West-Russell travel fund for providing monetary assistance to cover the expenses associated with travel and field work.

There is one last group of individuals whom I would like to thank in supporting me over the past three years, my family and friends. My parents have been supportive and encouraging, and my friends have provided laughter, humor, insight, advice, and recipes for tailgating. Lastly I would like to thank my beautiful girlfriend Kara Meyer, and my faithful and loyal dog Moose, without them this would not have been possible.

Table of Contents

Acknowledgements	ii
List of Tables	v
List of Figures	vi
Abstract	viii
1. Introduction	1
2. Literature Review	3
2.1 Introduction	3
2.2 Parabolic Dune Definitions and Morphology	4
2.2.1 Morphologic Parabolic Dune Types	6
2.2.2 Parabolic Dune Models and Their Applicability to North Padre Island, Texas	8
2.3 Factors Influencing Parabolic Dune Development	17
2.3.1 The Role of Wind Regime in Parabolic Dune Development	17
2.3.2 The Role of Climatic Conditions in Parabolic Dune Development	20
2.3.3 The Role of Vegetation in Parabolic Dune Formation	21
2.3.4 The Role of Sediment Supply in Parabolic Dune Formation	22
2.4 Parabolic Dune Age and Migration	23
2.5 Location of Parabolic Dunes	24
2.6 Discussion and Conclusions	24
3. Characteristics of North Padre Island, Texas	29
3.1 Introduction	29
3.2 Regional Setting	29
3.3 Climate	30
3.4 Geology and Geomorphology	33
3.5 Dune Geomorphology and Locations.....	35
3.6 Conclusions	40
4. Methods	43
4.1 Introduction	43
4.2 Digital Orthophoto Quadrangles (DOQQs) and Image Processing	43
4.3 Map Projection and Format	44
4.4 Total Station (TS) Surveys	44
4.5 Survey Grids and Digital Elevation Models (DEMs)	47
4.6 Calculating Dune Change and Shapefiles	48
4.7 Wind and Sand Roses	50
4.7.1 Wind and Sand Rose Data	50

4.7.2 Frequency Tables	52
4.7.3 Sand Roses and Sediment Drift Potentials	53
5. Parabolic Dune Geomorphic Maps and Profile Change	56
5.1 Introduction	56
5.2 Geomorphic Maps and Individual Dune Change	56
5.3 Parabolic Dune Profile Change	61
5.3.1 Parabolic Dune 1 Transect Profiles	61
5.3.2 Parabolic Dune 2 Transect Profiles	64
5.3.3 Parabolic Dune 3 Transect Profiles	68
6. Measurement of Parabolic Dune Change and Migration	73
6.1 Introduction	73
6.2 Parabolic Dune Migration Rates.....	73
6.3 Extent of Dune Change	77
7. Wind: Seasonal Patterns and Geomorphic Influences.....	84
7.1 Introduction	84
7.2 General and Seasonal Components of the Wind Regime	84
7.3 Observed Influence of the Wind Regime.....	89
7.3.1 Winter Season	90
7.3.2 Spring Season	93
7.3.3 Summer Season	96
7.3.4 Fall Season	99
7.3.5 Survey Winds	102
7.4 The Relationships Between Precipitation and Wind Regime	104
7.5 Conclusions	106
8. Conclusion	108
8.1 Introduction	108
8.2 Parabolic Landform Unit Change and Migration	108
8.3 Generalized Model of Parabolic Dune Development for Padre Island, TX	110
8.4 Data Limitations and Areas for Future Research	113
Bibliography	116
Appendix: Sand Rose Sediment Drift Potentials Tables.....	122
Vita	134

List of Tables

2.1 Dune classification types	6
2.2 Dune migration rates for various parabolic dune studies	24
3.1 Annual PAIS precipitation totals (inches) from 1968-3/2007.....	31
3.2 Monthly and seasonal precipitation totals for PAIS 1968 – 2006	32
3.3 Hurricane and tropical storm impact along the Central Texas Coast 1961-2006	33
3.4 List of observed vegetation at Padre Island National Seashore study sites	36
4.1 Wind classes and compass directions.....	52
4.2 Calculation table of weighting factors.....	55
6.1 Dune migration table for dunes 1, 2, and 3, 1996 – 2/11/2007	74
6.2 Migration rates for dune landform units.....	76
6.3 Total dune area and extent of change 1996 – 2007	79
7.1 Bullard (1997) classification of wind regime.....	85
7.2 Individual frequency distribution of wind speed classes.....	88
7.3 Frequency distribution of wind classes during the winter season.....	92
7.4 Frequency distribution of winds during the spring season.....	95
7.5 Frequency distribution of winds during the summer season.....	98
7.6 Frequency distribution of winds during the fall season	101
7.7 Frequency distribution of winds between surveys.....	103
7.8 Seasonal and annual measurements of wind and precipitation data.	105

List of Figures

2.1 Parabolic dune variants and forms	7
2.2 Parabolic dune classification, morphology, and occurrences	8
2.3 Hack dune type development model	9
2.4 The schematic parabolic dune morphology model presented by Landsberg	10
2.5 Cree Lake parabolic dune development model	11
2.6 Parabolic dune morphology model with dune landform units and profile	13
2.7 The Pye parabolic dune morphology model at Cape Flattery, Australia	15
2.8 Parabolic dune activation and stabilization model	16
2.9 Location and climate of major parabolic dune studies	25
3.1 General regional location of North Padre Island, Texas	30
3.2 Locations of hurricane and tropical storm landfall.....	32
3.3 Barrier island types	34
3.4 Cross section profile of North Padre Island	34
3.5 Examples of the dunefield.....	35
3.6 The active foredune on North Padre Island, TX	37
3.7 Dune 1 land form units.....	38
3.8 Dune 2 landform units	39
3.9 Examples of dune 3 landform units	40
3.10 Examples of the vegetation density along the trailing ridges	41
4.1 Schematic of the two person rod and prism survey method or 2PRM	47
4.2 Example of rasterized dune survey data.....	49
5.1 Geomorphic map of parabolic dune 1, 2004 to 2007.....	57

5.2 Geomorphic maps of parabolic dune 2, 1996 to 2007.....	59
5.3 Geomorphic maps of parabolic dune 3, 1996 to 2007.....	60
5.4 Individual dune transect locations.....	62
5.5 Parabolic dune 1 transect profiles.....	63
5.6 Parabolic dune 2 transect profiles.....	66
5.7 Parabolic dune 3 transect profiles	69
6.1 Map of dune 1 migration and change from 2004 – 2007.....	81
6.2 Map of dune 2 migration and change from 1996 – 2007.....	82
6.3 Map of dune 3 migration and change from 1996 – 2007	83
7.1 Wind velocity scale for wind roses.....	86
7.2 Weather station total wind and sand roses.....	87
7.3 Wind roses and sand roses for the winter season	91
7.4 Wind roses and sand roses for the spring season	94
7.5 Wind roses and sand roses for the summer season	97
7.6 Wind roses and sand roses for the fall season	100
7.7 Survey wind and sand roses	102
8.1 Generalized model of parabolic dune development.....	112

Abstract

The Texas barrier islands have been studied and well documented in relation to barrier island evolution and morphology (Leatherman, 1979; Morton, 1994; White and Weise, 1980). The detailed analysis and mapping of various dune types and systems that comprise Padre Island National Seashore, specifically parabolic dunes, is the focus of this research. Dune surveys and doqq's, along with wind and weather records were used to develop an improved morphodynamic model for parabolic dunes. The wind records were provided by the Padre Island National Seashore, the National Data Climate Center, and the Texas Coastal Ocean Observation Network. Individual dune surveys were performed on three separate parabolic dunes for this research. These dune surveys were converted to digital elevation models and raster data, where geospatial analysis was performed.

This research project investigates the geomorphic process of parabolic dunes in three parts. The first part/question of this project will be to assess the accuracy and completeness of current models (Pye, 1982; Thompson, 1983) in a barrier island environment different from the environments used in previous model development. The second part of the project will attempt to answer if long term wind and weather data provide insights into conditions that are related to dune growth or change. The third part of this project utilized the recent surveys and GPS data, along with doqq's from 1996 and 2004 to assess the migration of parabolic dunes on Padre Island National Seashore. Rates of parabolic dune movement ranged from 1.7 m a^{-1} for dune 1, to 17.7 m a^{-1} for dune 3. A new parabolic dune model was developed involving seven separate stages. The model

may help to provide an increased understanding of the geomorphic evolution of parabolic dunes.

1. Introduction

Parabolic dunes are aeolian features that initiate and develop in barrier island, mainland beach, and desert environments (Cooper, 1938; Jennings, 1957; McKee, 1979; David, 1982; Pye, 1982; Robertson-Rintoul, 1990; Wolfe and David, 1997). Parabolic dunes are characterized by their 'U' or 'V' shape, and generally develop in conjunction with vegetation (Cooper, 1958, 1967). The dunes studied for this research are coastal parabolic dunes located within Padre Island National Seashore, Texas.

This research was performed to investigate the geomorphic process of parabolic dune development in a barrier island environment. Specifically, the aims of this research are: to assess the current parabolic dune models and their applicability to the North Padre Island environment and wind regime, to identify relationships between parabolic dune migration rates and wind and climate records, and to develop a model which describes the evolutionary process of a parabolic dune development using field data, dune change measurements and digital data. The current models for parabolic dune development (Landsberg, 1956; Pye, 1982; Thompson, 1983; David, 1981; Wright and David, 1997) lack agreement on the morphodynamic processes and steps in parabolic dune evolution. The lack of agreement in dune literature and the absence of specific parabolic mapping in Padre Island National Seashore has allowed for an excellent opportunity to conduct meaningful research on barrier island parabolic dunes.

Three types of data were collected and analyzed for this research project: survey and field data, doqq data, and wind record data. A variety of methods were utilized for data analysis including: air photo interpretation, GIS analysis, remote sensing techniques, total station field survey, and wind data set organization and sand rose calculations. This research focuses on the utilization of rasterized dune survey data paired with doqq imagery and wind regime data to

measure dune migration and change, and then develop a parabolic dune morphodynamic model based from those measurements and dune change.

2. Literature Review

2.1 Introduction

In the following the broad literature on parabolic dunes is reviewed. In particular parabolic dunes are defined, morphological types are examined, and the factors influencing dune development are discussed.

Parabolic dune studies can be arbitrarily divided into three main time spans or periods; early (1800's to 1959), modern (1960-1995) and recent (1996-present). The early study of parabolic dunes began in earnest with work of Cooper (Cooper, 1923, 1938) and Hogbom (Hogbom, 1923). Initially, most parabolic dune study was linked to post-glacial climate study (Cooper, 1938; Hogbom, 1923; Hack, 1941; Landsberg, 1956; Melton, 1940) and interpretation of dune form was related to dune growth episodes, vegetation densities, and dune orientation (Cooper, 1938, 1958; Hack, 1941; Landsberg, 1956; Jennings, 1957). Also, many of the initial parabolic dune studies were conducted within inland environments (Cooper, 1935, 1938; Hack, 1941; Hogbom, 1923). The early parabolic dune studies generally focused on the relationship between vegetation and its response to climate change or variation (Cooper, 1935, 1938, 1958; Hack, 1941; Melton, 1940).

Many of the major studies of coastal parabolic dunes have been conducted during the modern period (1960-1995) in Australia (Coldrake, 1962; Pye, 1982, 1983, 1993; Story, 1982; Thompson, 1983), and coastal North America (Cooper, 1967; Fillion, 1987). The development of systematic parabolic dune morphology models (Pye, 1982, 1983, 1993; Story, 1982; Thompson, 1983, Fillion, 1987; David, 1977, 1981; Halsey, et al., 1990) and classification schemes (McKee,

1966, 1979; Semeniuk, et al., 1988; David, 1977, 1981) were important themes during this period.

The recent period (1996-present) of parabolic dune study has emphasized the episodic nature of parabolic development and its association with climate; (Abrogast, et al., 2002; Lees, 2006; Anthonsen, et al., 1996; Anthonsen, 1997; Forman and Pierson, 2003; Arens, et al., 2004; Marin, et al., 2005; Hugenholtz and Wolfe, 2005) and the integration of geographic information systems (GIS) for dune analysis (Arens, et al., 2004; Wolfe and Lemmen, 1999; Bailey and Bristow, 2004; Andrews, et al., 2002; Hugenholtz and Wolfe, 2005). The integration of GIS into parabolic (and blowout) dune studies have expanded from the work of Gares and Nordstrom (1995) to the recent work by Hugenholtz and Wolfe (2005). The use of GIS in coastal studies and management should continue to expand and evolve in the coming years (Bartlett and Smith, 2005).

2.2 Parabolic Dune Definitions and Morphology

Parabolic dunes are ‘U’ or ‘V’ shaped dunes that develop a form which is, wholly, or in part controlled by the stabilization of vegetation (Landsberg, 1956; Jennings, 1957). Cooper (1958, p. 74) defines parabolic dunes as “a trough blowout of major size with massive terminal and lateral walls, which because of its bulk has attained a state of quasi-permanence.” From his work in Navajo country, Arizona, Hack (1941, p. 242) defines parabolic dunes as “long, scoop hollows, or parabolas of sand, with points tapering to windward; with a much gentler windward slope than leeward slope.” Also, according to Melton (1941) parabolic dunes are oval shaped features with a ring of sand along the leeward side and with wings open towards the windward opening. Blowout dunes are defined by Hesp (2002, p 255) as, “a saucer or trough shaped

depression formed by wind erosion on a preexisting sand deposit.” Blowout dunes are composed of a depression (or basin) and depositional lobe, and depending on the internal depth of the depression an erosional wall will be present. Parabolic dunes differ from blowout dunes primarily due the development of well defined trailing ridges, which display well defined internal and external walls.

The characteristic form of a parabolic dune is a ‘U’ or ‘V’ shape, consisting of at least three basic features, a depositional lobe, trailing arms or ridges, and a deflation basin (McKee, 1979; Thompson, 1983). The depositional lobe can be defined as a mound of active to partially vegetated sand on the downwind extent of the dune (Thompson, 1983). The depositional lobe can also be defined as a precipitation ridge, which marks the extent of dune migration (Cooper, 1958). The deflation basin (DFB) is a low, flat, or concave to semi-concave area of active to vegetated sand in between the trailing ridges (Thompson, 1983). Cooper (1958) defines the deflation basin as a low, flat dune floor, where sediment is actively eroded and transported. The trailing ridges (TR) can be defined as partially to completely vegetated dune ridges that diverge and extend upwind from the depositional lobe and extend along the length of the dune, (Thompson, 1983). Also trailing ridges can be defined as steep or sloping parallel ridges that mark the external expanse of a parabolic dune (Cooper, 1958). A thorough list of descriptions for the morphologic features of parabolic dunes is provided by numerous authors (for partial list see McKee, 1979). The terms used in describing the morphologic features of parabolic dunes for this work is based on the combined descriptions of Thompson (1983) and Cooper (1958) and dune classification developed by and McKee (1979).

2.2.1 Morphologic Parabolic Dune Types

The general dune classification presented by McKee (1979) has been additionally used for this study, due to its comprehensiveness and organization. The McKee (1979) classification organizes dunes according to three classes: simple, compound, and complex. Parabolic dunes are also sub-classified by length to width ratio or LWR (McKee, 1979); lunate < 0.4, hemicyclic 0.4-1.0, lobate 1.0-3.0, and elongate >3.0. Compound parabolic dunes display a number of adjoining or superimposed forms (McKee, 1979). Accordingly, complex parabolic dunes are examples of two or more dune forms occurring simultaneously (McKee, 1979). There are four distinct variants of compound parabolic dunes, nested, en-echelon, digitate, and superimposed (McKee, 1979).

Table 2.1 Dune classification types, modified from McKee (1979).

Dune classification types	Parabolic dune subclasses	Parabolic dune variants
<i>Simple</i> : mounds or ridges with slipface, similar in size and character	<i>Lunate</i> : < 0.4 LWR	<i>Nested</i> : smaller formed parabolics developed within larger parabolics
<i>Compound</i> : mounds or ridges where smaller dunes of similar type are superimposed	<i>Hemicyclic</i> : 0.4 - 1.0	<i>En-echelon</i> : closely occurring parallel and/or overlapping parabolics
<i>Complex</i> : combination of two or more dune types	<i>Lobate</i> : 1.0 - 3.0	<i>Digitate</i> : a parabolic developing multiple slipfaces and depositional lobes
	<i>Elongate</i> : > 3.0	<i>Superimposed</i> : parabolics developing over a vegetated and stable parabolic

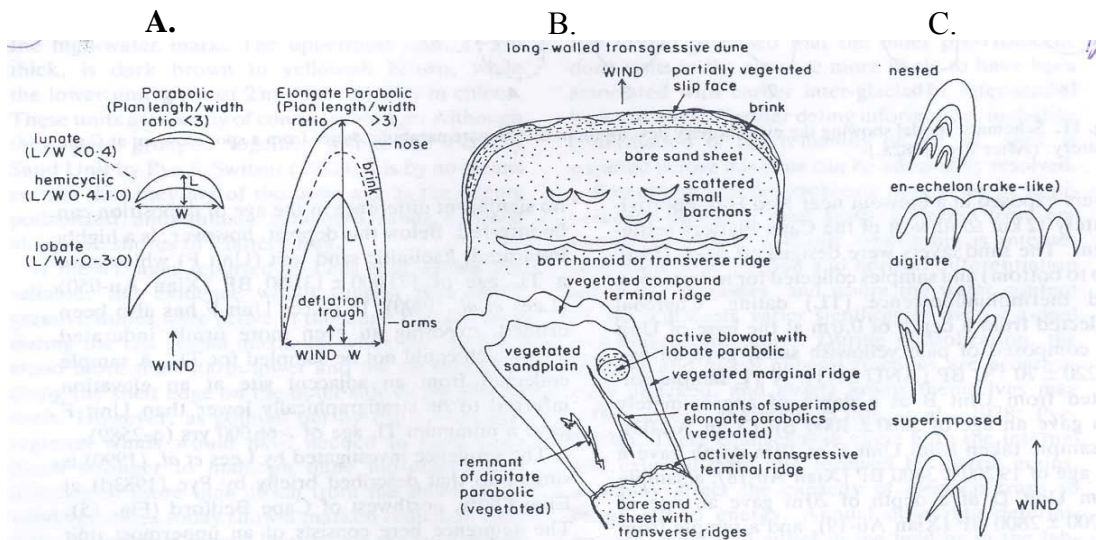


Figure 2.1 Parabolic dune variants and forms; (A) simple dunes, (B) complex dunes, (C) compound (source: Pye, *International Association of Sedimentology*, 1993)

Wolfe and David (1997) define five types of parabolic dunes: open, closed, unfilled-partially filled-filled, merged, and superimposed. The parabolic types are described by morphology, occurrence, and origin (Wolfe and David, 1997) thereby expanding the earlier classification work of David (1981). This work also highlights points made in previous works (Melton, 1940; Hack, 1941; Landsberg, 1956; Jennings, 1957; Pye, 1982, 1983, 1993; Filion, 1987; Thompson, 1983; Halsey, et al., 1990) about the relationship between wind speed and direction, sediment supply, and, vegetation density and moisture (Wolfe and David, 1997). The relationship emphasized by Wolfe and David (1997) is the specific factors listed above control dune morphology, as seen in Figure 2.2. In particular, Wolfe and David (1997) note that “unfilled” parabolic dunes with narrow depositional lobes are the byproduct of low sediment supply; while “partially filled” dunes and “filled” dunes with more well defined depositional lobes are the result of having a greater sediment supply. A dominant effective wind direction will produce an “open” or simple parabolic dune, where only sediment supply and vegetation density limit dune size and migration. However, in a region that experiences a more variable

effective wind regime the parabolic dune will develop a “back ridge” or closed entrance, due to sediment transported out of the deflation basin and depositing in dense vegetation near the dune throat (Wolfe and David, 1997).

2.2.2 Parabolic Dune Models and Their Applicability to North Padre Island, Texas

Parabolic dune model development began in earnest with the Hack model (1941) and the relationship it outlines to the three basic components necessary for parabolic dune development: the roles of vegetation, wind, and sand supply. The Hack model (1941) assumes that winds are constant and unidirectional, and parabolic dunes exist and develop where vegetation cover is between 30-70% and sediment supply is between 40-95%, and “where very great quantities of sand are moved by the wind” (Hack, 1941 p.260). Also, according to Hack (1941) wind regime must be strong enough to transport sediment 5-60% of the time.






A Simple Classification of Parabolic Dunes			
Modifier	Morphology	Occurrence	Origin
Individual dunes			
Open		Areas of sufficient sand supply and winds to form dunes	Moisture and / or vegetation are primary variables on dune morphology
Closed		Wings joined by a semicircular back ridge	Ridge formed behind deflation depression by vegetation trapping sand
Unfilled; partially filled; filled		Area between wings and head filled to varying degrees with sand	Filled according to amount of available sand
Compound dunes			
Merged		Two or more dunes attached and active simultaneously	Simultaneous dune activity
Superimposed		Dunes overriding one another	Successive dune activity

Figure 2.2 Parabolic dune classification, morphology, and occurrence (source: Wolfe and David, *The Canadian Geographer*, 1997)

The Hack model (1941) was developed from field work conducted in NE Arizona desert, where annual precipitation ranges from less than 5 inches to 16 inches and the wind regime is considered unidirectional out of the southwest. The climate is considered arid or BSk (arid, steppe, cold arid) according to the Koppen-Geiger climate classification, and the vegetation consists of shrubs, bunch grasses, and trees. The wind regime, climate, and vegetation cover are markedly different from the same respective characteristics of North Padre Island, which has a bimodal wind regime, BSh (arid, steppe, hot arid) Koppen-Geiger climate classification with a greater average annual precipitation (34.6 in), and a vegetation cover consisting mainly of grass species. Also, the Hack model (1941) is a conceptual model and does not present a systematic stage development of parabolic dunes. However, the Hack model (1941) presents a very generalized depiction of environmental influences and interactions and is applicable to North Padre Island.

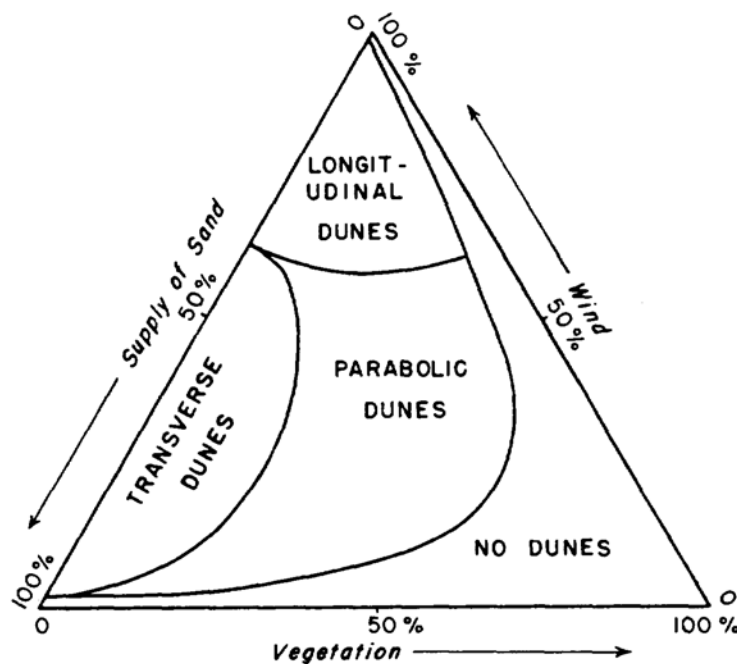


Figure 2.3 Hack dune type development model (source: Hack, *Geographical Review*, 1941).

Landsberg (1956), Jennings (1957), and Cooper (1958, 1967) also emphasized vegetation, wind regime, and sediment supply as the three main factors for parabolic dune development. However, of the previous three authors, only Landsberg (1956) presents a schematic stage model of parabolic dune morphology that presents form development and corresponding dune profile (Fig 2.4).

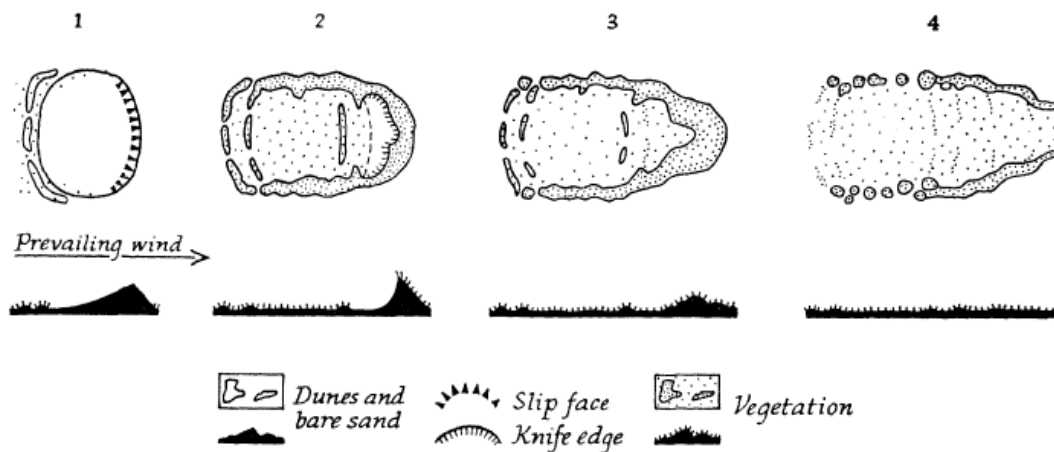


Figure 2.4 The schematic parabolic dune morphology model presented by Landsberg (source: Landsberg, *Geographical Review*, 1956).

Landsberg developed her model from field work conducted in coastal Britain and coastal Denmark. The vegetation cover in both Britain and Denmark is similar to North Padre Island, Texas, in the respect that the main vegetation cover is grass dominated, and both of Landsberg's locations have a Cfb (warm temperate, fully humid, warm summer) Koppen-Geiger climate classification. The wind regime at the British dune locations is narrow bimodal and the wind regime at the Denmark dune locations is unidirectional. The average wind regime velocities are greater in Landsberg's study locations as compared to North Padre Island, Texas, as her field sites are located between $57^{\circ} - 51^{\circ}$ N latitude. Overall, the Landsberg model (1956) is applicable to many locations due to its generalized nature, but it is based off of field work performed in

locations with unidirectional and narrow bimodal wind regimes, and appears to have been sediment supply limited.

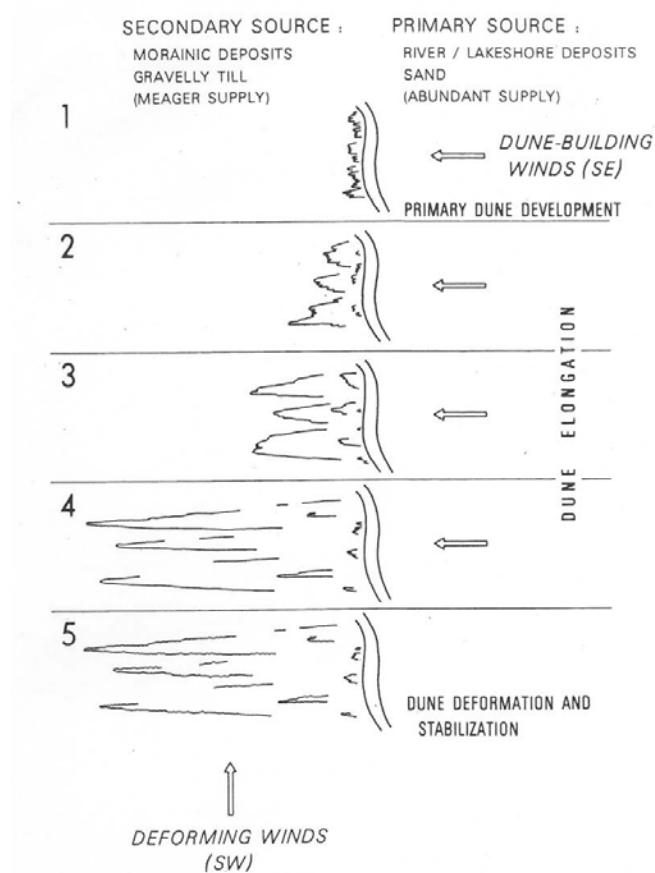


Figure 2.5 Cree Lake parabolic dune development model (source: David, *Canadian Journal of Earth Sciences*, 1981).

The parabolic dune models developed by David (1977, 1981) and Wolfe and David (1997) focus on dune morphology, the influence of perpendicular “deforming” or deflating winds, and classification (Fig 2.5). The influence of vegetation cover as the primary control on dune mobility and wind regime are discussed in association with sediment transport and dune form, also dune morphological features are defined (David, 1977, 1981; Wolfe and David, 1997). The David model (1977, 1981) is a continuous, five step model and model emphasis is placed on sediment supply and source.

The David model (1977, 1981) was developed based on field work conducted on stabilized parabolic dunes in a region that experienced unidirectional wind regime. After dune stabilization, the wind regime in the region changed towards the southwest and caused asymmetry and deformation of the stabilized dunes (David, 1981). The vegetation in Saskatchewan, in the areas of parabolic dune development, consists of pine and woody forest. The climate of Saskatchewan is classified as BSh (arid, steppe, cold arid) in the south and Dfc (snow, fully humid, cool summer) in the Cree lake region, and the parabolic dunes are located between 59⁰ – 50⁰ N latitude. The sediment size in this area is classified as coarse with a -1.32 to 0 ϕ value, and is much larger than North Padre Island, Texas sediments. The applicability of the David model (1977, 1981) to North Padre Island is partially limited due the environmental characteristics of where the model was developed, and the regional wind regime.

Thompson (1983) presents a basic morphologic model of parabolic dunes that defines parabolic features (Fig 2.6). While discussing the influence of wind regime on parabolic formation, shape and orientation, his work recognizes the influence of precipitation and standing water on internal structure of the dune, specifically the deflation basin (Thompson, 1983). Another point discussed by Thompson (1983) is the presence of “eroded remnants” present within the internal structure of active parabolic dunes and the influence of these “eroded remnants” on the morphology of deflation basins and depositional lobes.

The location of Thompson’s parabolic dune field sites in southern Queensland is classified as Cfa (warm temperate, fully humid, hot summer) according to the Koppen-Geiger climate classification. The annual precipitation averages between 120 – 170 cm (47.2 – 66.9 in) with an average annual temperature of approximately 22⁰ C (~71⁰ F), which is similar to the climate and precipitation in North Padre Island, Texas. The wind regime is predominately out of

the SW and displays some seasonal variability (Thompson, 1983). However, the Thompson model (1983) is primarily a simple dune illustration and schematic, and his work is primarily concerned with the soil composition in parabolic dunes. Therefore, the Thompson model (1983) has very limited application in respect to North Padre Island, Texas due to fact it is not a parabolic dune model in the traditional sense (no stages or concepts) and is focused on dune feature or landform unit description and not evolution or overall development of those dune landform units.

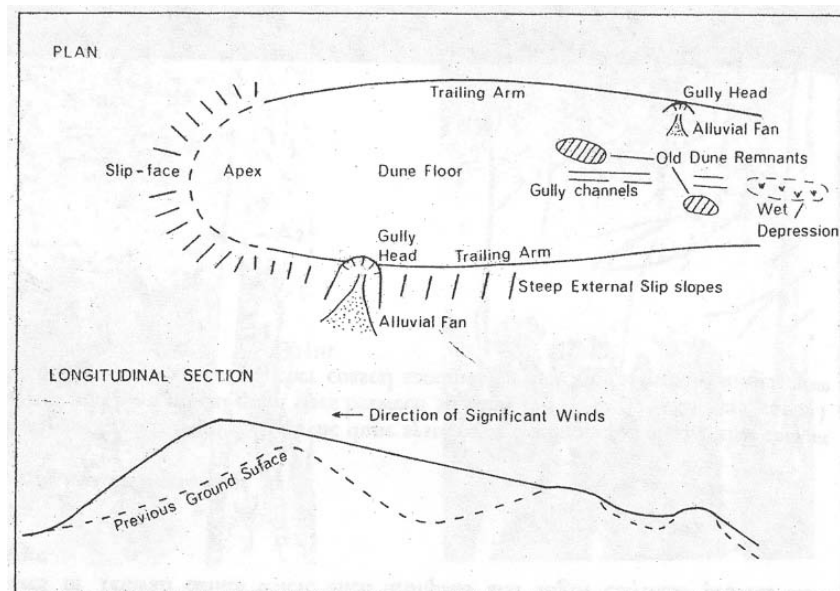


Figure 2.6 Parabolic dune morphology model with dune landform units and profile (source: Thompson, *Zeitschrift Fur Geomorphologie*, 1983).

The parabolic dune model developed by Pye (1982, 1993) is a systematic morphological model beginning with dune initiation as a blowout and developing to a ‘windrift’ dune (Melton, 1940) if conditions are optimal (Fig 2.7). Parabolic dune landform units are described and featured in a dune model schematic (Pye, 1982, p.224; 1993, p.34). Pye (1982) also differentiates between elongate parabolic dunes and common or non-elongate parabolic dunes. Thorough descriptions of elongate parabolic features are presented for the trailing ridges,

depositional lobe, and within the deflation basin (Pye, 1982, 1993). Stage 1a of the Pye model has been correctly reclassified as a blowout by Cooke et al (1993).

The Pye model (1982) was developed in a region of Australia that has a Koppen-Geiger climate classification of Aw (equatorial, winter dry) and receives an average annual precipitation of 178.4 cm (70.2 in). The wind regime in NE Queensland, Australia is unidirectional from the SE and the average temperature is approximately 26.5⁰ C (~80⁰ F). Sediment supply is not an issue for the parabolic dunes in the Cape Flattery region, due to the abundant sediment supply and the fact that active parabolics “cannibalize” relict parabolic dunes. The dominant vegetation is woody shrubs, pine, and rainforest, as the Cape Flattery parabolic dunes are located at ~14.5⁰ S latitude.

The Pye model (1982) is a systematic six set model and is characterized by dune elongation and the diverging and then converging of the parabolic dune trailing ridges. The Pye model (1982) is based in part on the work the Landsberg model (1956) but the model was applied to an area with different environmental qualities and sediment supply. North Padre Island, Texas experiences a bi-modal wind regime and has a different vegetation and environmental characteristics than NE Queensland. While some aspects of the Pye model (1982) are applicable to North Padre Island, Texas, like dune elongation and the development of more complex internal dune landform units like gegenwalle ridges. Also, the Texas coastal dunes are classified as lobate according to the McKee (1979) classification and differ from the elongate dunes in Cape Flattery.

A model of parabolic dune activation and stabilization is presented by David et al. (1999), which outlines phases of environmental change and the repetition of steps necessary for dune activation to occur (Fig. 2.8). Hugenholtz and Wolfe (2005) also present a dune activation

and stabilization model based off of work in the northern Great Plains of North America. The activation and stabilization of blowouts and incipient parabolic dunes is dependent on four assumptions: the dunefields are closed systems and continental, vegetation is the main limiting factor in aeolian activity, dune activity is balanced between biomass and active surface area, and drought or increased aridity in a region is the main disturbance in dunefield activation (Hugenholtz and Wolfe, 2005). Dune activation and stabilization is due to the interaction or influence of one or all of the assumptions listed above.

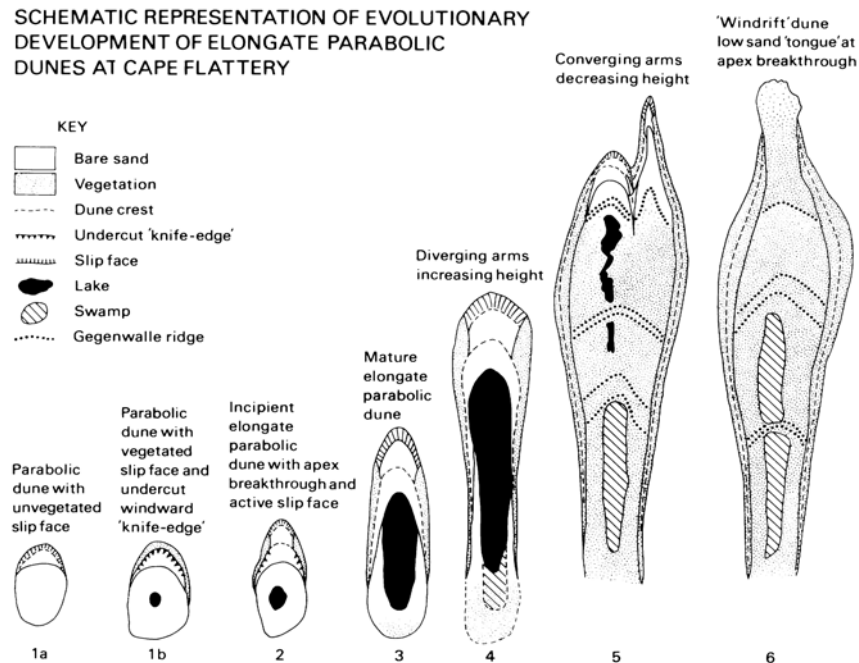


Figure 2.7 The Pye parabolic dune morphology model at Cape Flattery, Australia (source: Pye, *Geografiska Annaler*, 1993).

The David et al. stabilization and activation model (1999) is applicable to many locations where complete parabolic dune stabilization occurs especially since it is related to water table depth and climatic stresses and the variability of both. The region Seward Sand Hills region of Saskatchewan is classified as BSk (arid, steppe, cold arid) according to the Koppen-Geiger climate classification and receives approximately 37.5 cm (~14.8 in) of precipitation

annually of which one-third is snow. One aspect of the David et al. model (1999) is that needs clarification is differentiating between a parabolic dune back ridge and dune-track ridges. It appears that dune-track ridges are stabilized or partially vegetated back ridges, this is clearly a case of poor semantics and un-clarified dune feature or landform unit classification.

The evolution of other dune forms into a parabolic dune has been studied using computer modeling by Duran et al. (2006) and air photos by Anthonsen, et al (1996). The model by Duran et al. (2006) presents a numerical simulation for the change in vegetation density and its influence on dune form. The modeling performed by Duran et al. (2006) emphasizes that the growth rate of vegetation is necessary for the transformation of barchans to parabolic dunes. Analysis of aerial photographs, topographic maps, and wind data reveals a relationship between a change in wind regime and dune orientation, and the influence of increased vegetation cover (Anthonsen, et al., 1996) can have on dune form.

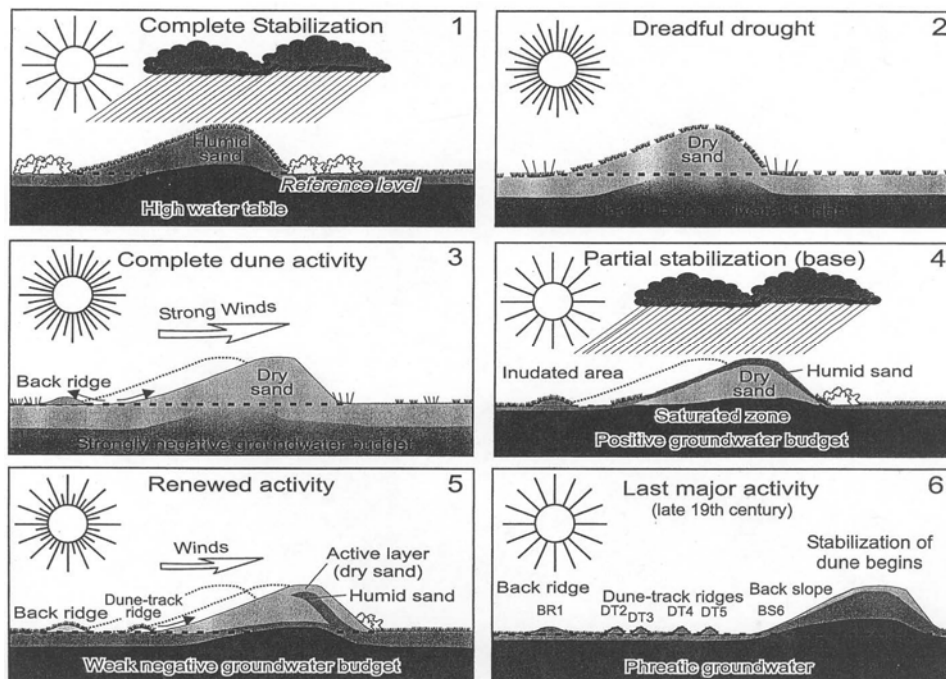


Figure 2.8 Parabolic dune activation and stabilization model (source: David et al, *Geological Survey of Canada*, 1999).

2.3 Factors Influencing Parabolic Dune Development

Four major factors have been identified as being the most influential in parabolic dune development: effective wind direction, climatic conditions, the role of vegetation and sediment supply. These four factors in parabolic dune development have been discussed in the majority of parabolic dune literature with authors placing varying degrees of emphasis on the importance and influence of each.

2.3.1 The Role of Wind Regime in Parabolic Dune Development

Landsberg was the primary author to emphasize the role of wind regime in parabolic dune development and to relate recorded wind data to dune orientation. To calculate the volume of sand moved and the direction of sediment movement Landsberg utilized Bagnold's equation (Eq. 1) and related the results to dune orientation. The Bagnold equation (1951):

$$A n (v - V_t)^3 \quad \text{Eq. 1}$$

where, A is a constant associated with the volume of sand moved; n is the number of directional winds; v is wind speed in m.p.h.; V_t is the constant given as the threshold velocity or 10 m.p.h. in this case (Bagnold, 1951). Landsberg (1956) utilized wind data from eleven stations near her selected study areas for her vector calculations. Dune orientation and dominant wind direction recorded at the weather stations did not correspond at all dune study locations (Landsberg, 1956). The conclusions reached to explain variations in parabolic orientation and curvatures are: changes in local topography in dune area, increased vegetation cover influencing sediment movement, and long-term changes in precipitation and wind regime.

Jennings (1957) work emphasized the role of the effective wind and the influence of onshore winds, in his work on King Island, Tasmania. His analysis of the wind data and coastal parabolic orientation led to his conclusion that the onshore component of wind regimes (Jennings, 1957) was most influential in dune orientation. The parabolic dune fields along the King Island coast migrate inland regardless of the coastal orientation. However, Jennings (1957) also notes there is a correlation between the lower density coastal vegetation and parabolic dune formation on the leeward coast of King Island.

Cooper (1958, 1967) associates parabolic dune development with the effective onshore winds of coastal California and Oregon. The onshore wind regime along the California and Oregon coasts allow for sediment to be transported inland and due to the combined influence of vegetation stabilization and density parabolic dunes develop. Cooper observed that parabolic dunes migrating through dense vegetation developed more elevated dune crests and depositional lobes and were generally shorter than parabolic dunes developing in forested (less dense) environments. Cooper drew similar conclusions from inland observations in Washington and Oregon about the relationship of uni-directional effective winds and vegetation density.

Fryberger and Dean (1979) work with directional wind data associates wind regime with dune form development. The results of their work indicate that parabolic dunes develop where wind regimes are: narrow uni-modal, wide uni-modal, or acute bimodal. The Fryberger and Dean method (1979) is used for calculating the potential net direction for sediment movement from directional wind data. The Fryberger and Dean method (1979) result in a histogram or sand rose, which displays the transport potential of each wind direction in vector units. The directional vector units are combined to calculate a resultant drift direction (RDD), displayed in

vector units, which represents the general direction of sediment movement. (For a complete review see section 4.7.2 and 4.7.3.)

The Australian parabolic dune research conducted during the modern period (1960-1995) focuses on the influence of effective winds and dune orientation, especially in regard to coastal parabolic dunes (Coldrake, 1962; Pye, 1982, 1993; Story, 1982; Thompson, 1983). The parabolic dune model developed by Pye (1982) was developed based on observations of coastal parabolic dunes with effective onshore winds. Using the Fryberger and Dean method (1979), Pye demonstrates parabolic dune alignment and migration is consistent with the onshore wind regime. Coldrake (1962) observed that parabolic dune orientation was consistent with the effective onshore (SE) wind regime, but also noted the influence of N and NE winds in sediment movement from the asymmetry of some blowout and parabolic dunes.

The parabolic dune work conducted in southern Saskatchewan, Canada (David, 1977, 1981; Wolfe and David, 1997; David et al. 1999; Wolfe and Lemmen, 1999; Hugenholtz and Wolfe, 2005, 2006) recognizes the uni-directional aspect of the summer wind regime and the influence of the seasonal high pressure system NE of this area. The parabolic dunes in the Great Sand Hills region are generally aligned with the recorded weather station data however local dune orientation varies due to topographic influence and slight differences in wind regime at the various study sites (Hugenholtz and Wolfe, 2005, 2006).

Wind regime can influence dune evolution and form, specifically in regards to transforming crescentic and dune forms to parabolic dunes (Anthonsen et al. 1996). Long term changes to wind regime ($> 30 \text{ a}^{-1}$) and an accompanying change in vegetation cover can lead to a change in dune migration direction and an increase in dune stability which will cause an evolution in dune form (Anthonsen et al. 1996).

2.3.2 The Role of Climatic Conditions in Parabolic Dune Development

The discussion of climatic change and vegetation cover are often linked in parabolic dune literature (Cooper, 1923, 1938, 1958, 1967; Hoggom, 1923; Melton, 1940; Hack, 1941; Pye, 1982, 1993; David et al. 1999; Arens et al. 2004; Forman and Pierson, 2003; Marin et al. 2005). The relationship between climatic change and vegetation cover is necessary to consider when determining factors in dune mobility and/or stabilization. The most obvious relationship between climatic conditions and vegetation is the precipitation levels that allow for short term and continued plant growth, while the relationship between water table and vegetation density is often not considered (David et al. 1999).

The early period (1800's-1959) parabolic dune studies of Cooper (1938), Hoggom (1923), Melton (1940) and Hack (1941) all formed conclusions that parabolic dune development and migration occurs in conjunction with a change in climatic conditions. The research by Cooper (1938) and Hoggom (1923) associate parabolic dune development with the climatic change at the end of the last ice age (~10K BP). With the end of the last ice age regional (central U.S. and northern Europe) precipitation increased and allowed for vegetation to anchor and eventually completely stabilize these parabolic dunes. Melton (1940) and Hack (1941) conclude from their respective research that increased regional (southern High Plains and NE Arizona) aridity is a factor in influencing dune migration. These conclusions were based on field observation of dune activity and comparison of historical air photos, to reveal patterns of dune migration.

A dune stabilization and activation model has been developed based on field research conducted in the Great Sand Hills region of Saskatchewan, Canada (David et al. 1999). Climatic conditions are the main factor in reactivation or stabilization of parabolic dune dunes (see Figure

2.8) where a change in climate and water table affects vegetation densities within the dune and can lead to reactivation of sediments or allow for an increase in vegetation growth. Similarly reactivation of parabolic dune sediments and dune migration has been linked to periods of drought ($\sim 4-10 \text{ a}^{-1}$) and seasonal decrease in precipitation (Arens et al. 2004; Marin et al. 2005; Forman and Pierson, 2003). Arens et al (2004) and Marin et al (2005) emphasize the interconnectedness of drought and the decrease in vegetation cover, which allows for more sediment to experience the potential for entrainment and therefore dune migration.

2.3.3 The Role of Vegetation in Parabolic Dune Formation

Vegetation is one of the primary factors in determining parabolic dune morphology, dune length, and migration rate. Parabolic dunes form in association with vegetation and vegetation density influences dune form (Cooper, 1958). Vegetation acts to stabilize the trailing ridges of a parabolic dune and provide a general “form” for the individual dune (Cooper, 1958, 1967; Pye, 1982, 1983, 1993; Thompson, 1982). Also vegetation may develop within the internal area of parabolic dunes depending on the surface moisture content and water table level and if climatic conditions are suitable vegetation will completely stabilize an active parabolic dune or dune field (Cooper, 1958, 1967; Anthonsen et al. 1996; David et al. 1999).

The types of vegetation most common in the areas of parabolic dune development are shrub-like plants, grasses, and occasionally woody plants (trees) (Hack, 1941; Cooper, 1958, 1967; Pye, 1982, 1983, 1993; Thompson, 1983). In the coastal environment the most common species associated with parabolic dunes are *Uniola sp.*, *Spartina sp.*, *Panicum sp.*, *Ammophila sp.* and *Spinifex sp.* (Pye, 1983, 1993; Carter et al. 1990). The sediment stabilizing properties of vegetation were initially documented by Melton (1940) and Hack (1941) in reference to plant

roots and ground stabilization. Vegetation also acts as a stabilizing agent for parabolic dunes by increasing the surface roughness parameter along the vegetated areas of the dune (Hesp, 1981; Pye, 1983). Therefore by increasing surface roughness a higher velocity wind speed is necessary to put sediment into entrainment and more sediment is sheltered by vegetation within the dune (Hesp, 1981; Pye, 1983).

2.3.4 The Role of Sediment Supply in Parabolic Dune Formation

Parabolic dune development and migration are dependent on the presence of an ample sediment supply to allow for dune landform unit development and continued dune evolution (Melton, 1940; Hack, 1941; Cooper, 1958, 1967; Pye, 1982, 1983, 1993; David, 1977, 1981; Wolfe and David, 1997). Many early period (1800's-1959) authors indicated that an ample sediment supply must be present in a region with wind regimes above threshold for blowout initiation to occur. Also the sediment supply and substrate must be thick enough for continued sediment transport and dune elongation, at least down to a non-erodible substrate, where dune migration will eventually cease (Melton, 1940; Hack, 1941; Cooper, 1958; Landsberg, 1956; Jennings, 1957).

Sediment supply is generally provided by sediments deposited by glacial retreat, fluvial deposits, or by coastal inputs. In the coastal environment parabolic dune sediment supply is provided by inputs from the backbeach, especially if a parabolic dune develops from a foredune blowout, and also from the substrate. The sediment supply and wind regime will determine the amount of dune elongation that is possible (Hack, 1941; Cooper, 1958, 1967; Pye, 1982,1983) Parabolic dunes that develop from glacial deposits are dependent upon substrate and potentially relict dunes for sediment supply for continued evolution and migration. Parabolic dunes that

develop from fluvial deposits are dependent upon substrate and seasonal sediment inputs especially in areas which experience water level fluctuations (Filion, 1987). In the instance of parabolic dune development in lee of the foredune the substrate acts as the sediment source, and sediment supply would increase if the active parabolic dune migrates over a relict or stabilized dune (Cooper, 1958, 1967; Pye, 1982, 1993; Thompson, 1983; Story, 1982; Inman et al. 1966; Arens et al. 2004).

2.4 Parabolic Dune Age and Migration

Parabolic dune migration rates vary due to climatic conditions, vegetation density, sediment supply and wind velocity (Inman, et al., 1966; Story, 1982; Pye, 1982; Wolfe and Lemmen, 1999; David, et al., 1999; Arens, et al., 2004). Early dune migration measurements were determined using air photo analysis, topographic maps, and field measurement (Inman, et al., 1966; Story, 1982; Pye, 1982). Recent advances in computer mapping technology, digital imagery, global positioning systems (GPS), and survey equipment have allowed for highly accurate dune migration measurement rate (Moore, 2000; Bailey and Bristow, 2004; Andrews, et al. 2002). Accordingly, the margin of error has been reduced (compared to using only field measurements) especially when integrating GPS data with field measurements and digital imagery (Moore, 2000).

The migration rates of individual parabolic dunes vary within dunefields (Bailey and Bristow, 2004; Arens et al. 2004; Marin et al. 2005; Wolfe and Lemmen, 1999) and also for individual dunes (Hugenholtz and Wolfe, 2006; Marin, et al., 2004). Parabolic migration rates range from 13.3 m a⁻¹ in Denmark (Anthonsen et al. 1996) to 6.5 cm a⁻¹ in northern Australia (Story, 1982). Previous studies indicate that migration rates generally range average from

approximately 5 m a^{-1} (Pye, 1982; Arens et al. 2004; Marin et al. 2005) in Queensland, Denmark, and Colorado, respectively, to approximately 2 m a^{-1} (David et al. 1999; Wolfe and Lemmen, 1999; Hugenholtz and Wolfe, 2006; Bailey and Bristow, 2004) in the Great Plains region of Canada, and the United Kingdom, respectively. The smallest migration rate noted was in northern Australia where some parabolic dunes advanced just 6.5 cm a^{-1} (Story, 1982).

Table 2.2 Dune migration rates for various parabolic dune studies.

Dune migration rates				
Author, year	Location	Total migration (m)	Annual migration (m a^{-1})	Period of migration (years)
Anthonsen et al. 1996	Denmark	1000	13.3	90
Arens et al. 2004*	Denmark	0-12 N, 0-7 L	3-1.75	2
Bailey and Bristow, 2004	U. K.	16	2	8
David et al. 1999	Saskatchewan	20	2	10
Hugenholtz and Wolfe, 2005	Saskatchewan	11	1.1	10
Inman et al. 1966	Baja California	65	18	~3.6
Marin et al. 2005**	Colorado	313-665	5-11	63
Pye, 1982	Australia	93	5.6	19
Wolfe and Lemmen, 1999	Saskatchewan	5.1	2.6	2

* Denotes two dune facies

** Denotes average of 13 dunes

2.5 Locations of Parabolic Dunes

Parabolic dunes develop in desert, tropical, semi-arid and arid environments (Pye and Tsoar, 1990), and are present in both coastal and inland dune fields (Pye and Tsoar, 1990).

Parabolic dunes generally develop in areas with a dominant prevailing wind direction (Jennings, 1957; Landsberg, 1956; Story, 1982; McKee, 1966, 1979; David, 1977, 1981; David, et al., 1999; Fryberger and Dean, 1979). Parabolic dunes may also occur in conjunction with intermediate beach types in areas of ample sediment supply (Short and Hesp, 1982).

2.6 Discussion and Conclusions

Multiple parabolic dune studies indicate that there are a few general themes that all common throughout the literature. The first prominent theme in the reviewed parabolic dune literature is that dunes migrate in the general direction of the effective wind regime. The

directional migration of parabolic dunes, in relation to effective wind regime, was initially noted by Hogbom (1923) and then Melton (1940). The Fryberger and Dean method (1979) provide a visual representation of the influences a of the sediment transport potential for a given wind regime. When the Fryberger and Dean method (1979) is utilized to analyze the wind regime in areas where parabolic dunes develop, the usual result is a wind regime that is uni-directional, and parabolic dune migration will be similar to the direction of the resultant drift direction (RDD) or the strongest effective wind.

Koppen-Geiger Climate Classification and Parabolic Fields

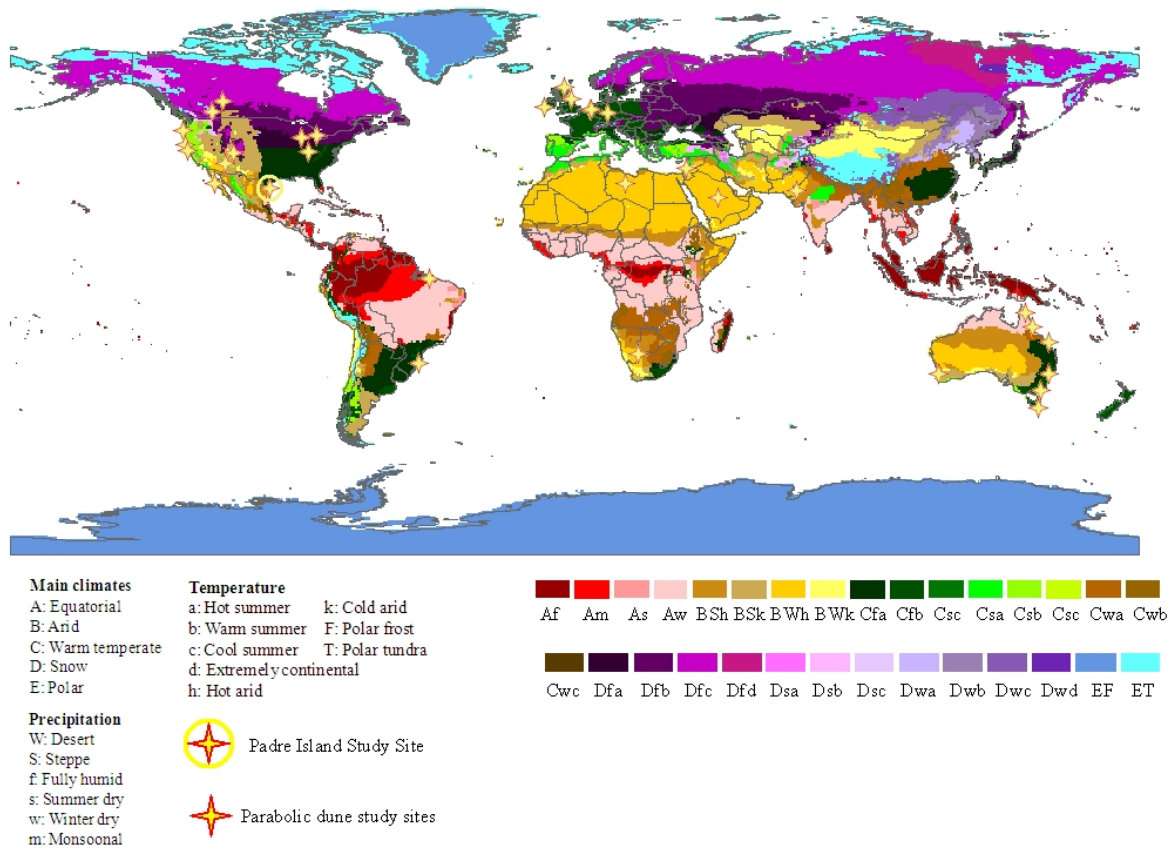


Figure 2.9 Location and climate of major parabolic dune studies.

The second major theme in the parabolic dune literature is the relationship between climate change and parabolic dune activity and/or activation. Cooper (1938), Melton (1940), and

Hack (1941), were the first authors to note that parabolic dune activity increases in periods of increased aridity. The increase in parabolic dune activity is due to the reduction of vegetation and the corresponding increase in sediments exposed to transport. Also, during periods of high aridity the water table lowers and the plant root systems weaken and eventually the vegetation dies off. The cohesive effects of a plant's root systems is lessened or negated during periods of prolonged aridity, allowing for more loose sediments to be transported. A parabolic dune stabilization and activation model based on climatic data and air photo analysis was proposed by David et al. (1999) (Fig. 2.8) that summarizes the observations documented in earlier studies (Cooper, 1938; Melton, 1940; Hack, 1941).

The third major theme in the parabolic dune literature is that parabolic dunes develop in a systematic fashion. Hack (1941) developed the first model for parabolic dune development that emphasized the relationship between vegetation, sediment supply, and wind regime. Landsberg (1956) developed a model based on her dune observations in Britain and Denmark. The modern period (1960-1995) of parabolic dune literature has produced three distinctive models for parabolic dune development: the Pye model (1982, 1993), the Thompson model (1983) and the David model (1977, 1981). The Pye (1982) and David (1981) models emphasize the systematic nature of parabolic dune development, while the Thompson model (1983) focuses on feature development within parabolic dunes due to environmental influences (i.e.: water). The parabolic models that have been developed during the recent period (1996-present) have focused on computer modeling (Duran et al, 2006), GIS analysis (Anthonsen et al. 1996; Anthonsen, 1997; Hugenholtz and Wolfe, 2005, 2006; Andrews et al. 2002) and the influence of climate (David et al. 1999; Marin et al. 2005; Abrogast et al. 2002).

There are a few noticeable gaps in the parabolic dune literature, particularly the lack of parabolic dune research conducted on barrier islands and the relative lack of long term monitoring (> 10 yr) of individual parabolic dunes. Coastal parabolic dune research has been conducted in multiple coastal locations, most notably in Australia, coastal Europe (and Britain) and the west coast of U.S. However, these locations consist of mainland beach environments and are not considered arid by the Koppen-Geiger climate classification (with the exception of Story, 1982). David et al. (1999) and Hugenholtz and Wolfe (2005, 2006) conducted long term parabolic dune monitoring (~ 10 yr), but dune surveys were conducted at irregular intervals, and climatic records were only analyzed in respect to the survey periods. The parabolic dune literature indicates that there is a heavy reliance on air photo interpretation, and only recently have GIS techniques been integrated into parabolic dune study. However, even with the recent utilization of GIS in parabolic dune studies, there has a lack of integration of rasterized parabolic dune survey data with doqq and aerial photo imagery to determine dune migration and change.

The focus of this research is to study parabolic dunes that develop in an arid barrier island environment, and determine parabolic dune migration and change using rasterized survey data and doqq analysis. Accordingly, a methodology has been developed that will allow other parabolic dune researches to integrate survey data with remotely sensed imagery, using GIS analysis and GPS data to determine and measure dune change. Weather station data has also been used to help determine dune migration direction and orientation, as well as to determine the seasonal influence of the wind regime.

The focus of this research therefore, is to study parabolic dunes that develop in an arid barrier island environment, and determine parabolic dune migration and change using rasterized

survey data and doqq analysis. Accordingly, a methodology has been developed that will allow other parabolic dune researches to integrate survey data with remotely sensed imagery, using GIS analysis and GPS data to determine and measure dune change. Weather station data has also been used to help determine dune migration direction and orientation, as well as to determine the seasonal influence of the wind regime. The research aims are to (i) examine communalities between previous studies and the behavior and evolution of parabolic dunes on Padre Island, (ii) to identify what factors and evolutionary mechanisms and products are similar and which are not, and why, (iii) to characterize the wind records for the region and attempt to match them to parabolic dune dynamics, orientation and geomorphology, and (iv) create a new parabolic dune evolutionary model for Padre Island parabolic dunes.

3. Characteristics of North Padre Island, Texas

3.1 Introduction

The dunes studied for this research are located on North Padre Island, Texas. This regional setting and barrier island environment are outlined in this chapter. The barrier island precipitation records, climatic conditions, sediment sources and a list of vegetation are presented for this area.

3.2 Regional Setting

North Padre Island is located along the south central Texas Gulf coast, west of Corpus Christi. North Padre Island is approximately 80 miles long and separated from South Padre Island by the Mansfield Channel in the south and from Matagorda Island by the Aransas Pass in the north (Fig. 3.1). The barrier island is separated from the mainland by Laguna Madre and the barrier island width varies from ~2.5 to ~5 miles (Weise and White, 1980). North Padre Island has a stable and aggrading foredune that is continuous along the backbeach, except where blowouts are present. The nearshore is characterized by three subaqueous shore parallel sand bars. The first two sand bars are approximately 50 and 100 meters from the high tide line, with the third sand bar approximately 75 meters seaward of the second bar. The beach at North Padre Island is classified as dissipative according to the Wright and Short (1983) morphodynamic beach model.

3.3 Climate

The climate of North Padre Island is semiarid and subtropical, or BSh (Arid, steppe, hot arid) by the Koppen-Geiger climate classification (Weise and White, 1980). The average annual temperature on North Padre Island is approximately 72°F, with an average of less than ten



Figure 3.1 General regional location of North Padre Island, Texas

days of freezing temperatures (Weise and White, 1980; PAIS weather data). North Padre Island experiences approximately 60% or 210-220 days of sunshine annually. Conversely, there are approximately 97 days of measurable precipitation (≥ 0.01 in) annually

(<http://www.srcc.lsu.edu/southernClimate/atlas/>).

Precipitation data (1968-3/2007) from Padre Island National Seashore ranger station indicates that average annual precipitation is approximately 34.6 inches or 76.1 cm. The wettest year for the recorded period was 1970 with a rainfall of 58.9 inches (149.5 cm) and the driest year was 1988 with a rainfall of 16.7 inches (42.3 cm). The seasonal component of the precipitation data indicates that the fall season (Sept.-Nov.) is the wettest with an average rainfall of 13.16 inches (~29 cm), with the winter season as the driest month with an average rainfall of 5.22 inches (~11.5 cm). Accordingly, the wettest month is September with an average rainfall of 6.42 inches or 42.3 cm and December is the driest month with an average rainfall of 1.35 inches or ~3 cm (PAIS precipitation data).

There have been ten hurricanes or tropical storms to strike, within a 65 nautical miles radius of Padre Island National Seashore ranger station since 1961 (www.nhc.noaa.gov/). Five hurricanes have impacted this area, with Carla in 1961, a category 5, being the most powerful storm to make landfall (<http://maps.csc.noaa.gov/hurricanes/viewer/html>). The central Texas coast averages one hurricane or tropical storm strike every 4.5 years (Fig 3.2).

Table 3.1 Annual PAIS precipitation totals (inches) from 1968-3/2007

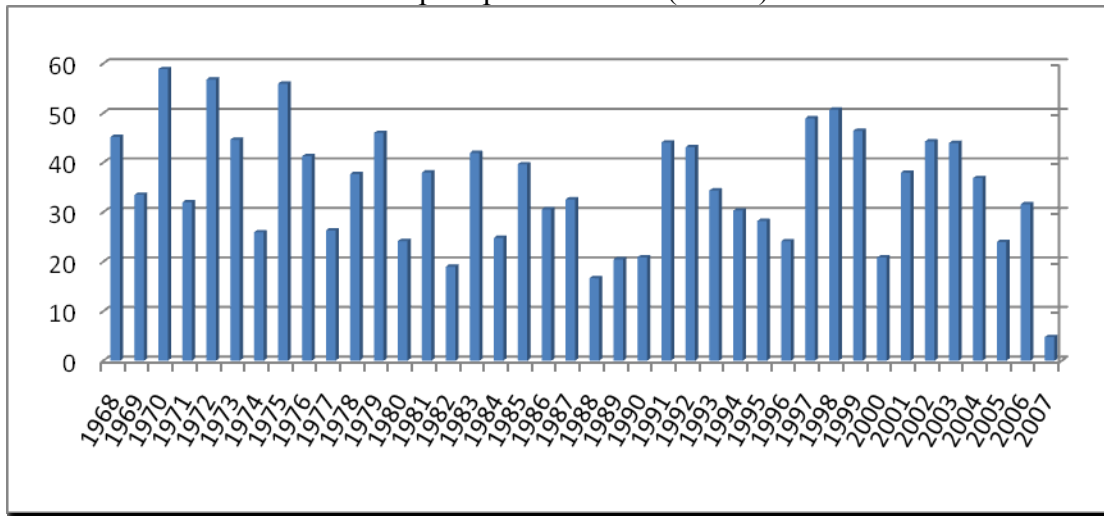


Table 3.2 Monthly and seasonal precipitation totals for PAIS 1968-2006

Monthly Totals	IN	CM	Seasonal Totals IN	
January	1.86	4.10	Spring	7.41
February	2.01	4.42	Summer	8.78
March	2.28	5.02	Fall	13.16
April	2.04	4.48	Winter	5.22
May	3.09	6.81	Seasonal Totals CM	
June	2.93	6.44	Spring	16.31
July	2.46	5.42	Summer	19.32
August	3.39	7.46	Fall	28.96
September	6.42	14.12	Winter	11.48
October	4.47	9.84		
November	2.27	5.00		
December	1.35	2.96		

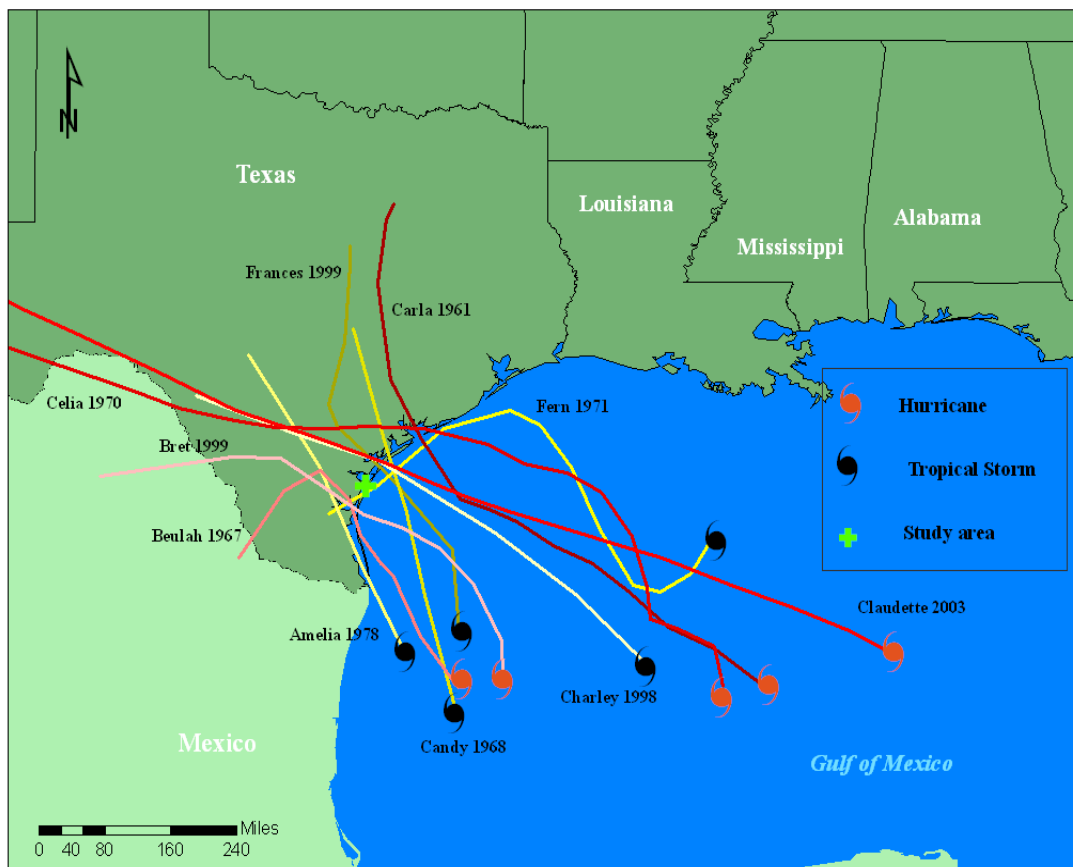


Figure 3.2 Locations of hurricane and tropical storm landfall along the Central Texas Coast 1961-2006

Table 3.3 Hurricane and tropical storm impact along the Central Texas Coast 1961-2006

Hurricanes			Tropical Storms		
Name	Category	Year	Name	Category	Year
Carla	5	1961	Candy	TS	1968
Beulah	2	1967	Fern	TS	1971
Celia	3	1970	Amelia	TS	1978
Bret	3	1999	Charley	TS	1998
Claudette	1	2003	Frances	TS	1988

3.4 Geology and Geomorphology

North Padre Island is an aggradational barrier island or a barrier island that is building and accreting in elevation, and not actively widening (Morton, 1994). The sediments composing the barrier island are well-sorted, fine to very fine sand with a mean grain size of 0.14 mm. Sediment analysis and radiocarbon dating has determined that North Padre Island formed approximately 4000 B.P.

The Holocene transgression and sea-level stabilization have allowed for sediments to be reworked up the continental shelf by wave action towards the central Texas mainland. The submerged Brazos-Colorado delta and Rio Grande delta sediments are the primary sources for the sediment composing North Padre Island. Also, sediments from the Pleistocene barrier-strandplain are incorporated into the barrier island sediment budget after the deposits were exposed on inner shelf after sea-level transgression (Morton, 1994).

The central portion of the Texas coast is a zone of convergence for littoral drift where sediments from north and south sources are deposited along the nearshore. The research area is also along the western most portion of the Texas coast and receives wave energy from northerly, southerly, and easterly directions. Under low energy wave conditions sediments are transported onshore from the offshore directions and sediment sources, and eventually are deposited on the subaerial beach (Leatherman, 1979; Morton, 1994; Shepard, 1960).

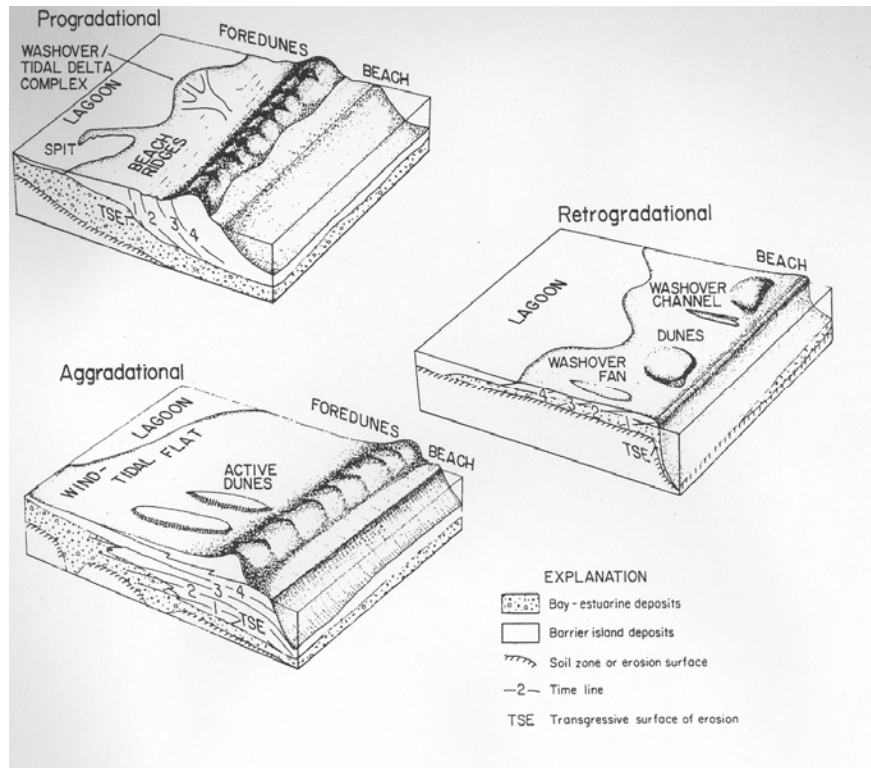


Figure 3.3 Barrier island types; North Padre Island is classified as aggradational (source: Morton, *Texas Barriers*, 1994)

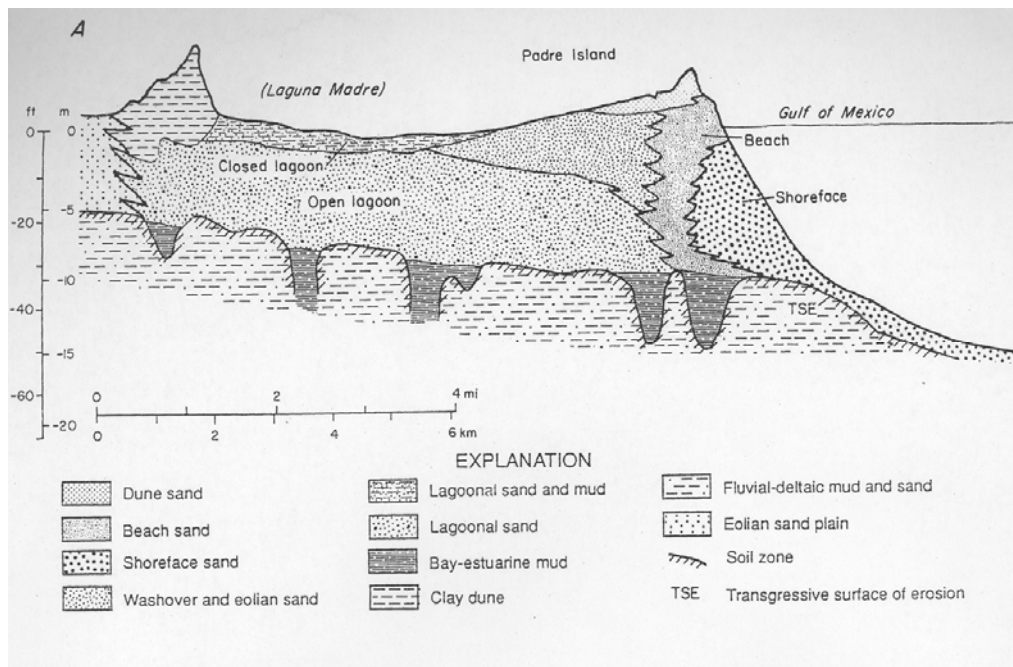


Figure 3.4 Cross section profile of North Padre Island (source: Morton, *Texas Barriers*, 1994).

The foredune and barrier island strand plain are densely vegetated across the extent of the research area. Prior to 1971, cattle was actively grazing across the strand plain that comprises Padre Island National Seashore and vegetation cover along the barrier island has steadily increased since that time. The increase in vegetation density along the strand plain and foredune is due to natural processes and re-vegetation efforts along with the removal of grazing animals. The foredune has been actively prograding since 1996 to the present based on doqq analysis, while blowout and parabolic dune activity has slightly decreased over the same period of time. The most abundant vegetation species along the foredune are: *Uniola paniculata*, *Panicum amarum*, *Croton punctatus*, and *Sesuvium portulacastrum*. The vegetation along the strand plain is varied and moderately dense to dense in the areas directly surrounding the dunes. The most abundant species across the strand plain are: *Fimbristylis castanea*, *Schizachyrium scoparium*, and *Paspalum monostachyum*. (See Table 3.4. for a complete vegetation list).

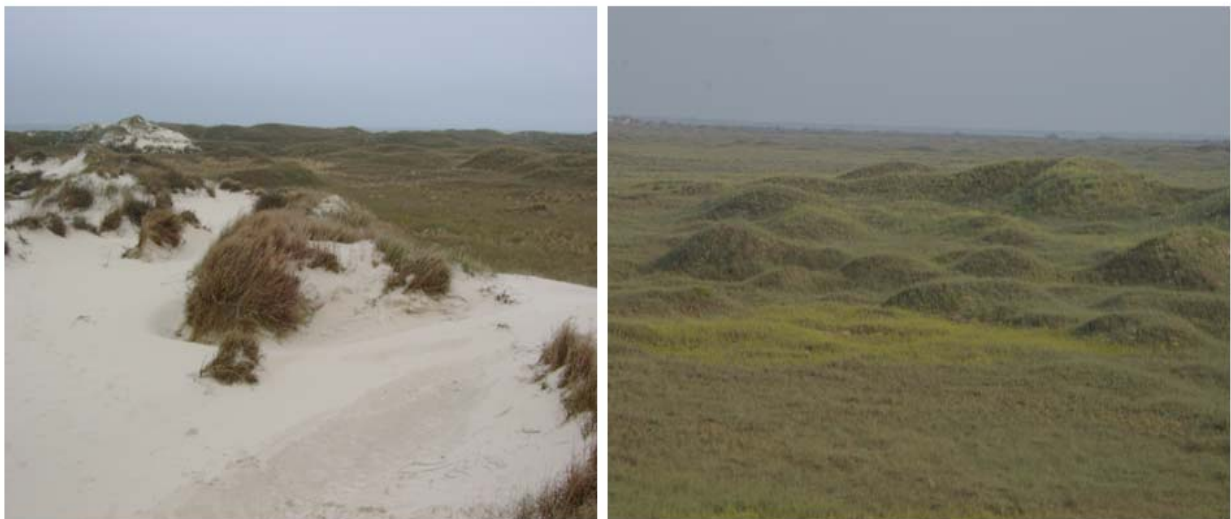


Figure 3.5 Examples of the dunefield surrounding the research dunes on North Padre Island, TX

Table 3.4 List of observed vegetation at Padre Island National Seashore study sites

	Dune vegetation types	Common name	Dune location
ANGL	<i>Andropogon glomeratus</i>	bushy bluestem	1,2,3
APSK	<i>Aphanostephus skirrhobasis</i>	lazy daisy	1,2,3
ATAR	<i>Atriplex arenaria</i>	quelite	2,3
BAMA	<i>Batis maritima</i>	vidrillos	1,2
CECI	<i>Cenchrus ciliaris</i>	buffel grass	2,3
CEIN	<i>Cenchrus incertus</i>	sandbur	1,2,3
CHFA	<i>Chamaecrista fasciculata</i>	partridge pea	1,2
CHCU	<i>Chloris cuclluata</i>	hooded windmill grass	2,3
COER	<i>Commelina erecta</i>	widow's tears	1,2,3
CODR	<i>Cooperia drummondii</i>	rainlily	1,2,3
COBA	<i>Coreopsis basalis</i>	coreopsis	1,2
COTI	<i>Coreopsis tinctoria</i>	golden wave	1,2
COMI	<i>Corydalis micrantha</i>	scrambled eggs	2,3
CRPU	<i>Croton punctatus**</i>	beach tea	1,2,3
CYTE	<i>Cyperus tenuis</i>	flat sedge	1,2,3
ERSE	<i>Eragrostis secundiflora</i>	red lovegrass	2,3
EUCO	<i>Euphorbia cordifolia</i>	spurge	2,3
FICA	<i>Fimbristylis castanea*</i>	fimbristylis	1,2,3
FUSI	<i>Fuirena simplex</i>	umbrella grass	2,3
HEPR	<i>Helianthus praecox</i>	sunflower	1,2,3
HYBO	<i>Hydrocotyle bonariensis</i>	sombbrero	1,2,3
IPIM	<i>Ipomoea imperati**</i>	beach morning glory	1,2,3
IPPE	<i>Ipomoea pes-caprae</i>	railroad vine	1
IVAN	<i>Iva angustifolia</i>	sumpweed	2,3
PAAM	<i>Panicum amarum**</i>	bitter panicum	1,2,3
PAMO	<i>Paspalum monostachyum*</i>	gulfdune paspalum	1,2,3
PHVE	<i>Philoxerus vermicularis</i>	silverhead	1,2
PHAU	<i>Phragmites australis</i>	common reed	1,2,3
POAL	<i>Polygala alba*</i>	white milkwort	1,2,3
RHAM	<i>Rhynchosia Americana</i>	snoutbean	3
SALO	<i>Sagittaria longiloba</i>	arrowhead	2,3
SABI	<i>Salicornia bigelovii</i>	glasswort	1
SCSC	<i>Schizachyrium scoparium*</i>	seacoast bluestem	1,2,3
SCPU	<i>Scirpus pogens</i>	bulrush	1,2,3
SEDR	<i>Sesbania drummondii</i>	rattlebush	2,3
SEPO	<i>Sesuvium portulacastrum**</i>	cenicilla/sea purslane	1,2,3
SOHA	<i>Sorghum halepense</i>	johnson grass	2,3
SPPA	<i>Spartina patens*</i>	marshhay cordgrass	1,2,3
SPVI	<i>Sporobolus virginicus</i>	seashore dropseed	2,3
UNPA	<i>Uniola paniculata**</i>	sea oats	1,2,3

*Denotes most prominent species

**Denotes prominent foredune species

3.5 Dune Geomorphology and Locations

The parabolic dunes studied for this project have developed on North Padre Island, Texas. The smallest parabolic dune (1) is located ~2.3 miles north of PAIS within the municipal limits of Corpus Christi. The larger two parabolic dunes are located within PAIS, ~1.6 miles (2) and ~2.5 miles (3) south of the off-road beach road; the three dunes are between UTM W672591, N3045309 NAD83 north to W666600, N3029757 south (Fig 3.3). As seen in Figure 3.5 the topography of North Padre Island is comprised of an irregular and hummocky dunefield and vegetation surrounding the dune locations can be considered dense to moderately dense (Blum and Jones, 1985; Morton, 1994; Weise and White, 1980).



Figure 3.6 The active foredune on North Padre Island, TX

Dune 1 is located ~50 m west of an active prograding foredune (W672591, N3045309). The general dune environment and location of dune 1 can be described as irregular and chaotic, with a relict foredune parallel to the dune blowout mouth, and an active foredune seaward of the relict foredune (Fig 3.7). There are multiple linear ridges present at varying angles with respect to the parabolic dune. There are also randomly arranged fully vegetated nebkas or mounds

covering the surrounding landscape. The external features of dune 1 are densely vegetated, as is the surrounding landscape particularly by *Spartina patens* and *Uniola paniculata*.



Figure 3.7 Dune 1 land form units from June 2006 (left) and November 2006 (right). The top pictures are of the depositional lobe and partial deflation basin. The bottom pictures are of the deflation basin facing towards the Gulf.

Dune 2 is located ~130 m west of the backbeach (W667035, N3031107) in a densely vegetated area with relatively flat surrounding topography and this parabolic dune is located , more than twice as far inland compared to the other dunes. The foredune ridges consist of a relict foredune and an actively prograding foredune. The active foredune has developed and prograded since 1996 based on doqq analysis (Fig 3.6). According to the McKee (1979) parabolic dune classification dune 2 is elongate with a LWR > 3, and of the three dunes only

dune 2 has this parabolic dune sub-classification. The landscape around dune 2 is relatively homogenous and flat to the W, SW and NW, with only a vegetated ridge north of the dune extending approximately half the length of the north trailing ridge. There is also a large sized blowout dune to the SE of dune 2 and multiple parallel ridges adjacent to the blowout and SE of dune 2.



Figure 3.8 Dune 2 landform units, depositional lobe slipface the summer 2006 on the left and winter 2007 on the right as seen from west of the dune. The deflation basin in summer 2006 as seen from the north trailing ridge (left) and the deflation basin winter 2007 as seen from the south trailing ridge (right).

Dune 3 is located ~45 m west of the backbeach and active foredune (W666600, N3029757). Similar to dune 2 the foredune ridge consists of a relict foredune and an actively

prograding foredune. It was determined from doqq analysis that dune 3 was developing and receiving sediment inputs from the backbeach as recently as 1996. Vegetation ground cover is ~100-90% to the N, E, SE, and W of the dune, except for an area along the W extent of the north trailing ridge and the depositional lobe, where vegetation cover is ~50%.



Figure 3.9 Examples of dune 3 landform units. Clockwise from top left: north trailing ridge and depositional lobe, surge lobe (summer 2006), internal north trailing ridge, deflation basin and internal south trailing ridge.

3.6 Conclusions

The regional setting of the study area is a unique location for parabolic dune study. The combination of having an abundant sediment supply with effective onshore winds, above threshold velocity are two of the factors in parabolic dune development on this barrier island.

The semiarid climate along with variations in seasonal and annual precipitation which influence vegetation densities are also factors that can influence parabolic dune formation, activity, and migration (David et al. 1999). The proximity of the parabolic dunes to relict foredunes indicates that dunes 1 and 3 received sediment inputs from the backbeach and evolved from blowouts along the foredune. The sandy substrate is also a sediment source for the parabolic dunes and the individual sediment budget for each dune can be considered unlimited.

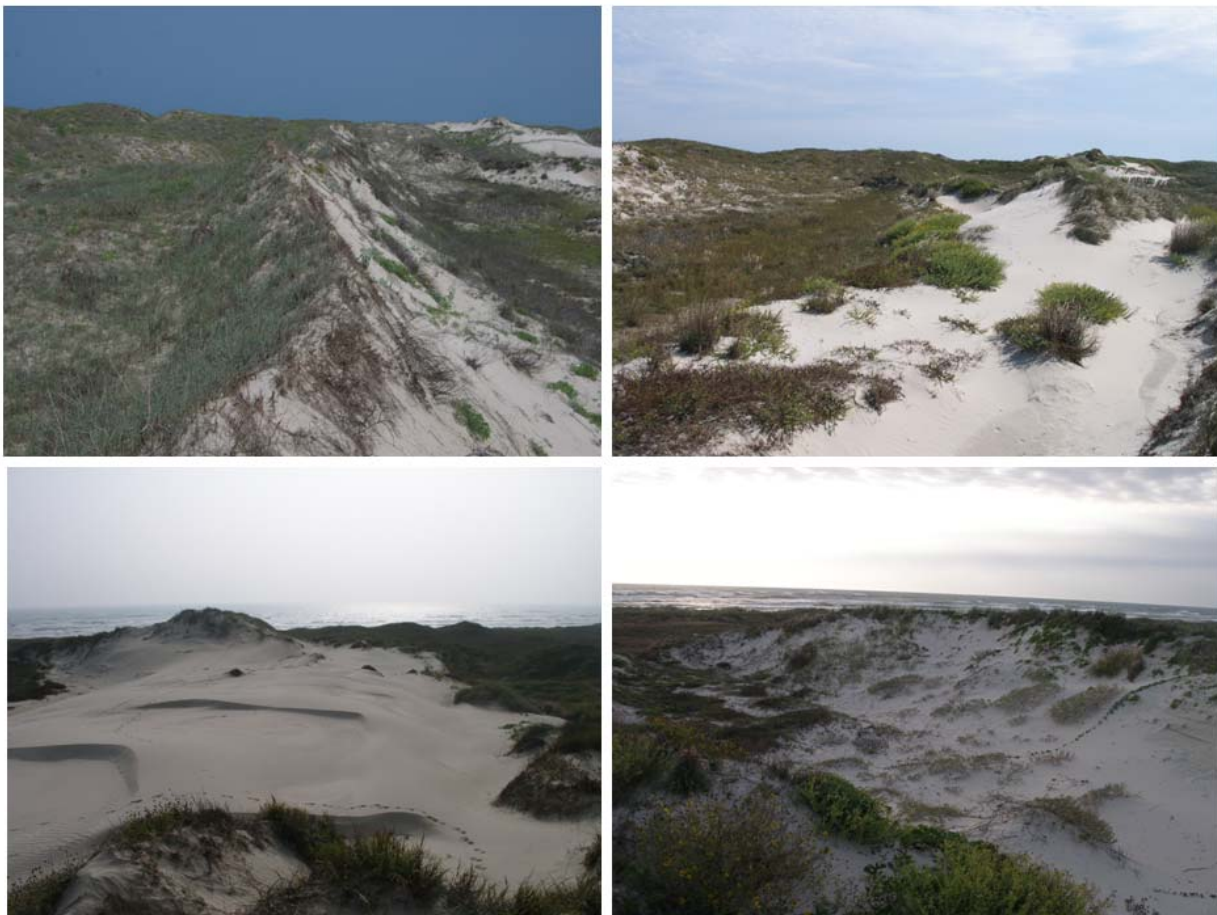


Figure 3.10 Examples of the vegetation density along the trailing ridges in dune 2 (top), dune 3 (bottom left) and dune 1 (bottom right)

North Padre Island has a dissipative nearshore zone with a high, continuous, moderate, to densely vegetated foredune with many blowouts and parabolic dunes active on the island.

Similar to the environment where the Short and Hesp (1982) beach dune model was developed,

this research area has a dominant onshore wind coupled with an abundant sediment supply.

Also, similar to the Short and Hesp (1982) beach dune model blowout and parabolic dunes have developed in this environment.

4. Methods

4.1 Introduction

A variety of methods were used in this research to analyze the data used in this research. The methods and analysis used can be divided into three classes: image preparation and analysis, field data acquisition and post processing, and wind data organization and analysis. Each class of methods is multipart and systematic, and familiarity with remote sensing, GIS, and digital elevation programs is valuable when performing data analyses.

4.2 Digital Orthophoto Quadrangles (DOQQs) and Image Processing

Few aerial photos are available for the study area because of a fire at the Padre Island National Seashore ranger station that destroyed the historical photos dating from the 1940s to the early 1990s. However, two sets of one meter resolution digital orthophoto quadrangles (DOQQ) images were acquired through the Texas Natural Resources Information System (TNRIS) homepage (www.tnris.state.tx.us/). The doqq's were flown in 1996 and 2004 with both sets were processed in color infrared. The doqq's were mosaiced in Erdas IMAGINE 9.0 to cover the entire length of the study area. The two images were then georeferenced using 25 ground control points, consisting of prominent man-made and natural features following methods outlined by Hugenholtz and Wolfe (2005).

A change detection function was performed in Erdas IMAGINE 9.0 on the classified and recoded subset images of the individual dunes (1, 2, and 3) to show the difference in dune migration and extent from 1996 to 2004. The change detection images were then imported into ArcMAP 9.0 for spatial analysis. Shapefiles were created to outline the extent of the individual

dunes, specific dune landform units, determine, area and change (Andrews et al. 2002; Hugenholtz and Wolfe, 2005).

4.3 Map Projection and Format

All doqqs, global positioning system (GPS) points, and images were projected in Universal Transverse Mercator or UTM format. The Utm projection was used because it displays data in a one meter grid format. Padre Island National Seashore and the surrounding areas of Texas belong to North Zone 14 of the UTM global map projection. All coordinates are presented in east-north (x, y) format.

4.4 Total Station (TS) Surveys

Bench marks were established within the individual dunes that were used as reference points to link surveys conducted from different survey locations. The surveys for parabolic 1, 2, and 3 were conducted using the Sokkia Total Station 3000 and Topcon CTD Total Station. The initial surveys were conducted from 13 – 17 June 2006 using the Sokkia TS and follow up surveys were conducted 13 – 14 January 2007 (1 and 3) using the Topcon TS, and 10 – 11 February 2007 (C) using the Sokkia TS. All surveys included morphological breaks and features in dune form as well as general dune landform units and specific GPS recorded benchmarks.

The 17 June 2006 Dune 1 survey consisted of 237 points and was entirely surveyed from control point BM-1 (672501, 3045315) located on the highest area along the southern trailing ridge. The survey was conducted with one person recording on the total station and one person manning the rod and prism. The morphological features present and surveyed in Dune 1 are the vegetated and non-vegetated areas of the deflation basin, trailing ridges, and depositional lobe.

The 13 January 2007 Dune 1 survey was performed using the Topcon CTD Total Station and consisted of 325 points; it was also conducted from control point ABM-1 (672501, 3045315). The second survey recorded 88 more points to record greater morphological accuracy and detail. The extra survey points were taken on the depositional lobe, deflation basin and along the outline of the north trailing ridge.

The initial dune 2 surveys were performed 14 – 15 June 2006. This dune survey consisted of three parts, with the first and second jobs performed 14 June from CBM-1 (666808, 3031249) along the south trailing ridge, consisting of 142 and 309 points, respectively. The third part of the dune 2, June survey was surveyed 15 June from CBM-4 (666893, 3031216) along the crest of the north trailing ridge and consisted of 42 points. All 493 points of the survey were performed with one person recording from the TS and one person manning the rod and prism. All morphological features and breaks were recorded including but not limited to: the dune outline and five meters into the vegetation, depositional lobe, deflation basin, trailing ridges, internal features (nebka/knobs), and gegenwalle ridge. The three parts of the total dune 2 survey were downloaded into Excel organized and edited to create a grid in Surfer 8.

The second dune 2 survey was performed 10 – 11 February 2007 and consisted of 718 points. The 2007 survey was conducted entirely from CBM-1 (666808, 3031249), in two parts (10 February, 392 points; 11 February, 326 points). The 2007 survey recorded 225 more points and was performed using the “two person rod and prism method.” The increased numbers of survey points were taken within the deflation basin, along the external wall and internal wall of the trailing ridges and in the deflation basin. The total station surveys were downloaded into Excel, organized and edited to create a grid in Surfer 8.

The initial dune 3 survey was performed 13 – 14 June 2006 and consisted of three survey jobs. The first survey job was performed on 13 June, from DBM-1 (666530, 3029768) on the highest point along the south trailing ridge and consisted of 345 points. The second survey job was performed 14 June, from DBM-3 (666555, 3029843) on the highest point along the north trailing ridge and consisted of 207 points. The third survey job was performed 14 June from DBM-4 (666384, 3029843) and consisted of 68 points. The total survey points recorded for the dune 3 June survey(s) was 620 points. As in other surveys all morphological features and breaks were recorded, including but not limited to: the trailing ridges and five meters into the vegetation, deflation basin, and gegenwalle ridge. All surveys were downloaded and imported into Excel for organization and editing (50 points were removed due to recording and instrument orientation error) for grid creation in Surfer 8.

The second dune 3 survey was performed 13 January 2007 entirely from DBM-1 (666530, 3029768) and consisted of 611 points. This survey was performed using the “two person rod and prism method” and included all morphological features and breaks, including but not limited to: the trailing ridges and five meters into the vegetation, depositional lobe, deflation basin, and gegenwalle ridge. The survey was downloaded into Excel for organization and editing for grid creation in Surfer 8.

The “two person rod and prism method” or 2RPM was modified from one person survey methods outlined by Brinker and Minnick (1995). The 2RPM consists of two persons spaced at four to six meters along the outside base, exterior and interior of the mid-lines of the trailing ridges and along the depositional lobes, moving in a coordinated pattern. The interior features of the parabolics, including the deflation basin and the elevated aspect of the deflation basin, were surveyed in a grid pattern with the two rod and prisms staggered and spaced three to five meters

apart. The staggered method allowed for more points to be recorded and decreased overall survey time. However, specific dune landform units and points were recorded to present the most accurate and realistic survey possible. All morphological features were accurately surveyed and more points were surveyed in a comparable amount of time to the one person method.

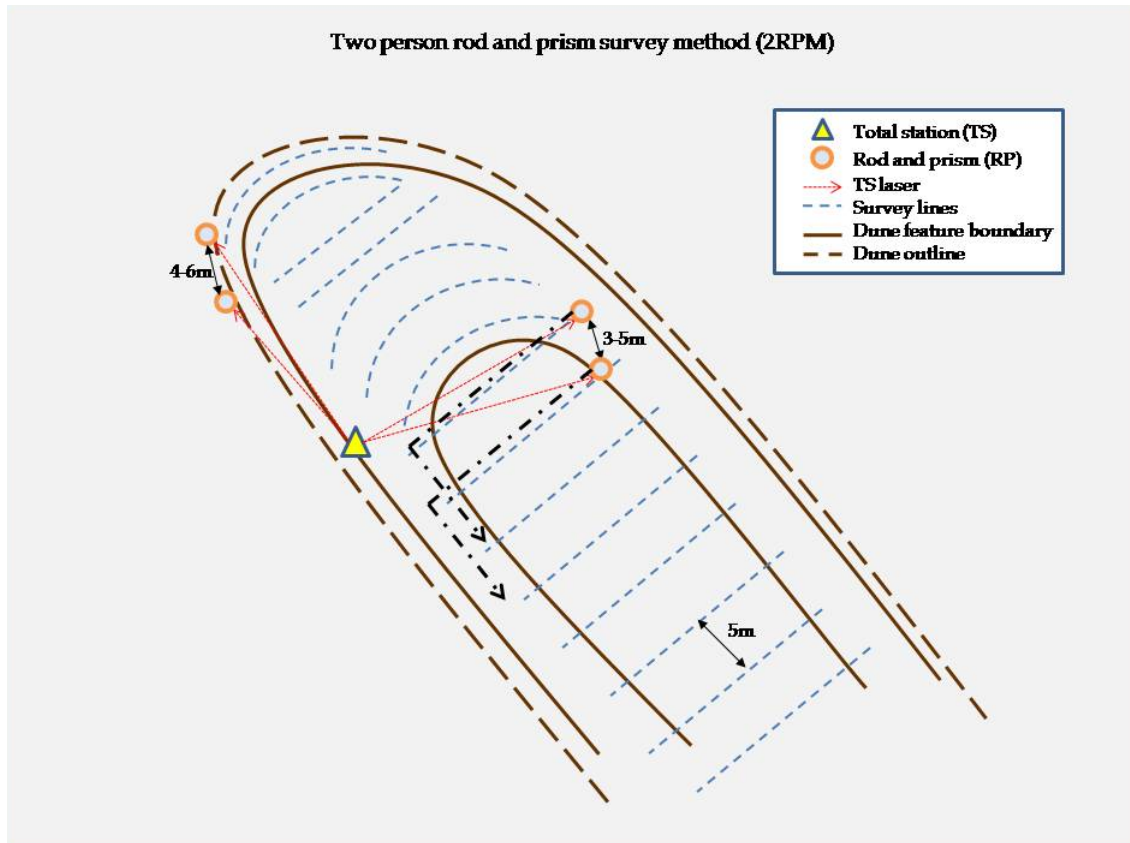


Figure 4.1 Schematic of the two person rod and prism survey method or 2RPM.

4.5 Survey Grids and Digital Elevation Models (DEMs)

All total station dune surveys were downloaded into Microsoft Excel and sorted to compare with field notes and edit, or remove any erroneous data. The survey data was output in ASCII format which allowed for ease in organization and editing. A copy of the raw survey data was converted into Utm values. The surveys values were converted by substituting the raw

survey benchmark coordinate (0, 0) with the TS Utm GPS coordinates and adding raw survey values to the Utm coordinates. Both sets of edited survey data for each dune were imported into Surfer 8 (Golden Software, <http://www.goldensoftware.com/>). Grids were created using the kriging method with one meter grid spacing to accurately depict geomorphic features and for ease when georeferencing (Andrews, et al. 2002). The grid pairs were imported into Erdas IMAGINE 9.0 and converted to images for GIS analysis in ArcMAP 9.0 (Andrew, et al. 2002). The Utm grid images were more easily georeferenced than the standard edited survey values. Since the Utm grid images, provide greater ease in identifying features for georeferencing, they had a lower root mean square error when rectifying the dune image with the doqqs.

4.6 Calculating Dune Change and Shapefiles

The change detection image and survey images were imported into ArcMAP 9.0 for spatial analysis. Polygon shapefiles were created outlining the dune forms from the change detection image to calculate the areas of individual dunes in 1996 and 2004. The polygon “dune” areas were calculated using X-Tools Pro extension for ArcGIS (www.xtoolspro.com). General dune area and feature area could only be calculated from doqqs due to the lack of elevation data contained within the data.

A variety of methods have been employed to measure dune migration rates (Inman, et al, 1966; Story, 1982; Pye, 1982; David, et al, 1999; Wolfe and Lemmen, 1999; Hugenholtz and Wolfe, 2005). Dune migration rates were calculated for this project using the “linear fit method” as described by Bailey and Bristow (2004) to determine a net dune migration. The parabolics were also measured by the right angle distance of the farthest extent of the dune from its GPS recorded bench mark in the east portion of the deflation basin to determine a maximum dune

migration. The deflation basin bench marks were present in the active dunes in both sets of images for dunes 2 and 3 (dune 1 activity began post 1996) and represent points from where dune migration can be quantified relative to a specific point.

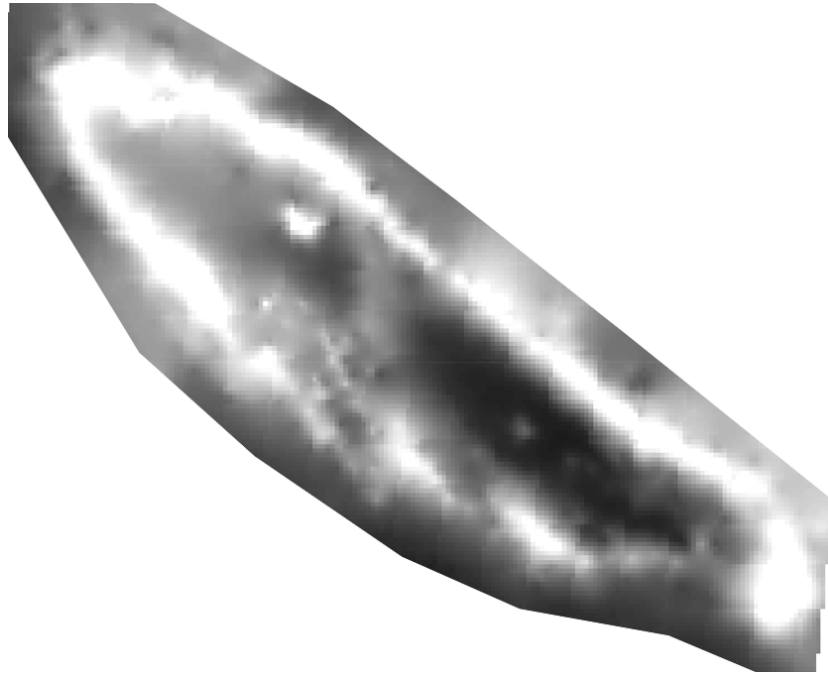


Figure 4.2 Example of rasterized dune survey data, dune C, 2007. The image is color ramped, brighter color indicates higher elevation

The linear trend method (Bailey and Bristow, 2004) involves using GIS and spreadsheet analysis of migration for the mean center point of a dune. The trend line is representative of the mean center point of the dune, from the farthest extent of the depositional lobe to the rear edge of the trailing ridges (Bailey and Bristow, 2004). Polylines were created in ArcMAP 9.0 outlining the extent of the depositional lobe of each dune during the surveys and from the doqqs (Bailey and Bristow, 2004). The polylines were converted to x, y point data in the ArcMAP and downloaded into Excel, where the point data was then used to create a linear trend line for each of the dunes (Bailey and Bristow, 2004). The linear trend method also allows for allows for an accurate measure of the change in dune orientation (Bailey and Bristow, 2004). The rectified

survey images were used when creating polylines for linear trend lines analysis, due to georeferencing the images with GPS points to accurately display the dunes.

4.7 Wind and Sand Roses

Wind and sand roses were created to present a graphic display of the main geomorphic factor that influences and contributes to parabolic dune development and formation. The wind roses were created using the program WRPLOT by Lakes Environmental (<http://www.weblakes.com/lakewrpl.html>). The wind data was organized in Excel with columns listing: year, month, day, hour, wind direction and wind speed. The Excel wind data was then imported into WRPLOT and where wind rose production was completed. The sand roses were created using the modified Fryberger and Dean method (1979), developed by Pearce and Walker (2005).

4.7.1 Wind and Sand Rose Data

The first data set of wind data were daily measurements collected from the Padre Island National Seashore (PAIS) ranger station. The data spans from 1 January 1968 to 20 February 2007 and was acquired from the climate station at PAIS, recorded at 10 meters elevation. The wind data was provided in Microsoft Access and imported into Microsoft Excel for data reorganization, classification and sorting. The PAIS data was recorded in sixteen primary compass directions and the compass directions were converted into corresponding degree measurements for wind and sand rose calculations (Pearce and Walker, 2005). The wind data was then reorganized and sorted to remove missing or erroneous data (i.e.: wind speeds > 430 mph), resulting in the removal of 863 days of data or 6% of the available PAIS wind data. This sorted wind data was then used for wind and sand rose calculations.

The PAIS wind roses were created using the sorted data and organized into seasonal classifications, as defined by the American Meteorological Society (AMS homepage, <http://www.ametsoc.org/>) and a total wind regime classification.

Wind data collected at Corpus Christi International Airport (CCIA) was also used to create wind and sand roses. The CCIA wind data is hourly data ranging from 1 January 1980 to 9 May 2006 recorded at 10 meters and downloaded from the National Climatic Data Center (<http://www.ncdc.noaa.gov/oa/ncdc.html>). The CCIA data was downloaded in the unedited format with measurements recorded at every ten degrees. There were 1552 missing or incomplete hours of wind data or 0.7% of the data set that was eliminated for wind and sand rose calculations. The unedited degree data was useful for wind rose calculations in WRPLOT, but potentially problematic for sand rose calculation. The CCIA data was then converted to sixteen primary compass directions using unbiased midpoint values (Pearce and Walker, 2005) for ease in sand rose calculations. The CCIA data was also classified according to the AMS seasonal definitions for sand and wind rose calculations.

Wind data was collected from two Texas Coastal Ocean Observation Network (TCOON) weather stations, located at Bob Hall Pier (BHP) on Padre Island and at South Bird Island (SBI) in Laguna Madre. The SBI station is located west of the North Padre Island barrier on a platform in the Laguna Madre Bay. These TCOON stations are maintained by Texas A&M University, Corpus Christi or TAMUCC and their Division of Nearshore Research, BHP location is also maintained as a NOAA NOS (National Ocean Station) station. The wind data collected from these stations were recorded as hourly data as determined from an eight minute average of wind speeds. Data from BHP spans from 1 January 1996 to 20 March 2007 recorded at 10m. The wind record at SBI spans from 1 January 1994 to 20 March 2007 and recorded at 10m. Both

TCOON data sets were downloaded from <http://lighthouse.tamucc.edu/TCOON/HomePage> in edited format allowing for ease in data organization and frequency calculations.

Table 4.1 Wind classes and compass directions, with corresponding degree measurements, used for calculating wind and sand roses modified from Pearce and Walker (2005).

Wind classes (m s^{-1})	Direction (compass)	Direction (degrees)
	N	0
WC 1, 0 to ≤ 3	NNE	22.5
WC 2, > 3 to ≤ 5.6	NE	45
WC 3, > 5.6 to ≤ 7	ENE	67.5
WC 4, > 7 to ≤ 8.7	E	90
WC 5, > 8.7 to ≤ 11.3	ESE	112.5
WC 6, > 11.3 to ≤ 14.3	SE	135
WC 7, > 14.3 to ≤ 17.4	SSE	157.5
WC 8, > 17.4 to ≤ 35	S	180
WC 9, > 35 to ≤ 50	SSW	202.5
WC 10, > 50	SW	225
	WSW	247.5
	W	270
	WNW	292.5
	NW	315
	NNW	337.5

4.7.2 Frequency Tables

Two-way frequency tables were created consisting of row (wind directions) and column (wind classes) classes that represent the occurrence of each possible (x, y) combination that occurs in the data set (Devore and Peck, 2001). The frequency tables were created using the edited wind data from PAIS, CCIA, BHP, and SBI. The data sets were organized with respect to sixteen compass directions and nine wind classes to present a reasonable distribution of wind speeds for calculating wind roses, sand roses and drift potentials (Pearce and Walker, 2005). The frequency table wind classes provide a representation of the wind velocities and regimes that are

responsible for potential sediment movement. The wind frequency tables were used to calculate sand roses and drift potentials. Fryberger (1979) does not define specific guidelines for establishing wind classes to calculate sand roses and drift potentials (DP) however for this work the presented wind classes were modified from the classes presented by Pearce and Walker (2005).

4.7.3 Sand Roses and Sediment Drift Potentials

The Fryberger and Dean method (1979) allows for a visual representation of potential sediment drift for a given wind regime. The sand roses were produced using the Fryberger and Dean method (1979) are, “circular histograms which represent potential sand drift from the 16 directions of the compass” (Fryberger, 1979). A sand rose has sixteen arms indicative of potential sand drift for each compass direction that are displayed in vector units (VU).

In order to determine the vector unit length, the prevalent sand drift direction and sediment drift potential, specific calculations must be performed. The Fryberger and Dean method (1979) provides the appropriate methodology for calculating sediment drift potentials, drift direction and vector units. The Fryberger and Dean equation (Eq. 3) is listed below:

$$Q = V^2(V - V_t) * t \quad \text{Eq. 3}$$

The Fryberger and Dean (1979) equation is a synthesis of previous threshold wind velocity equations and sediment measurements. The equation can be defined as:

Q = *annual sand drift rate,*

$V^2 (V - V_t)$ = *weighting factor of sediment,*

t = *time of constant winds, expressed as a percentage.*

The weighting factor can be defined as:

V = wind velocity at 10 meters,

V_t = impact threshold wind velocity at 10 meters (as the minimum velocity to keep sand in saltation)

Bagnold's equation (1941) defines the impact threshold wind velocity at 10 meters as:

$$V_t = 5.75 V^* t \log \frac{z}{z'} + V't. \quad \text{Eq. 4}$$

$$V^* t = A \left(\left(\sqrt{\frac{\rho_s - \rho_a}{\rho_a}} \right) * g d \right). \quad \text{Eq. 5}$$

Where A = constant for grain size larger than 0.25mm, or 0.1 (c Bagnold, 1941),

ρ_s = grain size density or 2650 kg/m³ for quartz sand,

ρ_a = air density or 1.2 kg/m³,

g = velocity of gravity or 9.8 m/s,

d = grain size diameter in meters or 0.00014 for Padre Island.

For the sediment grains on Padre Island $V^* t = 0.17259$ (this value is multiplied by 100 for calculation and display purposes).

$\frac{z}{z'} = 1000/d_{mm}$ according to Belly (1964), or $1000/0.14 = 7142.85$,

$\log \frac{z}{z'} = 3.853$ for Padre Island sediment grains.

$V't = 894*d_{mm}$ or $894*0.14$, which is the cm/s conversion of the measurement values initially proposed as miles per hour by Belly (1964); $V't = 125.16$ for Padre Island sediments. Therefore, for Padre Island sediments $Vt = 5.75 * 17.259 * 3.853 + 125.16$ or 507.416. The value 507.416 is then divided by 100 to reduce weighting factors to smaller values for ease in plotting wind roses (Fryberger, 1979).

Midpoint wind class values were used to calculate V for weighting factors (Pearce and Walker, 2005). Since all wind data was recorded and presented in m s^{-1} format all vector units (VU) calculated from weighting factors are also in m s^{-1} and used for wind energy environment classification (Bullard, 1997). The Fryberger and Dean Method (1979) also introduces three indexes to quantify the “direction and magnitude” of the vector units (Fryberger and Dean, 1979). The resultant drift direction (RDD) refers to the net trend in sediment movement from combined wind directions (Fryberger and Dean, 1979). The resultant drift potential (RDP) refers to the vector unit expression of the RDD, also RDP/DP is the directional variability of winds at a location (Fryberger and Dean, 1979). The weighting factors for the nine wind classes used in classification of Padre Island wind data are listed below.

Table 4.2 Calculation table of weighting factors for Padre Island sediment and wind classes modified from Fryberger and Dean (1979).

Wind classes (m/s)	V	Vsq	V-Vt	Vsq(V-Vt)/100
0 to ≤ 3	1.5	2.25	-3.57	-0.08
>3 to ≤ 5.6	4.3	18.49	-0.77	-0.14
>5.6 to ≤ 7	6.3	39.69	1.23	0.49
>7 to ≤ 8.7	7.85	61.62	2.78	1.71
>8.7 to ≤ 11.3	10	100.00	4.93	4.93
>11.3 to ≤ 14.3	12.8	163.84	7.73	12.66
>14.3 to ≤ 17.4	15.85	251.22	10.78	27.07
>17.4 to ≤ 35	26.2	686.44	21.13	145.02
>35 to ≤ 50	42.5	1806.25	37.43	676.00

5. Parabolic Dune Geomorphic Maps and Dune Profile Change

5.1 Introduction

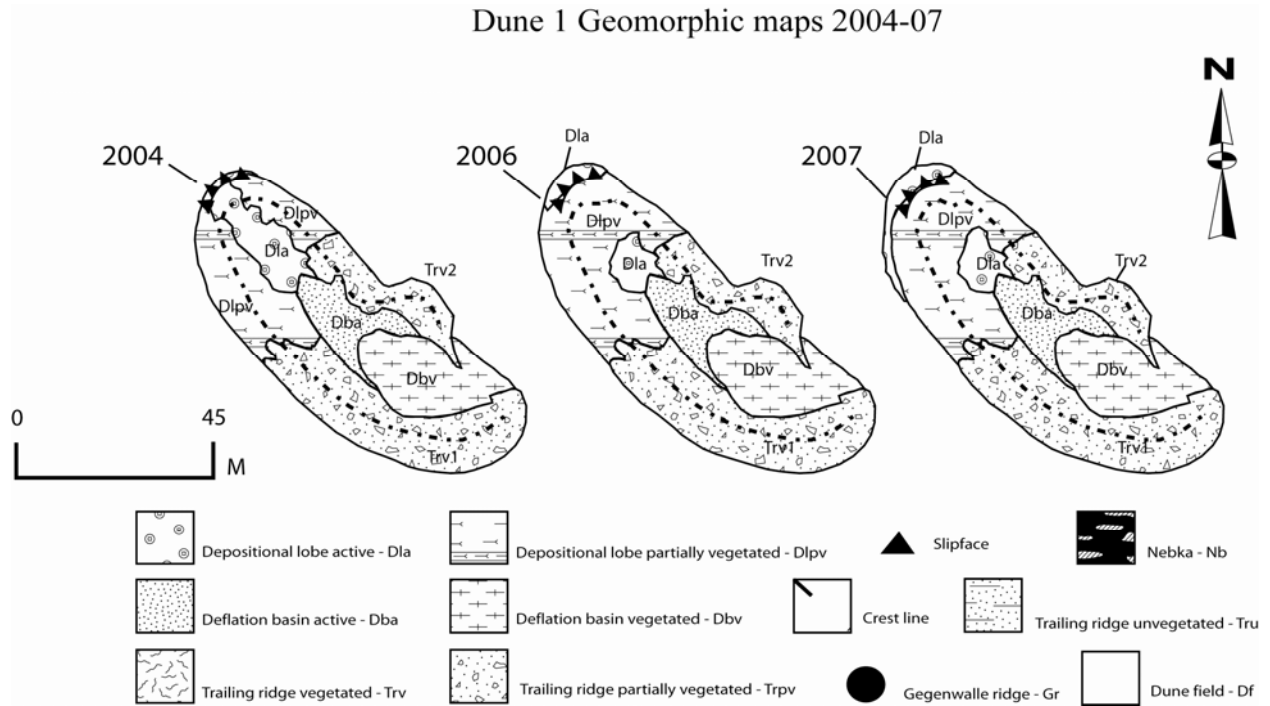
Dune profiles and geomorphic maps are presented for each parabolic dune based on doqq, total station surveys and GIS analysis. Doqqs were utilized to create geomorphic maps for each of the dunes, and to determine dune change from 1996 - 2004. Dune 1 development was initiated after the first doqqs were flown in 1996, therefore only one geomorphic map was created for this dune from doqqs and two geomorphic maps were created from survey rasters; while both dunes 2 and 3 have geomorphic maps created from 1996 and 2004 doqqs, and accompanying geomorphic maps created from survey rasters.

5.2 Geomorphic Maps and Individual Dune Change

Five geomorphic maps were produced from doqq analysis, which provides a visual representation of individual parabolic dune landform units from 1996 to 2004. Six geomorphic maps were produced from dune surveys and their accompanying raster images. As previously stated parabolic dune 1 development was post-1996, and the geomorphic maps provide insight into the individual parabolic dune development over the eight year period of doqq record and the six month period between surveys concluding in February 2007.

Parabolic dune 1 is an incipient parabolic dune with an active slipface or “Stage 2 parabolic dune,” as determined from the summer 2006 and 2007 surveys, according to the Pye (1982) model. Parabolic dune 1 was classified as a blowout dune from 2004 doqq analysis, as trailing ridge identification is difficult, and landform units are not prominent. As seen in Figure 5.1, dune 1 is unique compared to the two other dunes (Fig. 5.2, Fig. 5.3) in regards to having significant vegetation density on the depositional lobe. The trailing ridges are well defined and

identifiable in the 2006 and 2007 surveys. The north and south trailing ridges are both partially vegetated and, as seen from the profile data (Fig 5.7), are active and widening. The deflation basin is also divided into a vegetated portion and an active portion. The active portion of the deflation basin is depositing sediment onto the active depositional lobe and into some portions of the vegetated depositional lobe.



Parabolic dune 2 developed from a small parabolic dune with an active slipface, partially vegetated trailing ridges, an active deflation basin and an active depositional lobe. In 1996 parabolic dune 2 could be classified as a “Stage 1” (blowout) or possibly “Stage 2” parabolic dune according to the Pye (1982) parabolic dune classification, due to the difficulty in determining discernable trailing ridges. Parabolic dune development in the eight year period between doqq acquisitions, dune 2 evolved into a mature elongate parabolic dune. According to the Pye (1982) parabolic dune classification the 2004 dune 2 form would be considered a “Stage

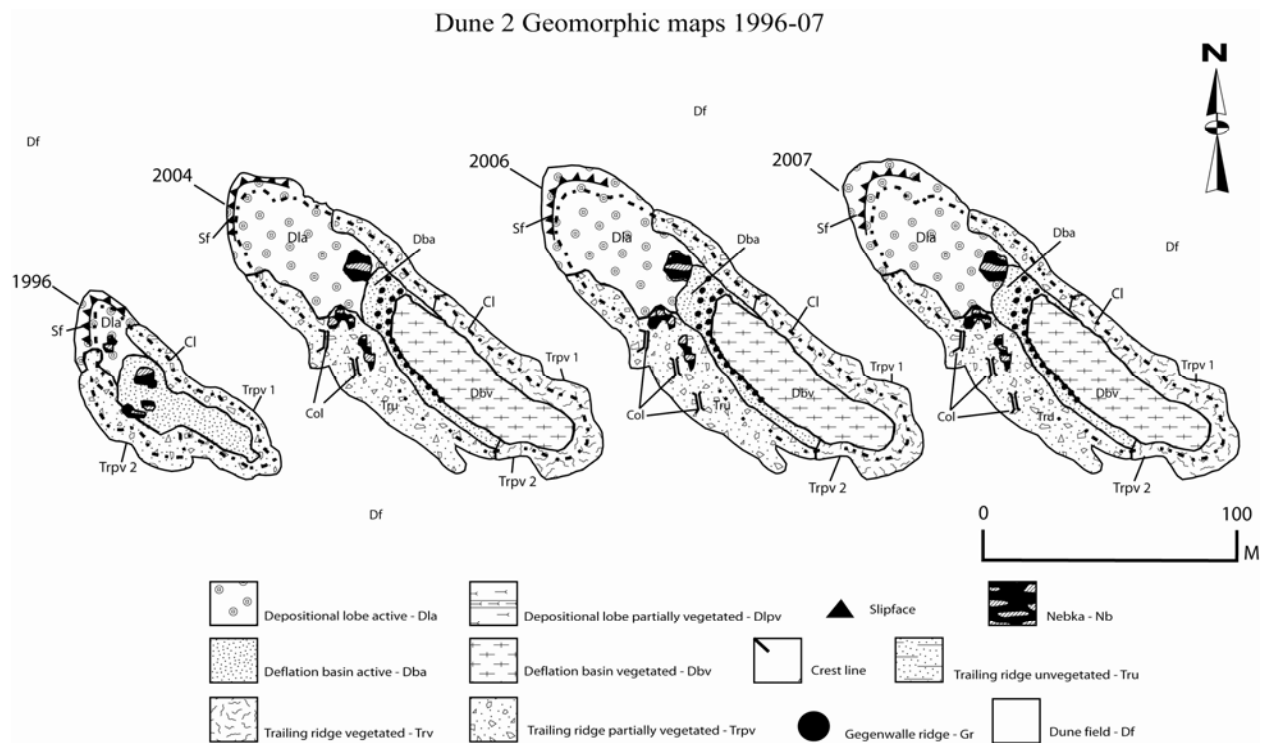
3” parabolic dune. By 2004, parabolic dune 2 had developed a gegenwalle ridge that formed a boundary around the low and vegetated deflation basin, two different and distinct trailing ridges, and the depositional lobe is marked by the presence of one very large nebka near the north trailing ridge. Dune migration distance and rate is noted in Table 5.1 and 5.2. and these rapid rates of migration may be helpful in explaining dune evolution.

The southern trailing ridge of dune 2 is currently active as indicated from the summer and winter survey data. Judging from doqq analysis and current observations of dune morphology the southern trailing ridge of this dune has been active since at least 2004. Survey data also indicated the depositional lobe and slipface of dune 2 is currently active and migrating towards the NW. Based on field observation, GPS data and survey data the vegetated portion of the deflation basin has been relatively stable between surveys and has experienced little change in extent since 2004 doqq acquisition. During rain events, the vegetated portion of deflation basin holds water forming a small “lake” and this store of water is conducive for vegetation growth and development. The nebka that is present in the 2004 doqq of dune 2 reveals the presence of three separate nebka present within the active depositional lobe. The largest of these three nebka is currently present within the depositional lobe. The two smaller nebka located near the south trailing ridge are currently experiencing erosion and are deflating, sediments from these small nebka were observed being transported towards the south trailing ridge during field work.

The southern partially vegetated trailing ridge or Trpv 2 in Figure 5.9 has experienced a decrease in vegetation density from the summer to the winter survey. The Trpv 2 has potentially been experiencing a decrease in vegetation for some time, but due to the absence of more extensive survey data or doqq records it is unknown. The vegetated portion of the north trailing

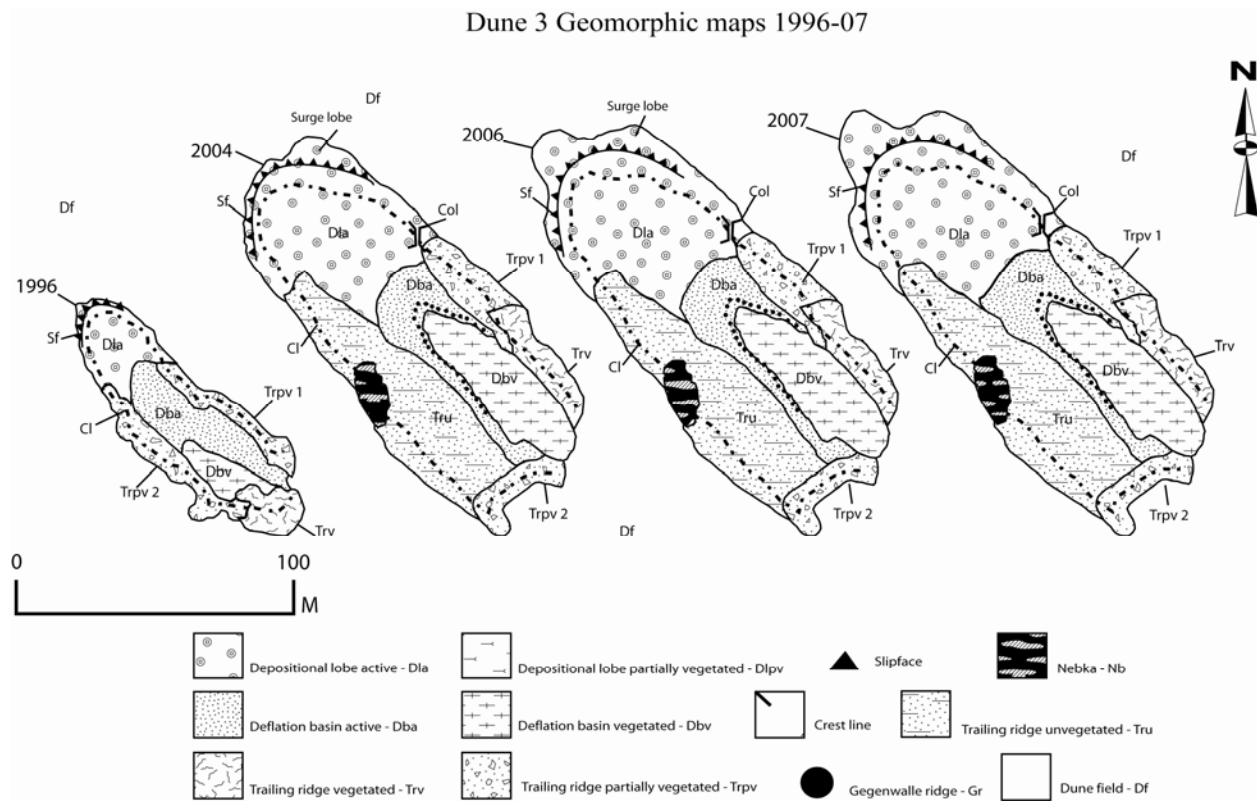
ridge or Trpv 1 in Figure 5.9 has developed from the partially vegetated north trailing ridge or Trpv 1, in 1996.

The north trailing ridge of parabolic dune 2 is continuous in both 1996 and 2004. The north trailing ridge also has migrated along the same relative axis from 1996 to 2007 and the last recorded survey. The closed eastern extent of parabolic dune 2 has expanded and widened since 1996. Although no discernable change was recognized between the summer and winter surveys of dune 2 across the dune throat, doq analysis indicates expansion of this feature.



Parabolic dune 3 has experience the greatest amount of dune landform unit change and migration since 1996. In 1996, parabolic dune 3 could be classified as a “Stage 3” parabolic dune, or a mature elongate parabolic dune according to the Pye (1982) parabolic dune classification. Currently parabolic dune 3 could be classified as a “Stage 4” or “Stage 5” parabolic dune according to Pye (1982), due to its characteristic diverging arms, however dune 3

is experiencing a decrease in depositional lobe elevation as evidenced from survey data. The most noticeable change in dune landform unit for parabolic dune 3 is the expansion and migration of the south trailing ridge. In 1996, the south trailing ridge or Trpv 2 has evolved into the large, unvegetated, and active south trailing ridge or Tru 1 in 2004. The feature Tru 1 was active and unvegetated during both the summer and winter surveys, and this feature has experienced widening and a slight decrease in elevation as evidenced from survey data. A surge lobe was present on dune 3 during 2004 doqq acquisition, and this same feature was present during the summer 2006 survey. However, the surge lobe was approximately 80-90% vegetated at the time of the winter 2007 survey, and was not an active feature of the dune.



A gegenwalle ridge has also developed surrounding the vegetated portion of the deflation basin, similar in location to the gegenwalle ridge in dune 2. Although not observed, it

is hypothesized that standing water is present during periods of heavy precipitation, due to the presence of the gegenwalle ridge and the marsh vegetation present within the deflation basin. The throat of dune 3 has remained open since 1996, but has increased in width during that time. Adjacent to the dune throat, just south of the entrance the vegetated trailing ridge or Trv 1 in 1996 has evolved into a partially vegetated trailing or Trpv 2 that is the location of highest point within the dune. It is from this location where the majority of the survey was conducted.

5.3 Parabolic Dune Profile Change

Parabolic dune profiles were measured across four transects of each dune: the dune length mid-line, the depositional lobe, dune width mid-line, and across the dune throat. The survey data was imported into Surfer 8 to create a digital elevation model or DEM, and that DEM was rasterized in Erdas IMAGINE 9.1. The rasterized survey image created in Erdas IMAGINE 9.1 was imported into ArcMap 9.0 for data analysis and profile measurement. Dune profiles were measured using the profile graph tool on the 3D Analyst tool extension in ArcMap. The dune transects were measured from the north edge of each dune towards the south west edge of each dune. The length wise transect of each dune was measured from the depositional lobe towards the dune throat. The transect profiles provide a visual representation of dune change across a narrow portion of the dune. The width transects of each dune display the influence of northerly winds over the survey periods.

5.3.1 Parabolic Dune 1 Transect Profiles

The parabolic dune 1 profiles display the influence of the northerly and south easterly winds between survey periods. Transect 1 or the long axis transect indicates a NW dune migration and a decrease in elevation on the depositional lobe between surveys. The NW

migration is to be expected, as indicated from sand rose data and the decrease in depositional lobe elevation is directly related to sediment transport from the depositional lobe to the edge of the migrating slipface.

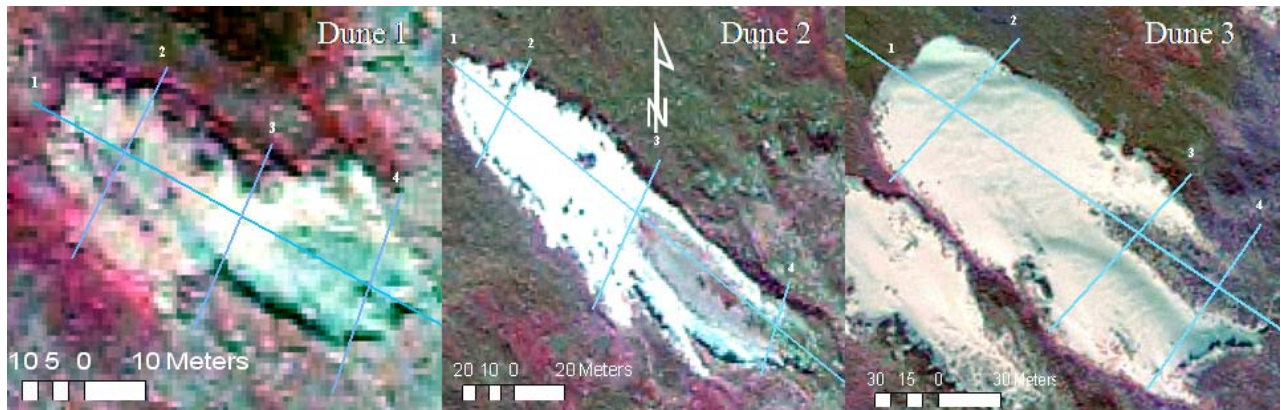


Figure 5.4 Individual dune transect locations.

The profile of transect 2 displays a decrease in elevation interior to the dune crest on the north aspect of the depositional lobe. This decrease in elevation near the north crest line is due to the influence of sediment transporting winds from the onshore direction. The crest line along the depositional lobe is vegetated on both the north and south aspects, and the stabilizing characteristics of vegetation, specifically the binding effects of plant roots has prevented or minimized change on the crest of the depositional lobe. However, the area where the decrease in elevation occurred is unvegetated and the binding properties of plant roots cannot prevent sediment transport.

Dune 1 profiles

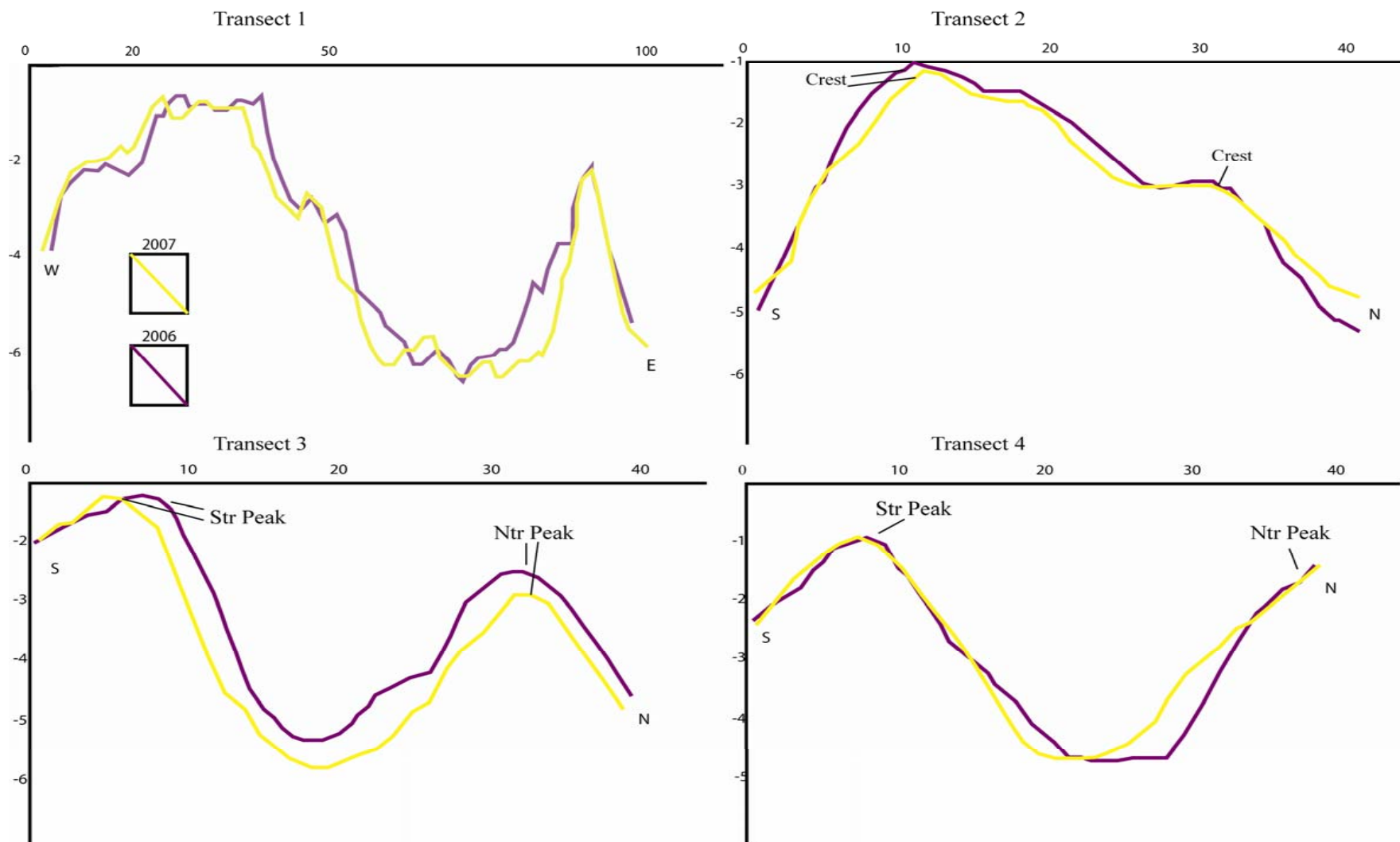


Figure 5.5 Parabolic dune 1 transect profiles taken from June 2006 and January 2007 dune surveys. Transect 1, mid-line of the long axis; transect 2, width of depositional lobe; transect 3, width of mid-line; transect 4, width of dune throat.

Parabolic dune 1 transects 3 and 4 both display similar profile changes between surveys. The internal slope of the north trailing ridge in transect 3 displays a slight decrease in slope angle from summer to winter surveys. The decrease in slope along the internal wall of the north trailing ridge is due to sediment transport from the crest line of the north trailing ridge onto the dune basin or dune floor. The transect 3 profile also indicates that dune 1 is experiencing a widening of the deflation basin, indicating sediment transport within the parabolic dune. The internal walls of the north and south trailing ridge were partially vegetated, providing enough unvegetated and open surface area for sediment transport to occur. Due to the available surface area for sediment transport to occur widening of the internal dune is not surprising. The transect 4 profile indicates that deposition has occurred on the internal wall of the south trailing ridge. The sharp angle at the base of the internal wall of the north trailing ridge and the deflation basin is indicative of error in profile generation as is the extreme decrease in elevation along the crest of the north trailing ridge. However, the general profiles of transect 4 are very similar and are valid for analysis of profile change.

5.3.2 Parabolic Dune 2 Transect Profiles

Transect profiles for parabolic dune 2 display the influence of both onshore and northerly winds. The long axis transect or transect 1 display some very noticeable changes that occurred between surveys. There is a decrease in the slope of the depositional lobe slipface that has occurred between surveys and a slight westerly migration of parabolic dune 2. The most noticeable differences between transect 1 surveys is the decrease in elevation of the second peak of the profile and the decrease in slope angle from the crest line of the depositional lobe towards the second peak of the parabolic dune profile. The decrease in elevation of the second peak that

is evident in the winter survey is evidence of erosion to the nebka on the depositional lobe, and of sediment transport across the depositional lobe and towards the slipface and crest line. The second peak in the dune transect, spans across the base of the nebka on the depositional lobe. The depositional lobe of parabolic dune 2 and the base of the nebka are almost entirely unvegetated and the lack of vegetation cover and open surface area are ideal conditions for sediment transport to occur.

The third peak in transect 1 profile is the gegenwalle ridge and to the right of that peak is the depositional lobe. The outline of the gegenwalle ridge is similar in both surveys and little change has occurred on this feature over this period. The differences in the profile of the deflation basin are due to differences in survey methods used in the winter compared to the summer survey. In the February 2007 survey, the majority of the deflation basin was filled with water, between the depths of three to ten inches. The water extent, depth, and weather conditions prevented the survey team from recording as many points along the dune transect.

The fourth, fifth, and six peaks of transect 1 profile display vegetated mounds within the dune. The fourth peak is the eastern edge of the deflation basin indicating the difference between the lowest area of the deflation basin and the surrounding basin. The fifth peak is small mound at the base of the closed end of the dune throat. The sixth peak is the dune crest along the closed edge of the dune throat, and where the north and south trailing ridges merge. The steep slope between the fifth and sixth profile peaks is a densely vegetated area and a location where onshore winds enter the dune.

Transect 2 was measured across the depositional lobe from north towards the south. The second profile displays change from the crest line on the north edge of the depositional lobe across to the external slope of the southern slipface. The summer profile displays one north peak

Dune 2 profiles

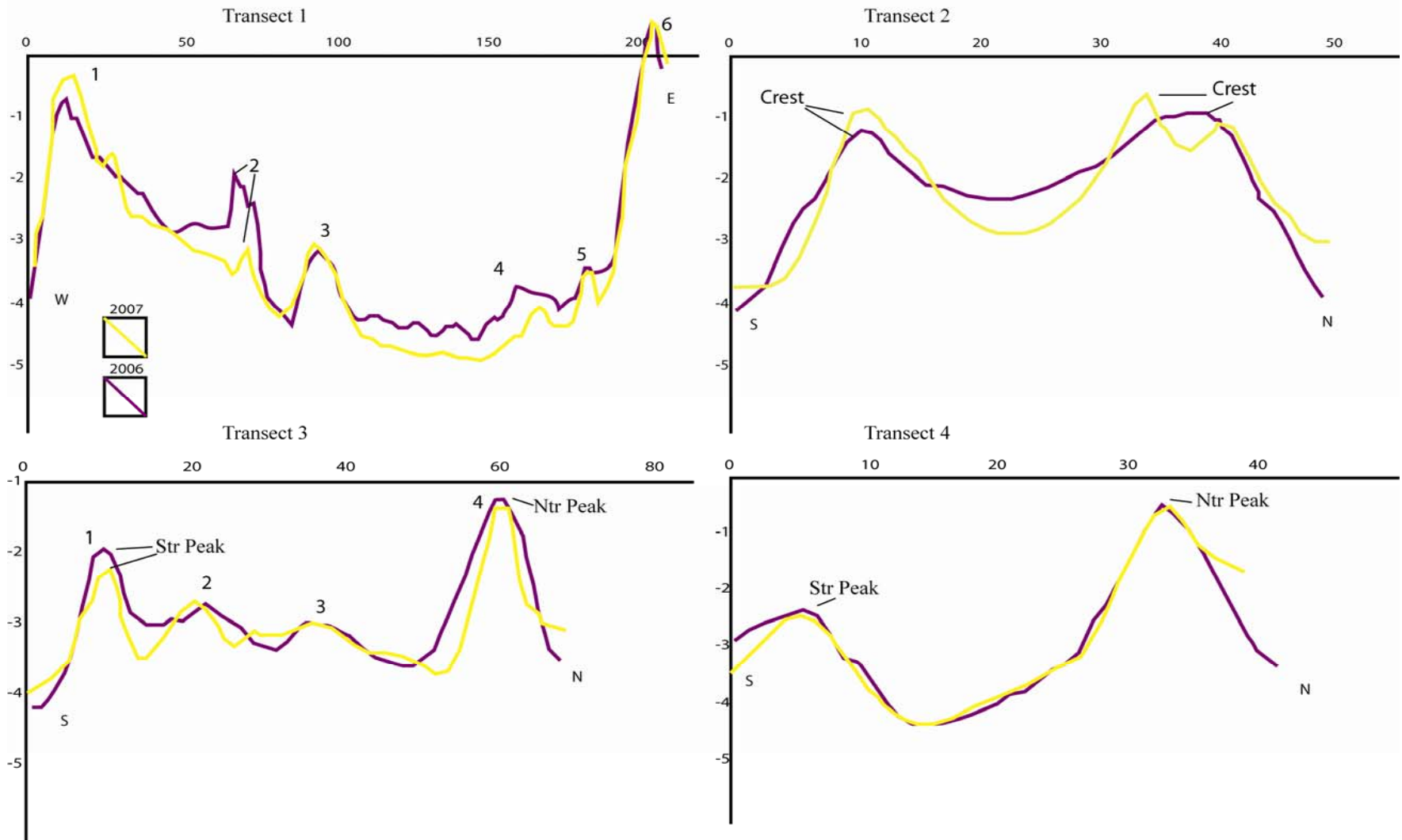


Figure 5.6 Parabolic dune 2 transect profiles taken from June 2006 and February 2007 dune surveys. Transect 1, mid-line of the long axis; transect 2, width of depositional lobe; transect 3, width of mid-line; transect 4, width of dune throat.

a regular slope across the internal depositional lobe and a regular slope up towards the south peak. The winter profile displays noticeable change to both the north and south peaks, and the internal depositional lobe, as compared to the summer survey. The northern peak from the summer survey has eroded and developed into two peaks at the time of the winter survey. The change in this north peak from summer to winter surveys is due to the influence of the northerly winds in an area with low vegetation density, and sediment deposition in adjacent vegetation on the depositional lobe. The internal depositional lobe for the winter survey has decreased in elevation since the summer survey, indicating sediment transport out of the depositional lobe or erosion to this feature of the dune. The southern peak of the depositional lobe is noticeably narrower and steeper for the winter survey compared to the summer survey; also the external slope of the southern peak is steeper and has experienced a slight slipface avalanche.

Transect 3 dune profiles were taken width length across the mid-line of the parabolic dune 2. The north peak for both, the summer and winter surveys, exhibit very little change between survey periods. There are two peaks along this profile that lie within the deflation basin. The northern of the two internal peaks is a mound on gegenwalle ridge that bounds the vegetated portion of the deflation basin. The winter profile indicates that this mound has widened and decreased in elevation compared to the summer survey profile. The third peak is a nebka near the south trailing ridge. This nebka was present during the summer survey, but has increased in width and height, while it has accreted from the summer survey to winter survey. The sediment transporting winds that have helped to build this nebka are both from northerly and onshore directions. The fourth peak on this profile is the southern trailing ridge. The southern trailing ridge lower in elevation compared to the northern trailing ridge, and has experienced minimal change between summer and winter surveys. The only noticeable change between

surveys was erosion along the internal base of the southern trailing ridge, likely caused by onshore winds.

Transect 4 for dune 2 was taken across the densely vegetated dune throat, near the convergence of the trailing ridges. The summer and winter transect profiles display no discernable change between surveys. The absence of profile change is due to dense vegetation cover inhibiting sediment movement and the lack of a nearby active sediment source.

5.3.3 Parabolic Dune 3 Transect Profiles

The transect profiles for dune 3 display the influence of onshore winds and northerly winds between summer and winter surveys. The transect profiles that displays the most change between surveys are the long axis or transect one profiles. The long axis transect from the summer survey characterized by four peaks: the depositional lobe, the western edge of the gegenwalle ridge, a mound in the vegetated deflation basin, and the base of the southern trailing ridge. The most apparent change in the profile between the summer and winter surveys is the change in slope and width of the depositional lobe between surveys. As seen in the transect one profile, the depositional lobe in the summer survey is wider across the dune crest compared to the winter survey and has a steeper slipface slope towards the leading dune edge. Also a small slipface is noticeable west of the crest on the depositional lobe. In the winter survey the depositional lobe has decreased in crest width, while the overall width of the depositional lobe has increased. The increase in depositional lobe base width is an indication of slipface avalanche, sediment transport towards the leading edge, and forward dune migration. Since the

Dune 3 profiles

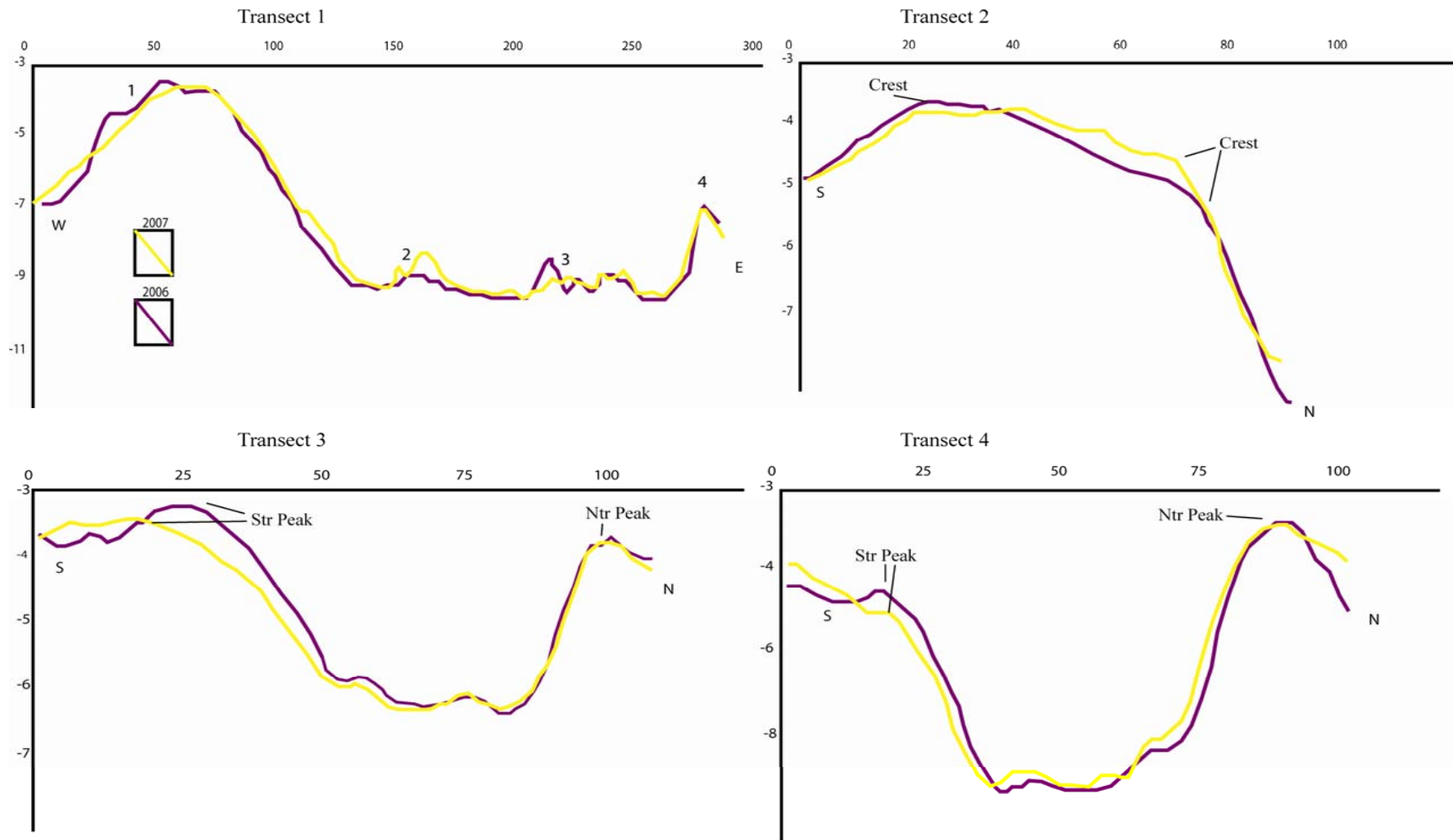


Figure 5.7 Parabolic dune 3 transect profiles taken from June 2006 and January 2007 dune surveys. Transect 1, mid-line of the long axis; transect 2, width of depositional lobe; transect 3, width of mid-line; transect 4, width of dune throat.

depositional lobe of dune 3 is completely unvegetated these changes are to be expected between surveys especially given the wind regime and resultant drift direction during that time.

The second peak along transect 1 is the gegenwalle ridge that outlines the extent of the vegetated deflation basin. There has been some deposition and an increase in elevation for this part of the gegenwalle ridge from the summer to winter survey due to sediments transported by multi-directional winds within dune 3. The third peak, or the cluster of small peaks, are closely spaced vegetated mounds within the vegetated section of the deflation basin. The differences in these peaks are assumed to be due to slight inconsistencies in surveying. During the winter survey more data points were recorded within the deflation basin, therefore providing a more detailed representation of geomorphic features. The summer survey, while accurate, did not record as many points within the deflation basin and for some features only base and apex points were recorded. Therefore it is difficult to determine what, if any, change occurred with these features. The fourth peak is the edge of the southern trailing ridge adjacent to the dune throat. There has been only slight change to this part of the southern trailing ridge and can barely be discerned from the transect profile.

Transect 2 profile was taken from south to north across the depositional lobe of dune 3. A regular and gentle slope can be seen from both the summer and winter survey profiles across the crest of the depositional lobe. The most noticeable change from the summer to winter survey is the overall decrease in elevation in the winter profile. However, two small peaks are present during the winter survey that are absent during the summer survey. These small peaks are two areas of slightly stabilized sediments around which sediment has been recently eroded. They are otherwise simple variations in elevation along the depositional lobe crest line.

Transect 3 was measured from south to north across the width of the dune mid-line, east of the nebka on the south trailing ridge. The first peak of this profile is the unvegetated and active portion of the south trailing ridge. The south trailing ridge crest line has widened between surveys and has also decreased in elevation since the summer. The onshore and northerly winds are largely responsible for the decrease in the south trailing ridge elevation and the widening of this feature. The northerly winds are largely responsible for transporting sediment from the crest line to the external slope. However, sediment bedforms observed during both the summer and winter surveys indicate sediment transport towards the NW in the general direction of dune migration. This sediment activity and transportation can be expected from wind rose data and due to the lack of vegetation along the south trailing ridge.

The second and third peaks in this set of profiles indicate the gegenwalle ridge outlining the southern and northern edge of the vegetated deflation basin. There is a slight change between the summer and winter survey, but judging from the profile shape, the differences may be due to recorded survey points. The fourth peak of these profiles is the north trailing ridge, which is vegetated along the external wall, crest line, and the top section of the internal wall. The base of the north trailing ridge along this transect is unvegetated and active sediment, and therefore susceptible to erosion and transport. There is a slight but noticeable widening at the base of the north trailing ridge between the wall and the adjacent gegenwalle ridge (third peak). This widening indicates erosion along the base of the internal north trailing ridge and can be anticipated due to the lack of stabilizing vegetation surrounding this area.

Transect 4 spans across the width of the dune, north to south, near the throat of the dune but west of the dune apex and survey area. The peaks along the fourth transect outline the same dune landform units as the third transect. Again, the dune landform units that displays the most

change between surveys is the south trailing ridge. Similar to the third transect the south trailing ridge crest line elevation has decreased, but sediments have deposited along the base of the vegetated “dogleg” portion of the south trailing ridge.

6. Measurements of Parabolic Dune Change and Migration

6.1 Introduction

Dune change measurements are presented for the three parabolic dunes analyzed for this research. Dune migration rates and GIS shapefiles measuring the extent of dune change are presented for each parabolic dune based on doqq, total station surveys and GIS analysis. The margin of error on all migration rate measurements has been estimated to be between 0.5 – 1.5 meters, as determined from doqq and survey raster images. The parabolic dune shapefiles, after area calculations were performed, were imported into Adobe Illustrator CS3 for schematic production and illustration.

6.2 Parabolic Dune Migration Rates

Parabolic dune migration rates vary for the three dunes according to the net trend method and the midline end point method. The net trend method measures the migration of the entire parabolic dune by determining the midpoint of the dune and measuring the migration of that point compared to the midpoint of the dune over time (Bailey and Bristow, 2004). The midline end point method has been used in many parabolic dune studies and is a simple method to measure the migration of the depositional lobe or other migrating dune landform units (Pye, 1982; Inman et al. 1966). The migration rates for dunes 1, 2, and 3 vary according to dune measurement method and dune size. The net trend method reveals that dune 3 has the highest migration rate for each measurement period, which corresponds with dune 3 having experienced the greatest change in area since 1996. The midline end point method reveals that dune 2 experienced the greatest migration distance of the three dunes during a measurement period, migrating 107.1 m from 1996 to 2004.

The migration measurements indicate a correlation between dune size and migration rate. Dune 3 also has the lowest density of vegetation cover of the three dunes and the most active depositional lobe and trailing ridges. The midline end point migration rates for dunes 2 and 3 correspond closely with the inland parabolic dunes studied by Marin et al. (2005) in southern Colorado and with the coastal dunes studied by Anthonsen et al. (1996) in Denmark (see Table 2.2). The midline end point migration rates for dune 1 correspond to migration rates for coastal parabolic dunes measured by Bailey and Bristow (2004), Arens et al. (2004) in the UK and Denmark, respectively, and inland parabolic dunes studied by Hugenholtz and Wolfe (2005) and David et al. (1999) in southern Saskatchewan.

Table 6.1 Dune migration table for dunes 1, 2, and 3 from 1996-2/11/2007. Note that Dune 3 experienced the greatest net trend migration average and the highest annual migration rate over a measurement period. Dune 2 experienced the farthest midline end point migration distance over any measurement period (1996-2004).

Parabolic Dune Migration Rates 1996 - 2/11/2007				
Dune 1 Migration Rates**				
Year	Net trend midpoint		Midline end point	
2004	672507, 3045327		672470, 3045343	
2006	672504, 3045329		672468, 3045345	
2007	672503, 3045328		672466, 3045345	
Migration	Meters	M/yr	Meters	M/yr
2004-06	3.4	1.7	3.4	1.7
2006-07*	1.3	2.6	1.3	2.6
Net	4.7	1.6	4.7	1.6
Dune 2 Migration Rates				
Year	Net trend midpoint		Midline end point	
1996	666881, 3031213		666858, 3031251	
2004	666831, 3031243		666764, 3031303	
2006	666830, 3031249		666763, 3031306	
2007	666828, 3031248		666763, 3031310	
Migration	Meters	M/yr	Meters	M/yr
1996-04	58.7	7.3	107.1	13.4
2004-06	6.1	3.1	3.6	1.8
2006-07*	2.4	4.8	4.3	8.6
Net	67.2	6.1	115.0	10.5

Table 6.1 continued.

Dune 3 Migration Rates

Year	Net trend midpoint		Midline end point	
1996	666504, 3029822		666462, 3029859	
2004	666449, 3029855		666376, 3029914	
2006	666438, 3029866		666345, 3029930	
2007	666435, 3029867		666344, 3029933	
Migration	Meters	M/yr	Meters	M/yr
1996-04	64.4	8.1	102.5	12.8
2004-06	16.1	8.1	35.4	17.7
2006-07*	3.8	7.6	4.1	8.2
Net	84.3	7.7	142.0	12.9

*denotes 6 months

**denotes parabolic dune development after 1996

The net trend method for parabolic dune migration indicates that the three dunes displayed varying degrees of mobility, and that dune migration has a directional component. Dune 1 migrated 3.4 meters towards the WNW direction from 2004 to 2006, and 1.3 meters towards the SW from 2006 to 2007. The directional migration towards the SW between surveys indicates that dune 1 has both expanded and migrated towards the south. Dune 2 migrated 58.7 meters towards the NW from 1996 to 2004, which is in the general direction of RDP for both the BHP and SBI total sand roses. From 2004 to 2006 parabolic dune 2 migrated 6.1 meters towards the NNW, signifying both westerly migration and dune expansion in the northerly direction. Between surveys, dune 2 migrated 2.4 meters in the westerly direction signifying a western migration and dune expansion or widening. Dune 3 migrated a distance of 64.4 meters from 1996 to 2004 in the NW direction. Dune 3 also maintains a general direction of migration towards the NW from 2004 to 2006 and between surveys. The lack of change in migration direction indicates that dune 3 expansions were relative to dune 3 migration.

Parabolic dune landform units were also determined from doqq analysis for dunes 1, 2 and 3. Using methods similar to those listed above, individual dune landform unit migration distance was measured. The length of depositional lobe, deflation basin, and trailing ridges were measured on dunes 1, 2 and 3 to determine feature migration distance and rate using the midline end point measurement. The landform units of dune 1 were not easily discernable from the 2004 doqq and determining landform unit migration was difficult. It was also determined that minimal trailing ridge and deflation basin migration occurred or that the migration was less than the determined margin of error. Parabolic dune landform unit migration rates and measurements are listed in Table 6.2 below.

Table 6.2 Migration rates for dune landform units as determined from doqq and survey image raster analysis

Parabolic dune landform unit migration rates (m a⁻¹) 1996 -2004, 2004-06, 2006-07						
Midline end point measurements						
	Meters		M/yr			
Dune 1	2004-06		2006-07			
Depositional lobe	3.4	1.7	1.3	0.7		
Deflation basin	2.5	1.25	1	2		
South trailing ridge	~0	0	~0.75	1.5		
North trailing ridge	~0	0	~0	0	Meters	M/yr
Dune 2	1996-04		2004-06		2006-07	
Depositional lobe	110.5	13.81	3.6	1.8	4.3	8.6
Deflation basin	50.4	6.3	2.4	1.2	0.5	1
South trailing ridge	111.7	13.96	~0	0	~0	0
North trailing ridge	91.3	11.41	~0	0	~0	0
Dune 3	1996-04		2004-06		2006-07	
Depositional lobe	106.5	13.31	35.4	17.7	4.1	8.2
Deflation basin	59.2	7.4	2	1	1.5	3
South trailing ridge	82.4	10.3	7	3.5	2.5	5
North trailing ridge	77.2	9.65	~0	0	~0	0

6.3 Extent of Dune Change

Shapefiles were created from doqq and image overlays, which show the extent of individual dune migration and change in dune area. General dune migration was in the resultant drift direction from the onshore winds, and specifically in the RDD of the Bob Hall Pier total wind regime data. The area of dune change was calculated using XTools Pro extension for ArcMap 9.0 and results are given in meters.

Dune 1 development occurred after the 1996 doqq were flown. Therefore only three periods of dune change were mapped. Dune change and migration occurred along the slipface and western extent of the dune. The other features of dune 1 are stabilized and only slight change has occurred external of the dune. The area of dune 1 in 2004 was 3051 m² and although dune development occurred after 1996, initiation potentially occurred shortly after the doqq were flown. Dune 1 increased in area 93 m² from 2004 to 2006 and dune expansion was in the NW direction, as expected. There was an increase in area of 46 m² from 2006 to 2007 (six months), approximately half the area of the dune expansion from 2004 – 2006. The direction of dune migration was more towards the westerly direction and the rate of expansion indicates that dune 1 may be experiencing increased activity and mobility along the western extent of the depositional lobe.

Dune 2 developed prior to 1996 and an incipient parabolic dune was present at this time. Four periods of dune activity were mapped and dune migration and expansion are towards the NW, with some small areas of expansion along the southern trailing ridge. The dune expansion and migration is largely unidirectional. Dune change occurred across the complete extent of the dune, especially across the depositional lobe and trailing ridges. The deflation basin has

expanded from 1996 to 2004, but little change in regards to migration in this particular landform unit was noticeable from 2004 to 2007.

The area in dune 2 was 2403 m² in 1996 and expanded 5570 m² from 1996 to 2004. The total area of dune 2 in 2004 was 7973 m² when the next doqqs were flown. Dune 2 expanded 315 m² from 2004 to 2006 to encompass a total area of 8288 m². Between summer and winter surveys dune 2 expanded 173 m² to for a total dune area of 8461 m². Dune expansion from 2006 to 2007 was more than half of the dune expansion from the previous two year measurement period. If the rate of dune expansion were to continue at the rate between surveys the two year increase in dune area would be 692 m². The present rate of expansion is much greater than the 2004 to 2006 migration.

Dune 3 migrated and expanded in the NW direction since the 1996 doqqs were flown. Dune 3 was present prior to 1996 as a mature parabolic dune. The dune expansion is occurs along the north trailing ridge, south trailing ridge, and depositional lobe between 1996 and 2004. The deflation basin also experienced expansion from 1996 to 2004; however it is difficult to determine the area of internal features in low density and unvegetated areas, as in the 1996 dune 3. As best determined from doqq analysis, the area of the deflation basin was 1570 m² in 1996 and 2763 m² in 2004. The area of dune 3 in 1996 was 4857 m² and parabolic dune development likely began between eight to ten before the doqq was flown, based on dune 1 size and age. The change in dune 3 area from 1996 to 2004 was an increase of 14617 m² and this change in dune area indicates a very high level of dune activity. The total dune area in 2004 had increased to 19574 m².

Dune 3 area increased 2377 m² from 2004 to 2006 to increase the total dune area to 21951 m². In the six months between dune surveys from 2006 to 2007 dune 3 expanded 452 m²

to bring the total dune size to 22403 m². The rate of dune expansion between surveys was less than half of the expansion rate from 2004 to 2006. Of the three dunes only dune 3 experienced a decrease in the rate of expansion from the survey time period compared to 2004 to 2006 measurement period.

Table 6.3 Total dune area and extent of change 1996 – 2007

Extent of dune area (m ²) change 1996 - 2007		
	Extent of change	Total area
Dune 1*		
2004**		3051
2006	93	3144
2007	46	3190
Dune 2		
1996**		2403
2004	5570	7973
2006	315	8288
2007	173	8461
Dune 3		
1996**		4857
2004	14617	19574
2006	2377	21951
2007	452	22403

*denotes parabolic dune development after 1996
 **initial extent of change not recorded

Individual dune areas are comparable for the different dunes over time. Dune 1 in 2004 is comparable in size to dune 2 in 1996, with a dune 1, 2004 having a greater total area of 648 m². As determined from doqq analysis both dune 1, 2004 and dune 2, 1996 are blowout dunes or potentially “Stage 2” parabolic dunes (Pye, 1982). Parabolic dune 3, 1996 is approximately twice the size of dune 2, 1996 and dune 3 in 1996 is a mature parabolic dune or “Stage 3” dune (Pye, 1982). Both dune 2 and dune 3 were well defined and active parabolic dunes in 2004, although dune 3 was more than twice the size of parabolic dune 2 in 2004. The similarity in dune size for the individual dunes over time indicates that blowout dunes generally have an area

that are less than approximately 3055 m² or thereabouts, and can be as small an area as 2400 m². Conversely, well defined and active parabolic dunes in this environment are present with dune areas that can vary between approximately 3140 m² to greater than 22403 m².

Parabolic Dune 1 Evolution 2004 - 2007

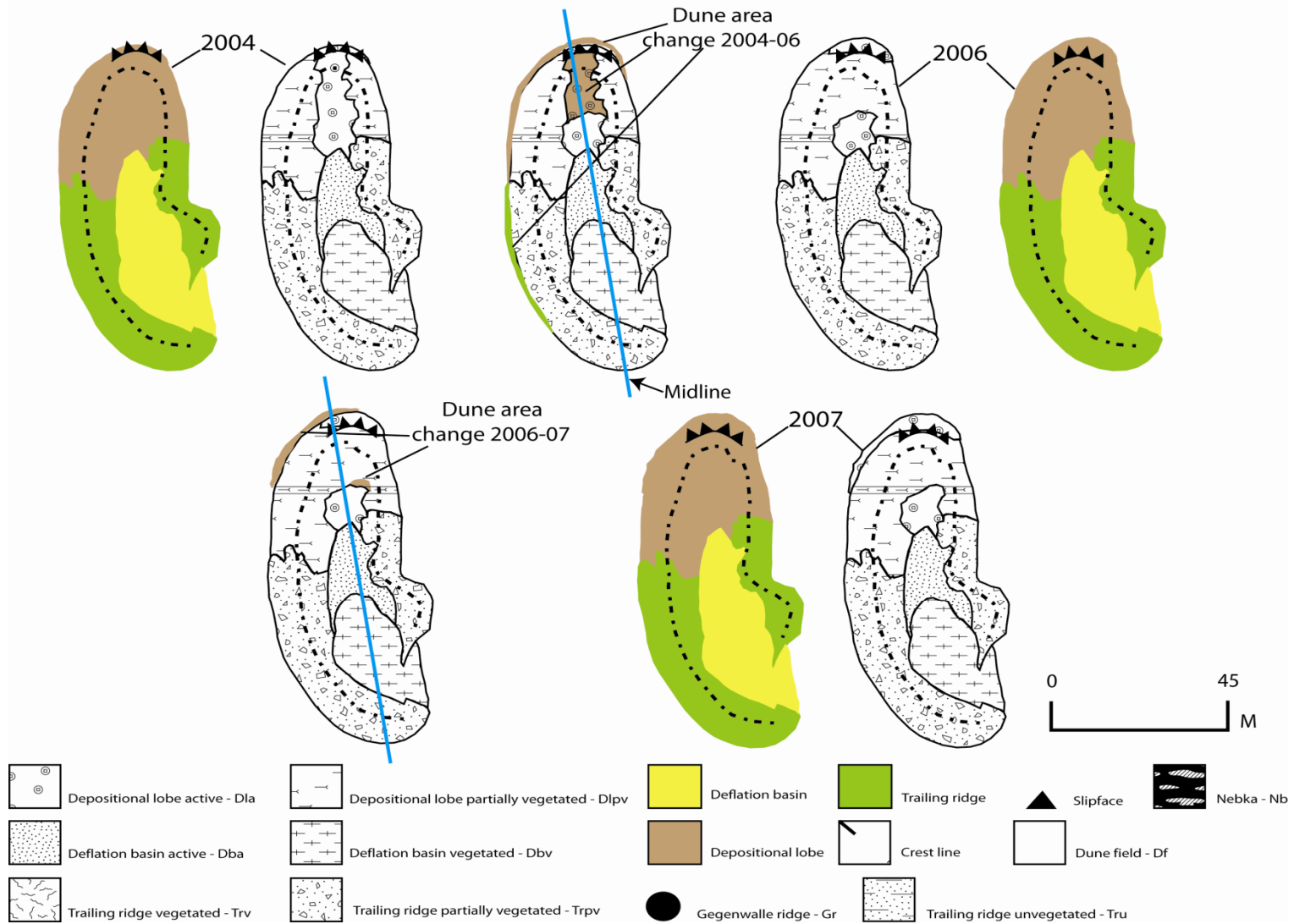


Figure 6.1 Map of dune 1 migration and change from 2004 – 2007

Parabolic Dune 2 evolution 1996 - 2007

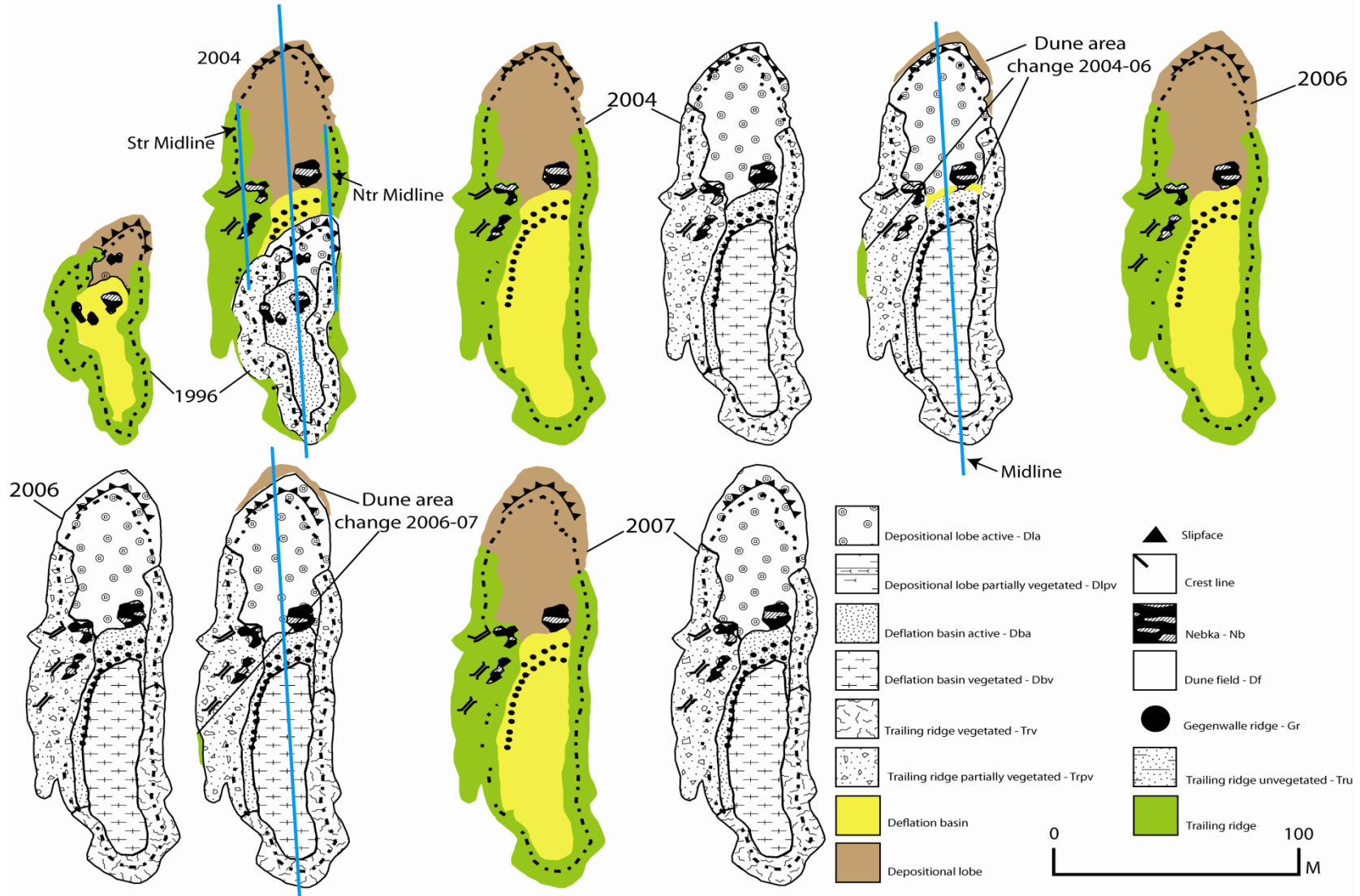


Figure 6.2 Map of dune 2 migration and change from 1996 - 2007

Parabolic Dune 3 evolution 1996 - 2007

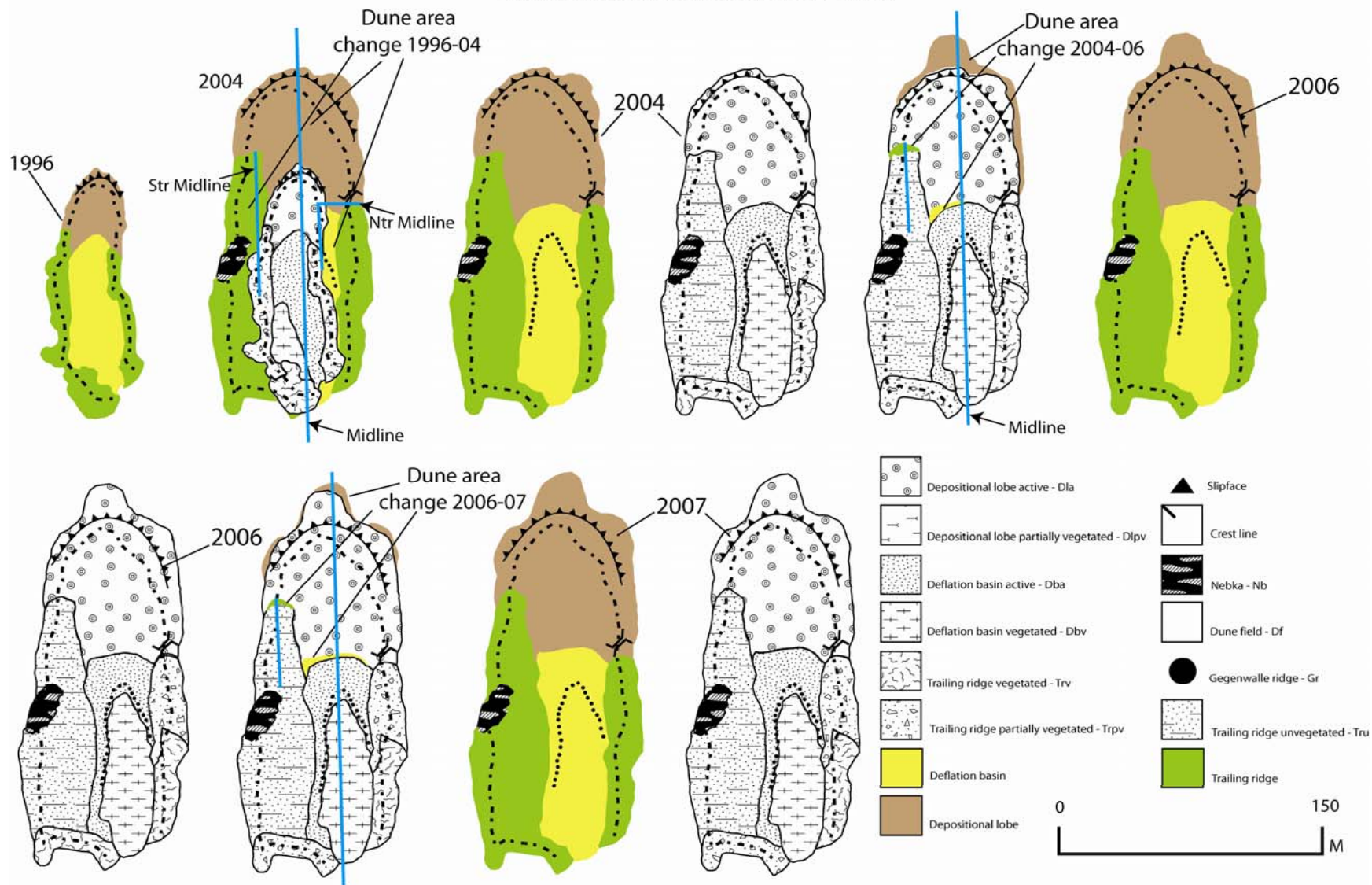


Figure 6.3 Map of dune 3 migration and change from 1996 - 2007

7. Wind: Seasonal Patterns and Geomorphic Influences

7.1 Introduction

In this chapter the wind regime of North Padre Island is examined in order to determine the geomorphic influence the directional components of wind regime has on dune form and development. Secondly, wind roses and sand roses are presented which show the general direction of wind direction and sediment transport. Also, observations of aeolian activity and its morphologic influence on dune orientation and dune symmetry are also presented. The relationships between winds above sediment transport velocity frequency, drift potential (DP), and seasonal precipitation are presented to determine which seasonal wind regime has the greatest influence on dune orientation and migration.

7.2 General and Seasonal Components of the Wind Regime

Wind data was collected from four weather stations: Padre Island National Seashore range station (PAIS), Corpus Christi International Airport (CCIA), Bob Hall Pier (BHP), and South Bird Island (SBI). The data collected from these stations were used for wind regime analysis, determining potential sediment transport, and determining the influence of the wind regime on dune orientation. However due to differences in weather station location, observation time (hourly versus daily), and data set time periods, there are some differences in wind and sand rose production. The most prominent component of the wind regime is the consistency of the SE and SSE, or onshore winds and the low frequency of westerly winds. The PAIS wind rose displays the most variation compared to the three other data sets because they consist of once daily 8 am observations. The morning observations do not provide a detailed

representation of the regional wind regime due to the higher frequency of north and southeast winds. The three other weather stations recorded wind data once an hour for 24 hours a day and therefore present a more accurate portrait of the wind regime.

The Texas Coastal Ocean Observation Network (TCOON) data stations (BHP and SBI) display the most similarities in total wind regime. The slight differences in these two wind roses may be due to weather station location and the influence of barrier island topography. The CCIA weather station is located inland and farther west than the other three stations and in this instance the wind data displays a greater frequency of north winds as compared to BHP and SBI locations.

The drift potentials for each weather station data set indicate that the North Padre Island wind energy environment is high (Appendix), according to the Bullard (1997) classification (see Table 7.1). Winds above sediment transport threshold, or winds greater than 5.6 m s^{-1} , occurred at varying frequencies as recorded at the individual weather stations. As seen in Table 7.2 the greatest frequency of winds above threshold were present at BHP (1996-2007) and the lowest frequency of winds above threshold occurred at PAIS (1968-2007).

Table 7.1 Bullard (1997) classification of wind regime based on the work of Fryberger and Dean (source: Bullard, *Journal of Sedimentary Research*, 1997)

Values of Drift Potential Calculated Using Wind Speeds in		Wind-energy Environment
Knots	ms^{-1}	
<200	<27	Low-energy environment
200-400	27-54	Intermediate-energy environment
>400	>54	High-energy environment

Fryberger and Dean (1979) identify five commonly occurring wind regimes: narrow unimodal, wide unimodal, acute bimodal, obtuse bimodal, and complex. This wind regime classification is useful for identifying the aeolian influence in varying desert and coastal environments. Also, dune types generally occur in conjunction with specific wind regimes, in particular parabolic dunes generally develop in environments that have narrow unimodal and bimodal wind regimes (Fryberger and Dean, 1979). A narrow unimodal wind regime is “characterized by having 90% or more of the drift potentials in adjacent directions or within 45° on the compass” (Fryberger and Dean, 1979). A wide unimodal wind regime consists of two peak drift potentials within a singular directional quadrant, but has a distribution of 45° or greater. An acute bimodal wind distribution consists of two modes forming an angle less than 90° , accordingly an obtuse bimodal wind distribution has two modes forming an angle greater than 90° (Fryberger and Dean, 1979). A complex wind regime is characterized by having a wind distribution with three or more nodes or with “poorly defined nodes” (Fryberger and Dean, 1979).



Figure 7.1 Wind velocity scale for wind roses

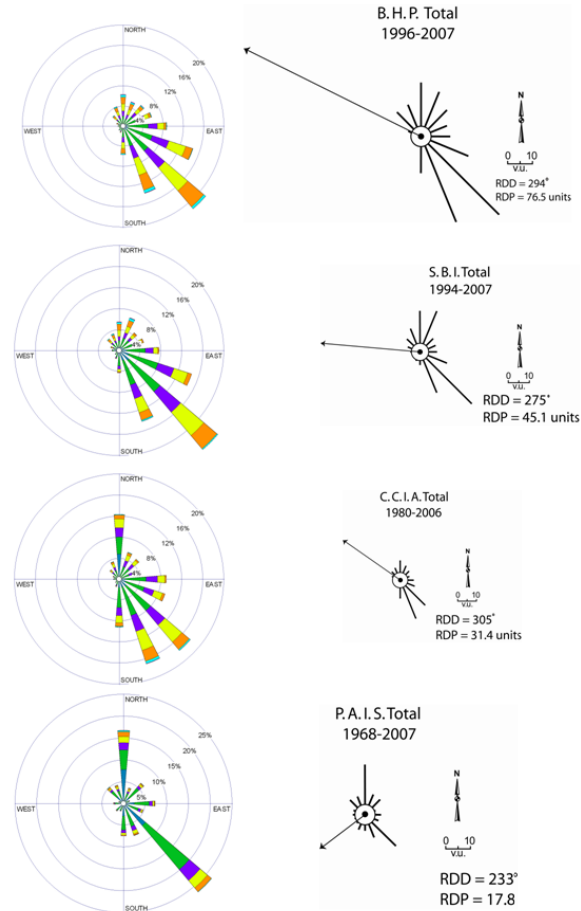


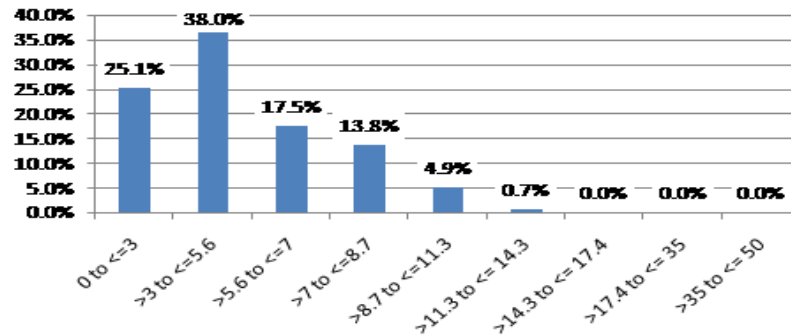
Figure 7.2 Weather station total wind and sand roses. Sand roses indicating direction of potential sediment transport direction (RDD), magnitude of sediment transport (RDP), and frequency of directional winds. The southeasterly component of the wind regime is the most influential in sediment transport.

The sand roses for the total wind regime data indicate that PAIS, BHP, and SBI, all have an obtuse bimodal wind distribution. The sand rose data from CCIA indicate a wide unimodal wind distribution in its recorded location. The wind rose data for the weather stations indicate that both PAIS and CCIA have obtuse bimodal wind regimes, and both BHP and SBI have acute bimodal wind regimes. The most influential wind direction for sediment transport is either the SE or SSE and drift direction is towards the NW and WNW. As noted previously, the PAIS wind data displays a bias in the N and SE directions.

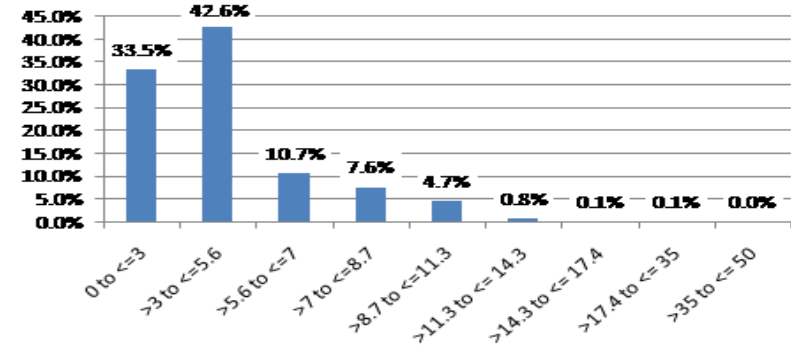
Table 7.2 Individual frequency distribution of wind speed classes at each weather station location. Charts also indicate frequency of wind speeds above transport threshold ($>5.6 \text{ m s}^{-1}$) at each location. Frequency of winds above threshold: CCIA, 36.9%; PAIS, 23.9%; BHP, 58.2%; SBI, 47.1%

Total wind regime frequency totals

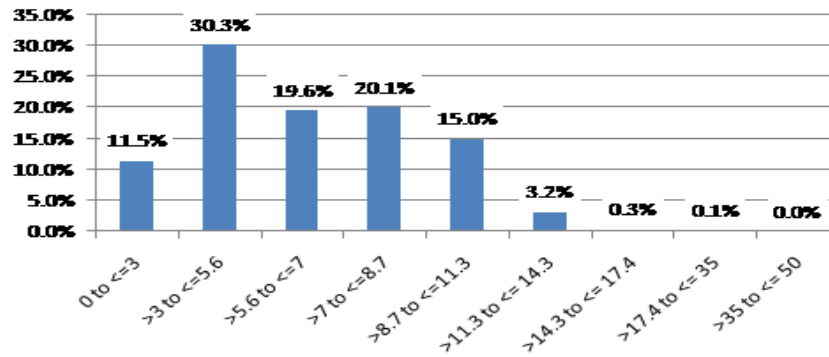
Corpus Christi International Airport 1980-2006



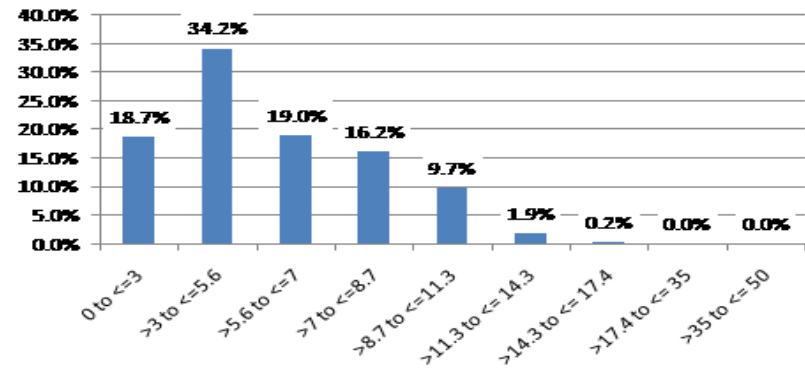
Padre Island National Seashore 1968-2007



Bob Hall Pier 1996-2007



South Bird Island 1994-2007



Dune orientation and resultant drift direction or RDD corresponds most closely with the BHP and CCIA total wind data. However, there is enough variation in the orientations of the three dunes that the sand rose of one data set does not completely account for the varying orientations.

7.3 Observed Influence of Wind Regime

Field observations and two sets of total station surveys provide insight into the geomorphic influence of seasonal and total wind regimes. Field notes were compiled during four trips to the study sites, 13 June to 17 June, 2006; 11, 12 November, 2006; 13, 14 January, 2007; and 10, 11 February, 2007. The general dune orientation aligns with SE winds, which is approximately 103° to 111° to the shoreline orientation. The length wise dune orientation varies for each dune from $\sim 310^{\circ}$ NW for dune 3, $\sim 320^{\circ}$ NW for dune 2, and $\sim 290^{\circ}$ NW for dune 1 as determined from TNRIIS 2004 doqqs. The shoreline orientation at dunes 3 and C is 31.8° E and 23.3° E at dune 1.

The most obvious directional influence of the wind regime is the SE, SSE, and ESE components. These three directions compose the onshore component of the wind regime and are responsible for the general dune orientations (Jennings, 1957; Story, 1982; Pye, 1982; Thompson, 1983), and direction of migration (Jennings, 1957; Story, 1982; Pye, 1982; Thompson, 1983; Wasson, et al., 1983). Variability between seasonal wind regimes accounts for differing degrees of influence for the onshore and alongshore wind directions. However, the onshore component of the wind regime has undoubtedly the most geomorphologic influence (Landsberg, 1956; Jennings, 1957).

Northerly winds N, NNW, NNE, NW, and NE also influence dune shape, orientation, and direction of migration (Landsberg, 1956; Jennings, 1957; Wasson, et al., 1983). The southern features of each dune's, trailing ridge, depositional lobe, and deflation basin display the influence of northerly winds. The south trailing ridge of each dune displays three characteristics compared to the north trailing ridge, a gentle internal slope, lower vegetation density, and greater ridge width. The southern aspect of the depositional lobe of each dune displays a higher elevation and lower vegetation density as compared to the northern aspect. Sediment has been observed depositing along the southern aspect of the depositional lobe due to winds associated with passing cold fronts, and evidence of deposition can be seen from comparing surveys. The deflation basins of each dune display the influence of northerly winds as evidenced by the development of gegenwalle ridges along the southern aspect of vegetated basin. The gegenwalle ridges in dunes 2 and 3 developed from sediment deposition on germinated vegetation that grows on the wet extent of the active deflation basin. Sediment deposition and gegenwalle ridge aggradation continues due to the influence of northerly and multidirectional winds.

7.3.1 Winter Season

According to the BPH, SBI, and PAIS data sets the dominant sediment transporting winds during the winter season (1 December to 28 February) were northerly winds (N, NNE, and NE), the CCIA data set indicates that the SSE winds are the most dominate sediment transporting winds during the winter season. The frequency of sediment transporting winds is lower for the winter season compared to the average annual frequency of winds above threshold and the lowest of the four seasons.

The wind rose data indicates that the winter season wind regime is classified as obtuse bimodal for all four weather stations. The sand rose data indicates that BHP, SBI, CCIA winter sediment transporting wind regime is obtuse bimodal, with the strongest sediment transporting nodes in the N and SE quadrants. The PAIS sand rose data indicates a wide unimodal sediment transporting wind regime during the winter season. The resultant drift directions for the winter season range from 272° - 194° and have an average RDD of 218° signifying a sediment transport towards the SW. The winter season is the second most active for total sediment transport as indicated by the average of drift potentials for each data set.

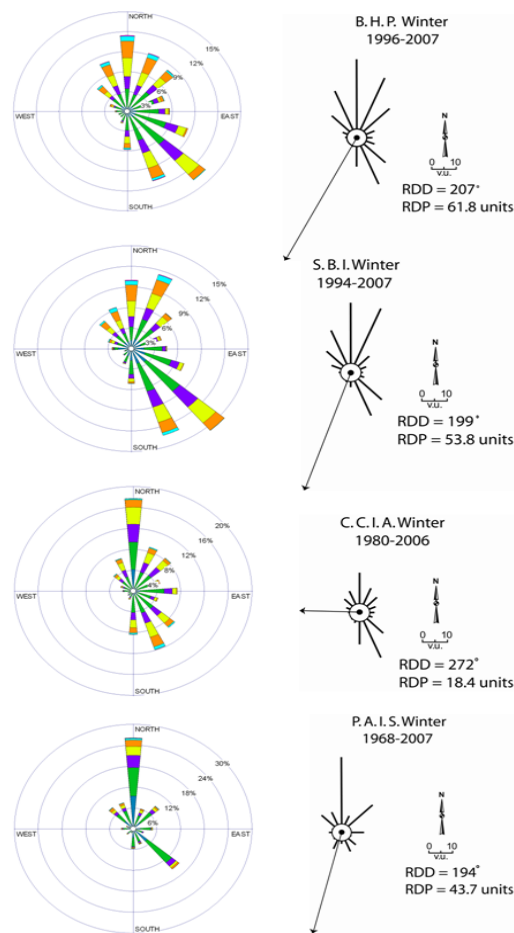
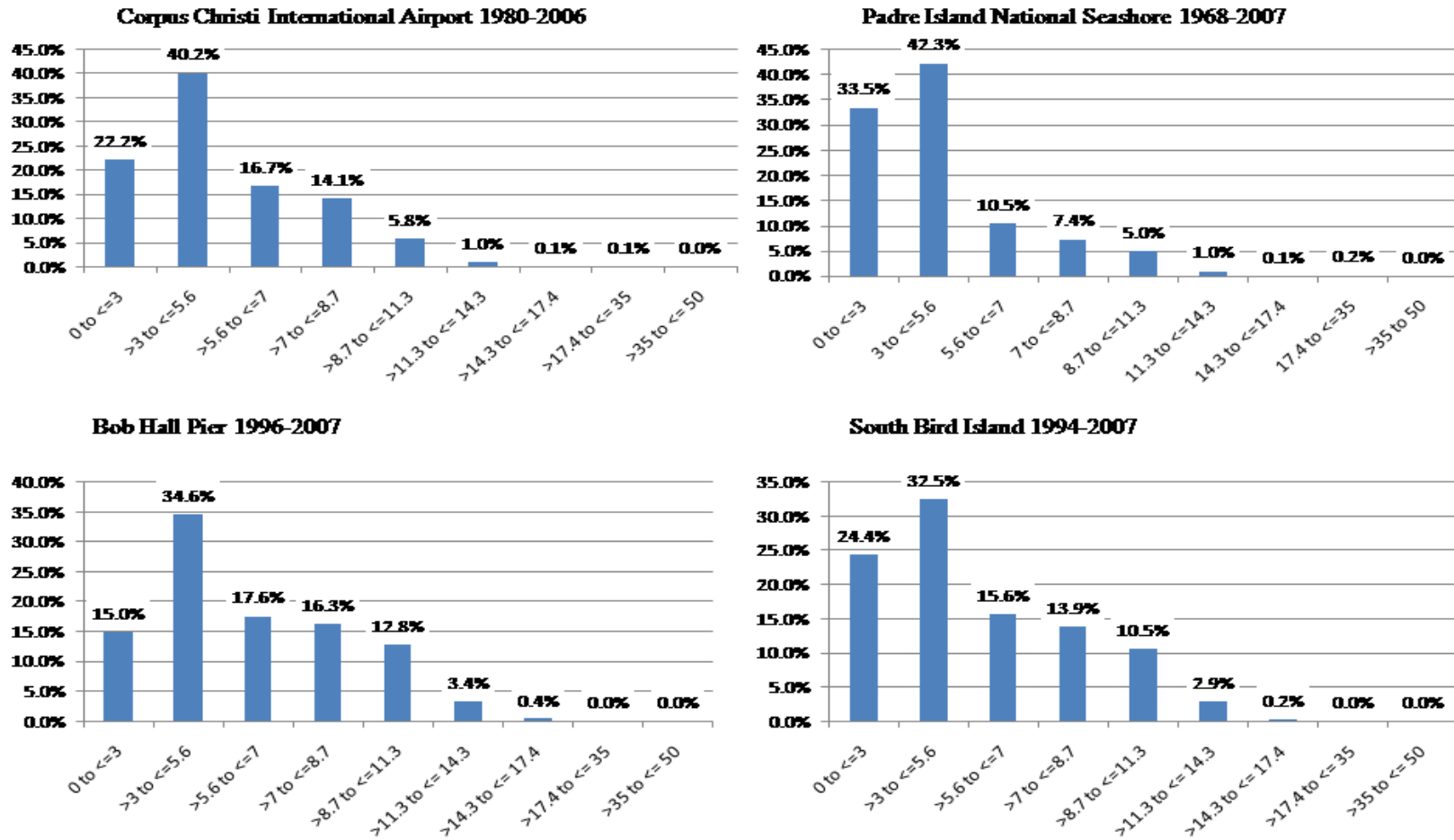


Figure 7.3 Wind roses and sand roses for the winter season.

Table 7.3 Frequency distribution of wind classes during the winter season. Frequency of winds above sediment transport velocity: CCIA, 37.6%; PAIS, 24.2; BHP, 50.4%; SBI, 43.1%

Winter wind regime frequency totals



The winter season also experiences the lowest average seasonal precipitation and the influence of the winter wind regime can be observed on dunes *A*, *C*, and *D* in some specific features of dune morphology. The southern aspect of the depositional lobe of each of the dunes has a higher elevation as compared to the northern aspect, and the topographic surveys display evidence of deposition from the summer to winter surveys. The southern trailing ridges of all three dunes display evidence of sediment deposition due to increased elevation along the base of the southern trailing ridge. In the case of dune 2 there was deposition south through the cols as determined from summer to winter survey comparison. The influence of the winter winds is also a factor in determining individual dune asymmetry by depositing sediment along the southern dune features.

7.3.2 Spring Season

The spring season is characterized by the occurrence of strong SSE and SE winds along the coast and the high frequency of winds above sediment transport threshold. The spring sand roses are similar in overall resultant drift direction (RDD) for the four data sets. The spring sand roses also display the highest average of drift potentials (133.5 vector units) for any season, indicating that this is the seasonal period of most sediment transport activity. The resultant drift directions for the sand roses are between 281° - 314° with an average of 293.5° and indicate the general direction of sediment transport and dune migration is between the WNW and NW.

The spring season wind regime can be classified as wide unimodal according to the CCIA and BHP wind rose data, while SBI indicates a narrow unimodal wind regime. However the PAIS wind rose data classifies the spring season wind regime as obtuse

bimodal and is similar to the sand rose for the total wind regime except for occurrence of stronger winds from the SE. The sand roses for the spring season display more variance in relation to the sediment transporting potential of the wind regime. The sand rose data indicates that BHP, SBI, and PAIS weather stations experience an obtuse bimodal wind regime during the spring season. The CCIA sand rose displays the characteristics of a narrow unimodal wind.

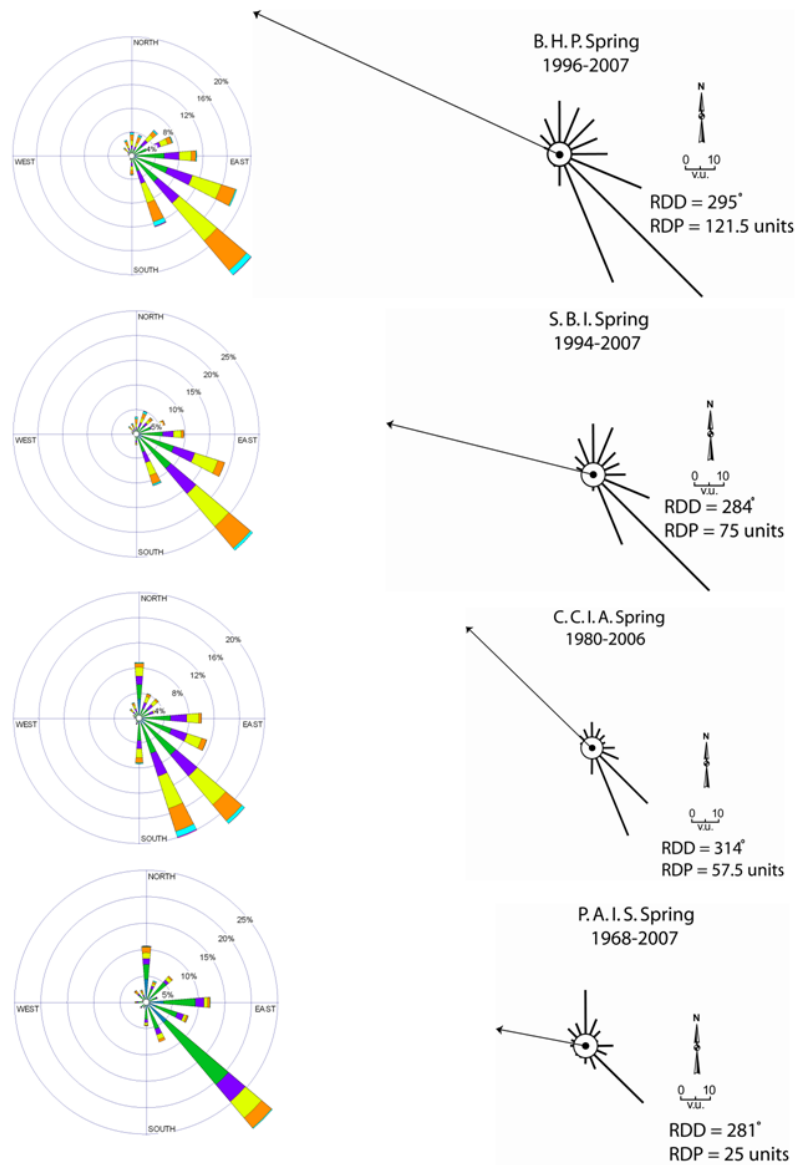
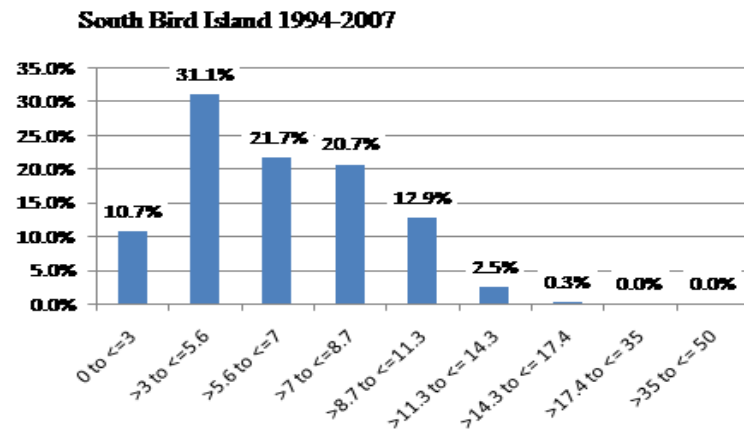
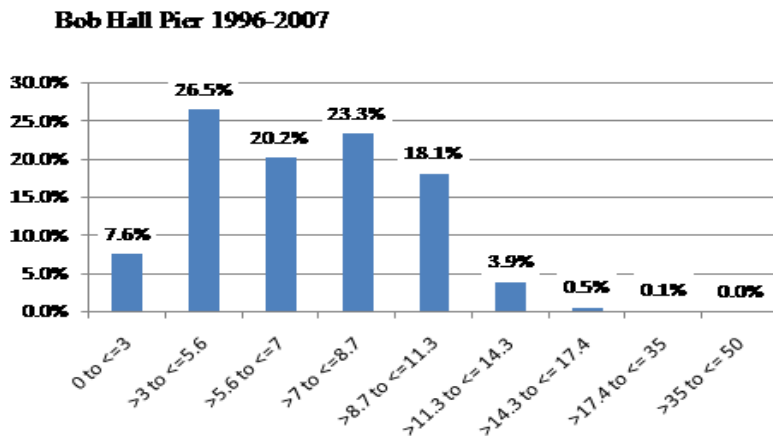
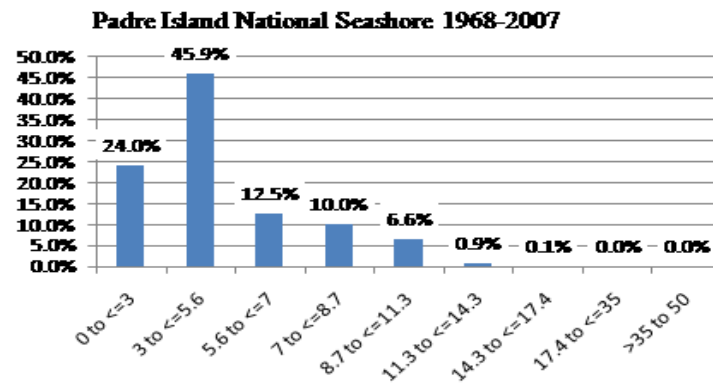
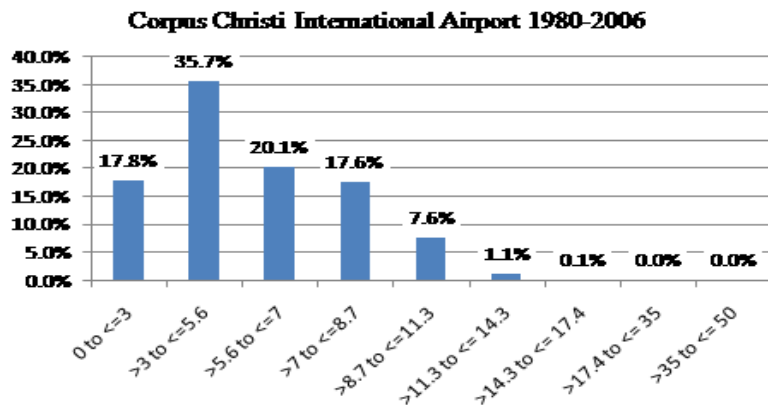


Figure 7.4 Wind roses and sand roses for the spring season.

Table 7.4 Frequency distribution of winds during the spring season. Frequency of winds above threshold: CCIA, 46.5%; PAIS, 30.9%; BHP, 65.9%; SBI, 57.6%

Spring wind regime frequency totals



Evidence of sediment transport and deposition by the spring seasonal winds is observed in the direction of dune orientation. The long axis and specifically the north trailing ridge of each parabolic dune is most closely aligned with the RDDs of the BHP and SBI sand roses indicating the influence of the spring season wind regime. The trailing ridges of each parabolic dune are also nearly parallel to each other and the RDDs of the BHP and SBI sand roses indicating the geomorphic influence of the spring winds.

7.3.3 Summer Season

The summer season winds are characterized by the strength of SE and SSE winds and the absence of northerly and westerly winds. The average resultant drift direction of the summer season sand roses are most closely aligned of any season with a range of 318° - 306° and an average RDD of 314° . The weather station wind data also indicates that the average resultant drift potential for the summer season is the highest of the four seasons with an average RDP of 72.2 vector units and that directional sediment transport is greatest during the summer. The summer season sand roses are similar to the spring sand roses in general resultant drift direction, as both seasons display the influence of the SE and SSE wind directions.

The summer season wind regime is classified as acute unimodal according to wind rose and sand rose data from all weather stations. The agreement in summer wind regime classification and similarity in resultant drift directions indicates the consistency of the onshore wind directions and absence of northerly winds recorded at each weather station site. The orientation of parabolic dunes 1, 2, and 3 is similarly aligned with the resultant drift directions of the summer sand roses. Although the summer average of

resultant drift directions is slightly more northerly than the spring average of resultant drift directions the RDDs are similarly aligned. The difference in average resultant drift direction from the summer (RDD: 314°) and spring (RDD: 293.5°) wind regimes is 20.5°. The combined summer and spring wind regimes for North Padre Island represent the general direction of orientation and these two seasons are most influential in determining parabolic dune orientation, migration, and geomorphology.

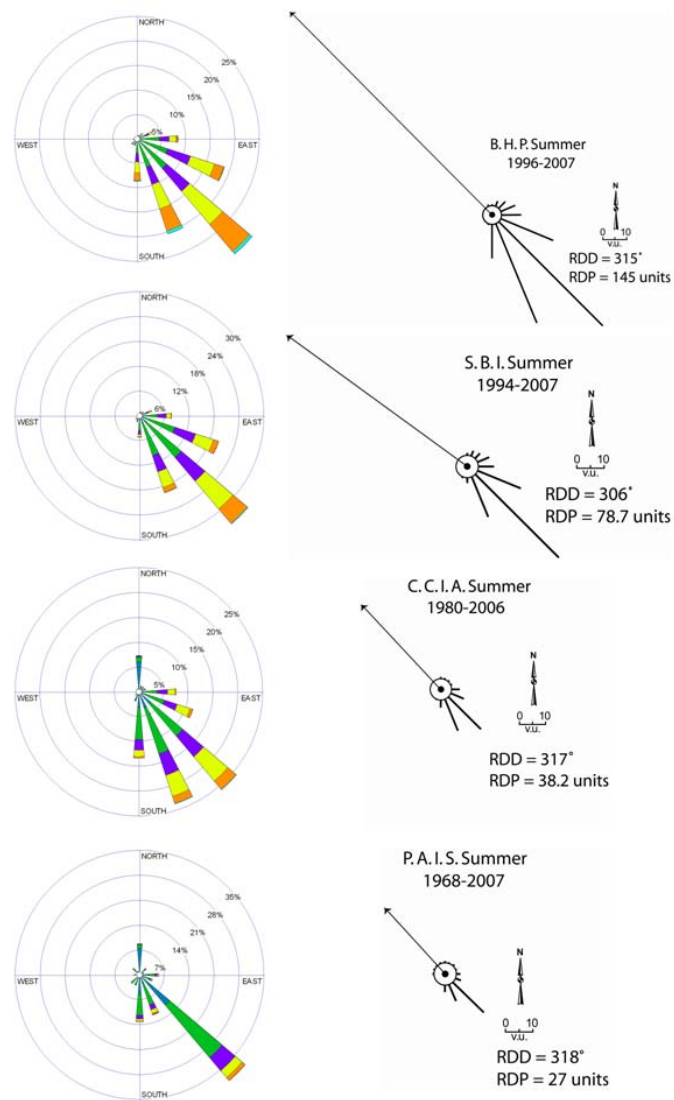
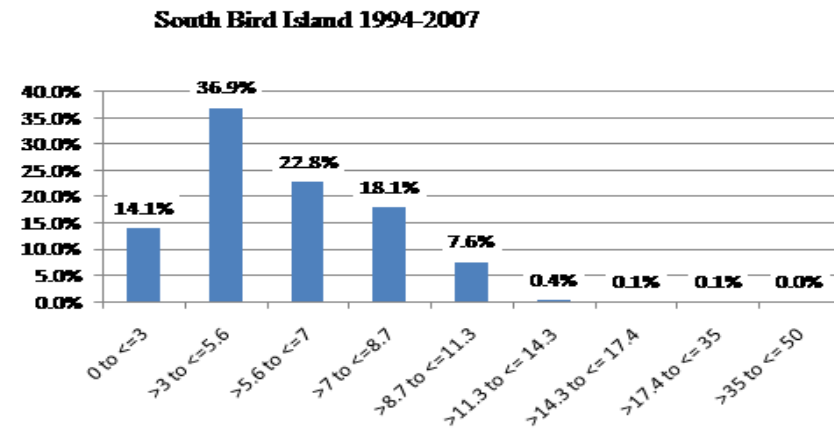
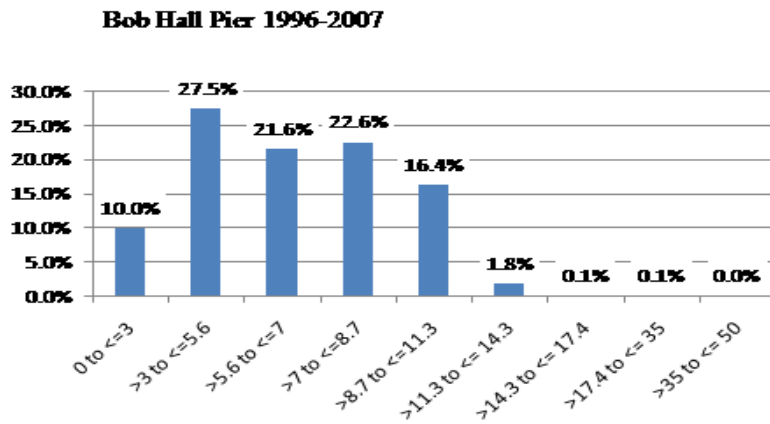
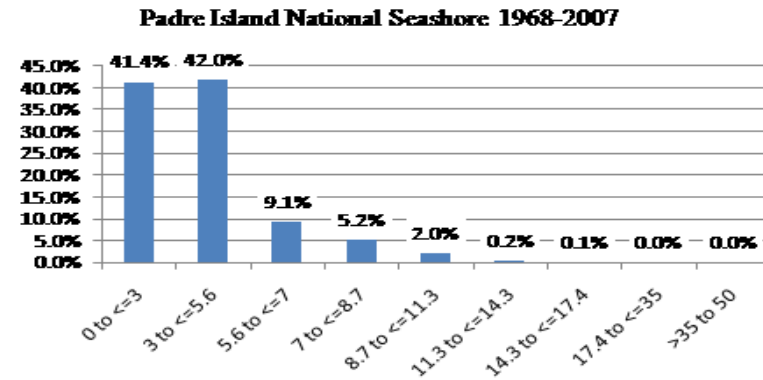
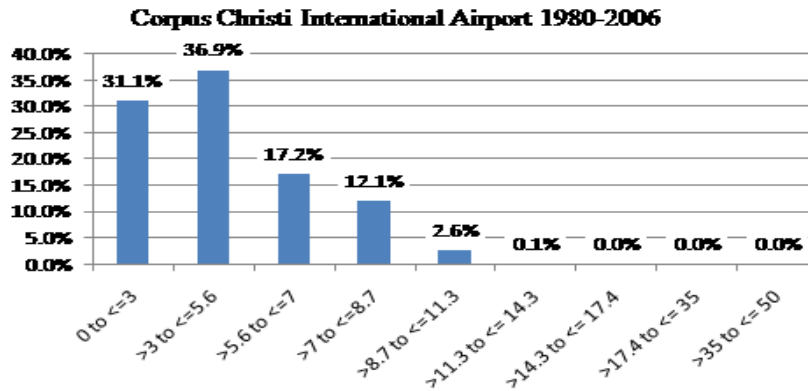


Figure 7.5 Wind roses and sand roses for the summer season.

Table 7.5 Frequency distribution of winds during the summer season. Frequency of winds above threshold: CCIA, 30.5%; PAIS, 16.6%; BHP, 62.5%; SBI, 49%.

Summer wind regime frequency totals



7.3.4 Fall Season

The fall season is characterized by the variability in wind directions and their corresponding drift potentials. According to the weather data sets the fall season has the lowest: wind velocities, total drift potential, average drift potential, frequency of winds above threshold, and average resultant drift potential. The fall season sand roses display the most variability in resultant drift direction. The average resultant drift direction for the fall season is 250.75° , the RDDs range from 305° - 203° , and the average resultant drift potential is 38 vector units. The fall season experiences the highest average rainfall, and coupled with the low average resultant drift potential for the fall season indicates that the fall wind regime has the least geomorphic influence for any of the seasons.

The wind rose data for the fall season indicate that each weather station experiences a bimodal wind regime. However, the BHP and SBI weather stations experience lower frequencies of northerly winds compared to the CCIA and PAIS weather stations during the fall. The fall sediment transporting wind regime for North Padre Island is classified as obtuse bimodal according to the BHP, SBI, CCIA and PAIS sand rose data. Interestingly enough the SBI and CCIA sand roses have resultant drift directions that differ by 85° from the NW to the SW. Accordingly the BHP and PAIS bimodal obtuse sand roses have resultant drift directions that differ by 72° from the WNW to the SSW. The differences in the directions of resultant drift and the variability of resultant drift directions present an inconsistent and variable wind regime during the fall. The average frequency of winds above sediment transport velocity for the weather stations was also the lowest of all seasonal frequency averages.

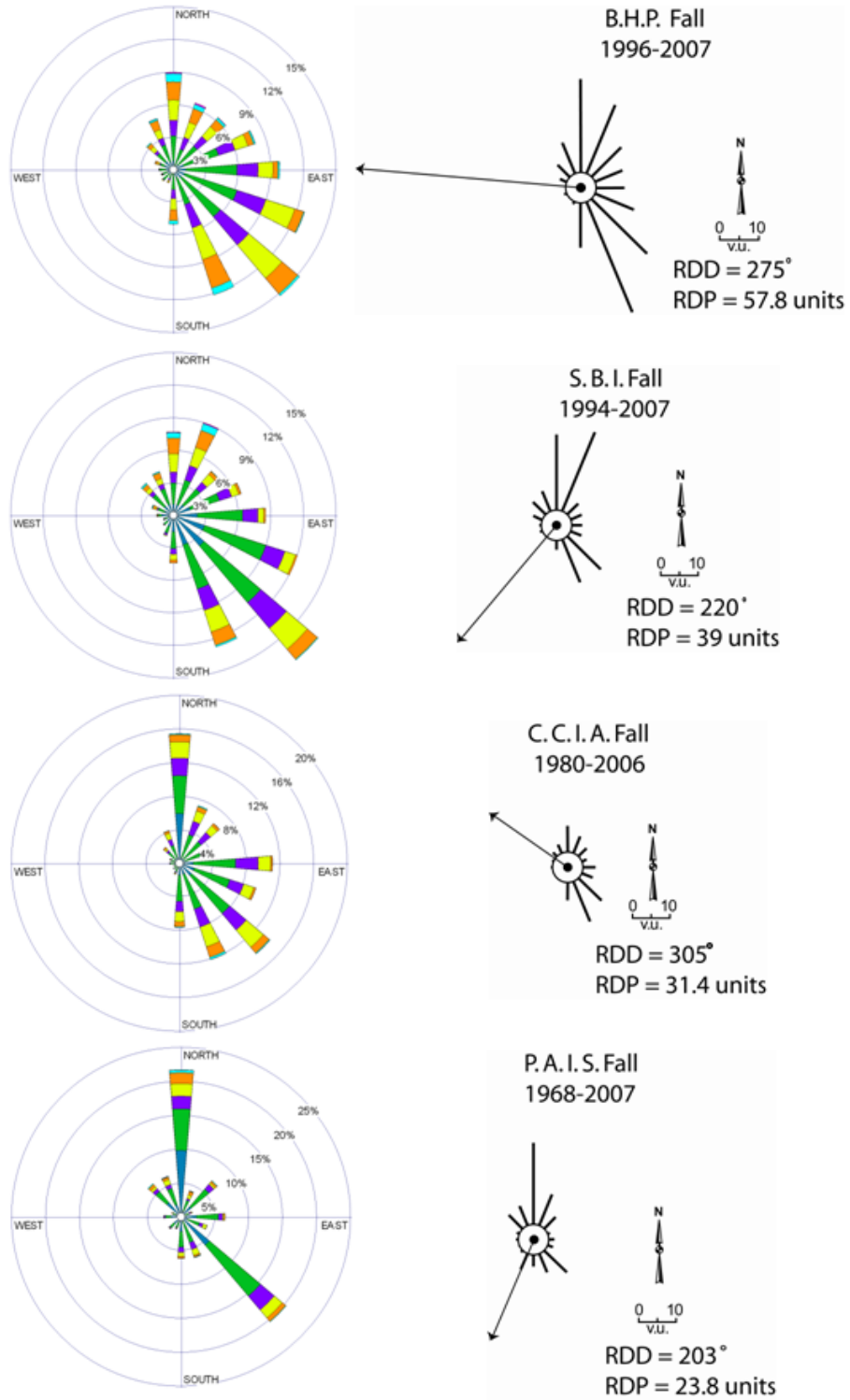
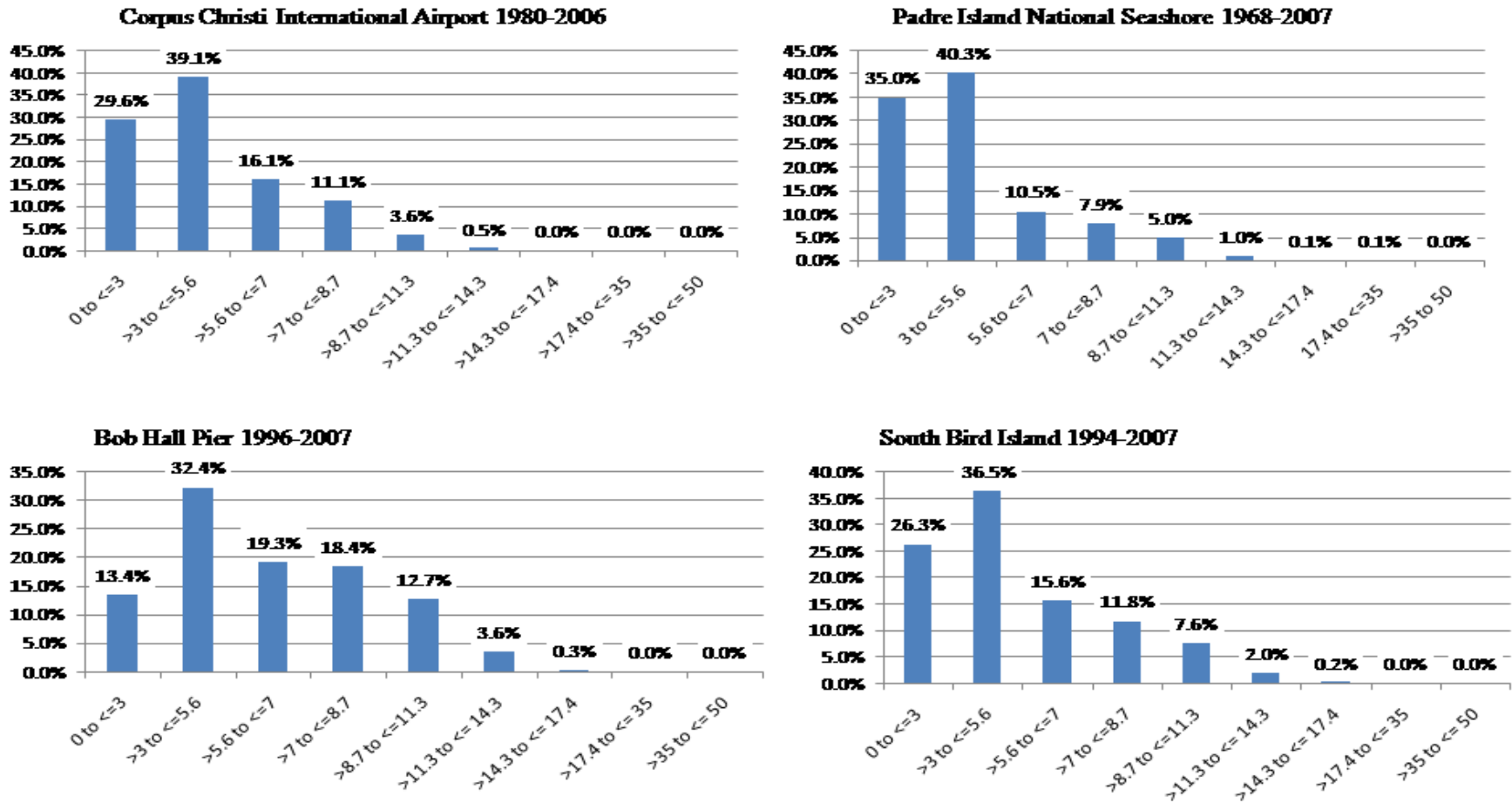


Figure 7.6 Wind and sand roses for the fall season.

Table 7.6 Frequency distribution of winds during the fall season. Frequency of winds above threshold: CCIA, 31.3%; PAIS, 24.7%; BHP, 53.2%; SBI, 37.2%.

Fall wind regime frequency totals



7.3.5 Survey Winds

Wind data was available for three weather stations: BHP, SBI, and PAIS (CCIA data was not posted for late 2006 and early 2007). The wind regime for this time period is classified as acute bimodal for the BHP and SBI wind rose data sets. The PAIS wind rose data classifies the wind regime as obtuse bimodal with directly opposing peak nodes. The sand rose data classifies the sediment transporting wind regime as obtuse bimodal for the both the BHP and SBI data sets and acute bimodal for the PAIS data set. The resultant drift directions for the three sand roses range from 323° - 248° with an average of 286° , indicating sediment transport to the WNW. The average resultant drift potential for the three weather stations is 36.6 vector units.

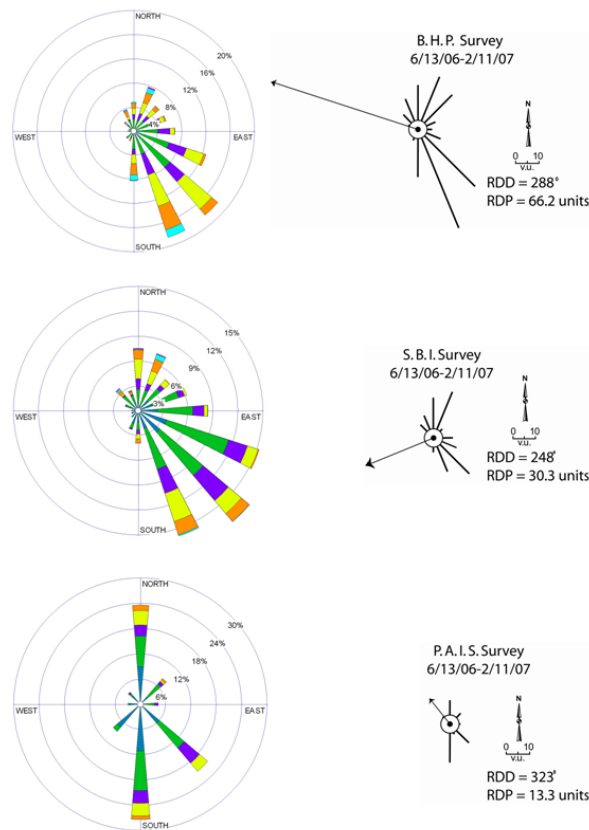


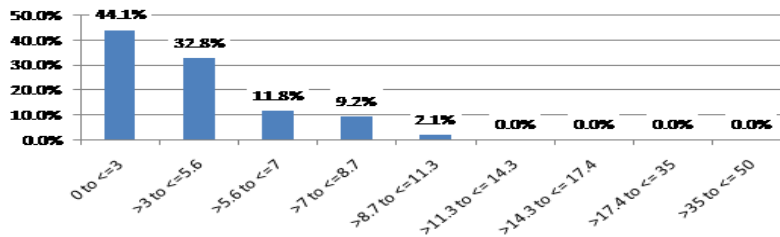
Figure 7.7 Survey wind and sand roses for weather stations near the parabolic study sites

Total station surveys and field observations confirm dune migration and sediment transport in the general direction of resultant drift directions calculated from the survey period wind data. The three sand roses display a high drift potential from the north. This northerly component of the wind regime was observed during field work and verified from dune 2 and 3 profiles, which displayed an increase in elevation along the southern aspect of the depositional lobe.

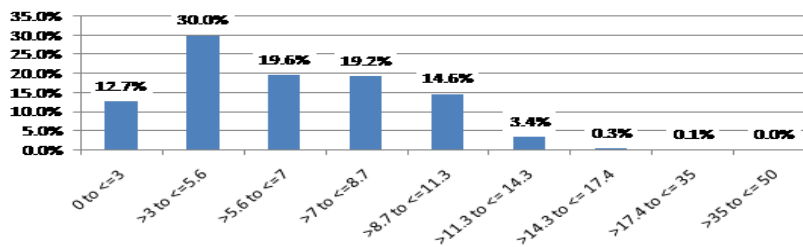
Table 7.7 Frequency distribution of winds between surveys. Frequency of winds above threshold: PAIS, 22.9%; BHP, 57.3%; SBI, 59.9%.

**Survey wind regime frequency totals
6/13/2006 – 2/11/2007**

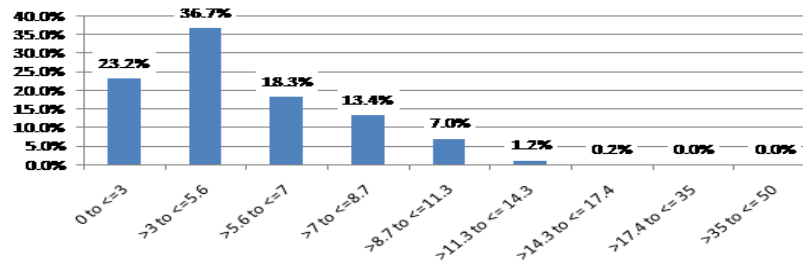
Padre Island National Seashore



Bob Hall Pier



South Bird Island



7.4 The Relationships Between Precipitation and Wind Regime

The Fryberger and Dean method (1979) was developed as a means to determine which directional component of the wind regime is most influential in determining the direction of sediment transport and dune migration. While the Fryberger and Dean (1979) method provides a systematic means for determining the directional transport of sediment, it also indicates the strength or potential for transport of each wind direction in vector units. However, Fryberger and Dean (1979) do not account for the influence of precipitation or surface moisture on sediment transport. The relationship between potential for sediment transport and seasonal precipitation should indicate some relationships are present between the seasonal wind regimes and precipitation data.

The relationships between wind regime and the precipitation data are a means to help understand which seasonal wind regime has the most influence on the Padre Island National Seashore parabolic dune forms and migration. The precipitation data, as noted in Chapter 3, was obtained from Padre Island National Seashore ranger station, and all calculations were performed using the same wind data sets used to calculate wind and sand roses.

Table 7.8 lists the seasonal precipitation data for each weather station (all PAIS precipitation data, wind frequency above sediment transport threshold (WFAT), and the ratio of wind frequency above transport threshold to seasonal precipitation. The table provides an easy reference to view the variability between wind data sets, and how each wind data set relates to the seasonal precipitation records. As seen in Table 7.8 the wind data sets display a range of variability for each wind data classification. The variability in the wind data sets provides insight into which data set provides the most accurate

representation of the winds that have the most geomorphic influence on parabolic dune development and evolution.

The spring and summer seasons have the highest percentage of winds above sediment transport velocity. Therefore, blowout initiation potentially occurs most frequently during the spring and summer season. Seasonal precipitation is the highest during the fall and this is the season which has the highest potential for revegetation.

Table 7.8 Seasonal and annual measurements of wind and precipitation data. The ratio of RDP to precipitation indicates the seasonal potential for directional sediment transport activity for wind regimes; higher values indicate greater potential sediment transport activity; WFAT/precipitation indicates general potential for sediment transport.

	BHP	SBI	CCIA	PAIS	Averages
Precipitation (cm)					
Winter	13.25	13.25	13.25	13.25	13.25
Spring	18.83	18.83	18.83	18.83	18.83
Summer	22.3	22.3	22.3	22.3	22.3
Fall	33.43	33.43	33.43	33.43	33.43
Annual average	87.81	87.81	87.81	87.81	87.81
Survey	78.7	78.7	78.7	78.7	78.7
Wind Frequency Above Threshold (WFAT) %					
Winter	50.4	43.1	37.6	24.2	38.83
Spring	65.9	57.6	46.5	30.9	50.23
Summer	62.5	49	32	16.4	39.98
Fall	53.2	37.2	31.3	24.7	36.60
Annual average	58.2	47	37	23.8	41.5
Survey	57.3	40.1	NA	23.1	40.17
Ratio of WFAT/Precipitation					
Winter	3.80	3.25	2.84	1.83	2.93
Spring	3.50	3.06	2.47	1.64	2.67
Summer	2.80	2.20	1.43	0.74	1.79
Fall	1.59	1.11	0.94	0.74	1.09
Annual average	0.66	0.54	0.42	0.27	0.47
Survey	0.73	0.51	NA	0.29	0.51

7.5 Conclusions

The long term effect of the wind regime on parabolic dune orientation and morphology is in the overall dune migration towards the NW, primarily due to the influence of onshore winds from the SSE and SE directions. The asymmetry of the individual parabolic dunes' trailing ridges is primarily due to the influence of the northerly winds, generally associated with the passage of cold fronts generally occurring during the fall and winter seasons. Sediment deposition and the widening of specific landform units were recorded by the total station surveys. Specifically, northerly winds are thought to be responsible for sediment deposition that was recorded along the southern aspect of the depositional lobe and the widening of the south trailing ridge for each parabolic dune.

During the four periods of field observations sediment transport was observed on each occasion, but to varying degrees of activity. Sediment transport activity was most common on the highest and least vegetated portions of the individual dune landform units. The vegetation density within and around the individual dunes increased from the summer to the winter field observations. During the November 2006 field observations, sediment transport was observed across the depositional lobes of each dune from the north to southerly direction. This southerly sediment transport was due to the winds associated with the passing of a cold front, which occurred during the study site visit.

It is assumed the greater the amount of seasonal precipitation the less potential for seasonal sediment transport, due to the cohesive properties of moisture. The fall season receives the highest amount of seasonal precipitation and the winter season receives the lowest amount of seasonal precipitation. It can therefore be inferred that the winds that

occur during the fall season have the least influence on dune morphology and the winter wind regime has the greatest influence on dune morphology. However, the summer and spring wind regimes are very similar and display similarities in resultant drift directions (RDD). The combined influence of the summer and spring season wind regimes can be seen in the general orientation of parabolic dunes 1, 2, and 3, as all three dunes are similar in orientation to the summer and spring seasonal resultant drift directions.

The individual dunes all experienced westerly migration from June 2006 to February 2007 and dune migrations were recorded in the total station surveys. The individual dune landform units expanded over the course of the field observations, with the most noticeable migration and expansion of landform units occurring along the depositional lobes of dune 2 and dune 3. A longer period of extensive field observations would reveal more insight into the dynamics of sediment deposition and individual dune morphology.

8. Conclusion

8.1 Introduction

This chapter is divided into three parts: conclusions based on data analysis and field observation, a parabolic dune development model, and directions for future research. The results of this research indicate that parabolic dunes on North Padre Island, Texas develop and evolve in a systematic fashion, as indicated from doqq analysis, field survey and observation, and wind data analysis. The wind regime for this coastal location displays a seasonal component in regards to the direction of effective winds and resultant drift direction. The directional aspects of the wind regime that have the most influence on parabolic dune migration and orientation are winds from the onshore directions, out of the SE and SSE, and northerly winds out of the N, NNW, and NNE. Based on the available data and field observations an three stage model of parabolic dune evolution has been developed for North Padre Island, Texas. This parabolic dune development model is based from parabolic dunes developing from blowout dunes.

8.2 Parabolic Landform Unit Change and Migration

General dune migration rates for the three parabolic dunes studied for this research are similar to migration rates observed in coastal locations by Anthonsen et al. (1996) in coastal Denmark and Pye (1982) in Queensland, Australia in inland locations by Marin et al. (2005) in SW Colorado. Parabolic dune migration rates for the three individual dunes vary according to the method of measurement, and range from 17.7 m/yr to 1.6 m/yr depending on the individual dune (see Table 6.1). Accordingly, overall dune migration is less than individual dune landform unit migration rates. The

depositional lobe is the most rapidly migrating feature, followed by the trailing ridges, and then the deflation basin. The south trailing ridge of three parabolic dunes is wider and has a lower elevation compared to the north trailing ridge. All three dunes exhibit this dune asymmetry in reference to the south trailing ridge and also in regards to having a lower vegetation density compared the north trailing ridge.

The lowest rate of parabolic dune migration occurs in the smallest dune (dune 1) and the highest dune migration rate occurs in the largest parabolic dune (dune 3). Individual landform unit migration varies for each of the three dunes studied and all migration rates are detailed in Table 6.2. The dune landform unit which displays the highest individual rate of migration is the depositional lobe of parabolic dune 3 which is 35.4 m/a^{-1} from 2004 – 06. However, the same landform unit in dune 2 displays the highest rate of migration in both 1996 – 2004 and from 2006 – 07 at 13.81 m/a^{-1} and 8.6 m/a^{-1} (Table 6.2). Within the dunes individual landform unit migration and development varies. For example, depositional lobes expand from 0.7 to 1.7 m/a^{-1} in dune 1, from 1.8 to 13.8 m/a^{-1} in dune 2, and 8.2 to 17.7 m/a^{-1} in dune 3. Similarly, deflation basins migrate at rates that vary from 1.25 to 2 m/a^{-1} for dune 1, from 1 to 6.3 m/a^{-1} for dune 2, and 1 to 7.4 m/a^{-1} in dune 3. The rates of trailing ridge migration vary from approximately zero to 1.5 m/a^{-1} for dune 1, to $\sim 14 \text{ m/a}^{-1}$ to approximately zero for dune 2, and from 10.3 m/a^{-1} to approximately zero for dune 3. Accordingly, individual dune landform unit expansion and change in area also varies as noted in Table 6.3. Vegetation density within individual landform units is the main factor in influencing migration rates, due to the sediment trapping properties and stabilizing effects of the vegetation root systems.

The depositional lobe and south trailing ridge display the influence of northerly winds as evidenced by survey data. Also, all three dunes are active under the current climatic conditions, and migrating in the northwesterly direction between $\sim 290^{\circ} - 320^{\circ}$. The orientation of these three dunes is similar to the resultant drift directions of the total wind regime sand roses for the Bob Hall Pier and Corpus Christi International Airport, and the summer sand roses for each weather station. Within the mature parabolic dunes 2 and 3, gegenwalle ridges have developed surrounding the vegetated portion of the depositional lobe, which indicate the activity of converging winds inside the parabolic dunes.

8.3 Generalized Model of Parabolic Dune Development for Padre Island, TX

The parabolic dunes along North Padre Island have initially developed from blowout dunes that formed along the foredune and within the dune field. Once a blowout dune has established and revegetation has not occurred, the potential for parabolic dune development exists, due to the combined factors of sediment supply, variations in vegetation density, environmental conditions, (i.e.: climate and precipitation) and the sediment transport potential of the wind regime. If all of these factors exist in this barrier island environment along the Central Texas coast then parabolic dune development can be anticipated.

Since parabolic dune development and evolution initiates from a blowout dune, the first stage in the generalized parabolic dune model for Padre Island, TX (GPMPI) is an incipient parabolic dune as seen in Fig. 8.1. “Stage 1” consists of an incipient parabolic dune characterized by simple and well defined parabolic dune landform units:

depositional lobe, trailing ridges, and deflation basin. The “Stage 1” parabolic dune is oriented in the general direction of the resultant drift direction (RDD) and most closely corresponds to the sand rose calculated from the Bob Hall Pier (BHP) data. The trailing ridges are nearly symmetrical and display a slight influence of the northerly winds generally associated with the passing of cold fronts. At this initial stage the parabolic dune is lobate with a length to width ratio (LWR) of 1.0 to 3.0. The “Stage 1” parabolic dune may either be closed or open at the throat of the dune, for the purpose of model display “Stage 1” is closed.

The second stage of the GPMPI is divided into two aspects: 2 and 2'. “Stage 2” indicates parabolic dune development from a “Stage 1” parabolic dune into a more complex elongate parabolic dune. At “Stage 2” the parabolic dune has migrated in the direction of the RDD, with minimal widening of the dune, specifically in regards to widening of the south trailing ridge. The “Stage 2” parabolic dune displays asymmetry in regards to the trailing ridges, which indicate the influence of the northerly winds. However, the “Stage 2” parabolic dune still maintains its elongate characteristics and form. There is potential for complete revegetation of the “Stage 2” parabolic dune and this change in morphology is indicated in “Stage 2a”. Complete parabolic dune revegetation was observed in the eight year period between doqqs (1996 to 2004), where areas of up to 2.2 acres of active sediment were observed being stabilized.

The parabolic dunes that develop and evolve on Padre Island are also likely to continue development from a “Stage 1” parabolic dune into a “Stage 2' ” dune, which differs from a “Stage 2” dune by its lobate shape. The “Stage 2' ” parabolic dune is distinguished from the “Stage 2” dune by the increase in dune width that is accompanied

Generalized Model of Parabolic Dune Evolution and Development for Padre Island, TX

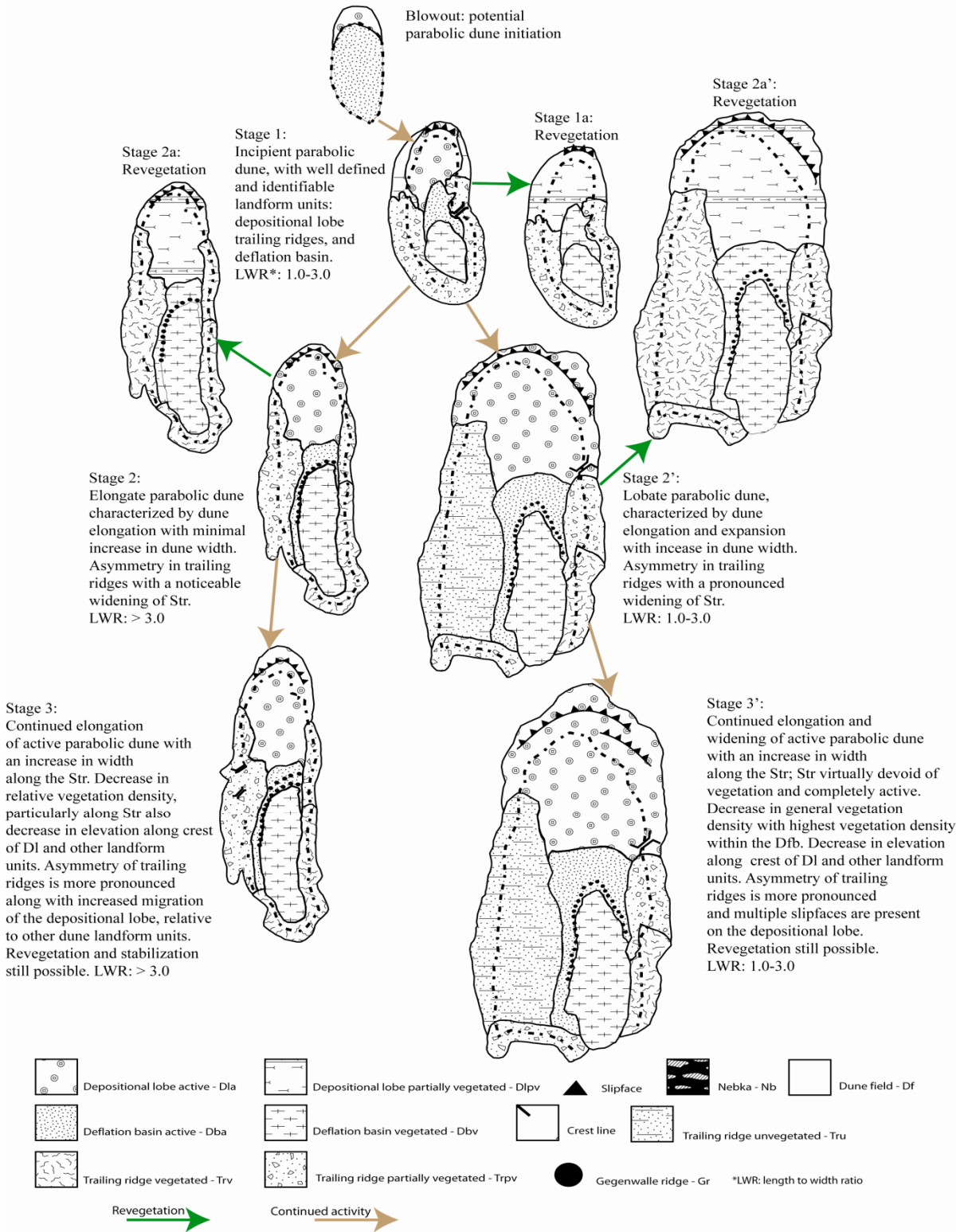


Figure 8.1 Generalized model of parabolic dune development for Padre Island, TX based on field observations, surveys and doqq analysis

by dune migration and elongation. The south trailing ridge of the “Stage 2’ ” dune is wider and more elongate than the north trailing ridge and trailing ridge asymmetry is pronounced generally due to the influence of northerly winds and the surrounding topography. There is still potential for complete dune stabilization and revegetation, which is noted in “Stage 2a’ ”.

The final stages in Padre Island parabolic dune evolution are “Stage 3” and “Stage 3’ ”. The “Stage 3” parabolic dune is a continuation of the “Stage 2” parabolic dune, but characterized by a decrease in elevation along the crestline of the depositional lobe and other landform units. The “Stage 3” parabolic dune continues to maintain its elongate form, although the LWR decreases slightly. The vegetation density within the parabolic dune decreases and sediment transport within the dune and along the trailing ridges increases allowing for continued downwind migration towards the northwest. The decrease in vegetation within the parabolic dune also allows for greater morphological influence of the northerly winds and particularly in regards to the south trailing ridge. The “Stage 3’ ” parabolic dune corresponds to the morphological changes that accompany the “Stage 3” dune, but the “Stage 3’ ” dune maintains its lobate form. Due to its larger sediment supply relative to a “Stage 3” parabolic dune of the same length, the “Stage 3’ ” parabolic dune develops a more complex depositional lobe, which may develop multiple slipfaces and en-echelon dune forms.

8.4 Data Limitations and Areas for Future Research

Due to a fire at the Padre Island National Seashore ranger station (PAIS) aerial photos dating from at least the 1940’s were destroyed. A more extensive historical

record of aerial photos would have provided a more complete reference to gauge parabolic dune migration rates, changes in dune vegetation density, and landscape change. The wind records demonstrate there were inconsistencies in wind record data sets, specifically the PAIS wind data set. The wind data recorded at PAIS was recorded daily at 10 am and the daily record does not provide an accurate description of the regional wind regime, as seen from the three other data sets. The PAIS ranger station is located approximately 700 meters from the shoreline. The location of the ranger station relative to the dune locations would provide an excellent reference of wind regime at an inland location, if hourly wind data was recorded at this location. The Bob Hall Pier and South Bird Island weather stations probably provide the most accurate depiction of the local wind regime. The location of the Bob Hall Pier weather station is over the Gulf of Mexico and does not experience any influence from the topography, unlike at the dune locations. The South Bird Island weather station is located over open water on a platform in Laguna Madre, west of the dune locations. The South Bird Island weather station probably experiences the influence of north winds more intensely than at the dune sites, due to the lack of surrounding topographic influence.

Future parabolic dune research at Padre Island National Seashore would benefit from conducting more frequent dune surveys, and from using more accurate mapping and survey equipment. A “backpack” GPS system, such as the Topcon GMS 110 GIS mapping system or the Sokkia GSR 2650 LB system would allow for data acquisition needing only one person, therefore reducing the need for field assistants and therefore increase the potential for increased survey frequency.

Parabolic dune research in Padre Island National Seashore and at other locations would benefit from an extensive month long (or longer) monitoring of multiple or an individual parabolic dunes. Establishing a weather station within the deflation basin of a parabolic dune would provide a wind and weather record for conditions within the dune, and present an insight into the micro climate within a parabolic dune. Surface moisture measurement could also be recorded on specific dune landform units and locations to present conditions under which moist sediment is transported within the dune. The biological and environmental components of parabolic dunes also could be studied to understand the relationships between dune biology and animal species.

Bibliography

- Abrogast, A., Hansen, E. and Van Oort, M., 2002. *Reconstructing the geomorphic evolution of large coastal dunes along the southeastern shore of Lake Michigan*. *Geomorphology*, 46: 241-256.
- American Meteorological Society. <http://ametsoc.org>
- Andrews, B., Gares, P. and Colby, J., 2002. *Techniques for GIS modeling of coastal dunes*. *Geomorphology*, 48: 289-308.
- Anthonsen, K., 1997. *Evolution of a parabolic dune, Rabjerg Mile, Skagen Odde, and its relationship to other Danish dune formations*. EUCC Dune seminar, Skagen, Denmark: 22-26.
- Anthonsen, K.C., L. and Jensen, J., 1996. *Evolution of a dune from crescentic to parabolic form in response to short-term climatic changes: Rabjerg Mile, Skagen Odde, Denmark*. *Geomorphology*, 17: 63-78.
- Bagnold, R., 1966. *An Approach to the Sediment Transport Problem from General Physics. Physiographic and hydraulic studies of rivers*, 422-I. United States Geological Survey Professional Paper, Washington D.C.
- Bailey, S. and Bristow, C. 2004. *Migration of parabolic dunes at Aberffraw, Anglesey, north Wales*. *Geomorphology*, 59: 165-175.
- Barbour, M. 1992. *Life at the leading edge: the beach plant syndrome*. Coastal Plant Communities of Latin America. Academic Press, New York, 392 pp.
- Bartlett, D., and Smith, J., 2005. *GIS for coastal zone management*. CRC Press, Boca Raton, 392 pp.
- Blum, M., and Jones, J., 1985. *Variations in vegetation density and foredune complexity at North Padre Island, Texas*. *The Texas Journal of Science*, 37(1): 63-74.
- Boak, E., and Turner, I., 2005. *Shoreline definition and detection: a review*. *Journal of Coastal Research*, 21(4): 688-704.
- Bullard, J., 1997. *A note on the use of the "Fryberger Method" for evaluating potential sand transport by wind*. *Journal of Sedimentary Research*, 67(May): 499-502.
- Coaldrake, J., 1962. *The coastal sand dunes of southern Queensland*. *Proceedings of the Royal Society of Queensland*, 22(7): 101-120.

- Cooper, W. 1923. *The recent ecological history of Glacier Bay, Alaska: the interglacial forests of Glacier Bay*. Ecology, 2(1): 93-128.
- Cooper, W. 1938. *Ancient dunes of the upper Mississippi Valley as possible climatic indicators*. Bulletin of the American Meteorological Society, 19(May): 33-45.
- Cooper, W. 1958. Coastal Sand Dunes of Oregon and Washington. The Geological Society of America, Inc, Boulder, 169 pp.
- Cooper, W., 1967. Coastal Dunes of California. The Geological Society of America, Inc, Boulder, 131 pp.
- David, P., 1977. *Sand dune occurrences of Canada: A theme and resource inventory study of eolian landforms of Canada*. Sand dune occurrences of Canada. Indian and Northern Affairs National Parks Branch, Montreal.
- David, P., 1981. *Stabilized dune ridges in Northern Saskatchewan*. Canadian Journal of Earth Science, 18: 286-311.
- David, P., Wolfe, S., Huntley, D., and Lemmen, D., 1999. *Activity cycle of parabolic dunes based on morphology and chronology from Seward sand hills, Saskatchewan. Holocene Climate and Environmental Change in the Palliser Triangle: A Geoscientific Context for Evaluating the Impacts of Climate Change on the Southern Canadian Prairies*. Geological Survey of Canada, Montreal.
- Duran, O., Schatz, V., Herrman, H. and Tsoar, H., 2006. *Transformation of barchans into parabolic dunes under the influence of vegetation*.
- Filion, L., 1987. *Holocene development of parabolic dunes in the central St. Lawrence lowland, Quebec*. Quaternary Research, 28: 194-210.
- Filion, L. and Morriset, P., 1983. *Eolian landforms along the eastern coast of Hudson Bay, Northern Quebec*. Nordicana, 47: 73-85.
- Forman, S. and Pierson, J., 2003. *Formation of linear and parabolic dunes on the eastern Snake River Plain, Idaho in the nineteenth century*. Geomorphology, 56: 189-201.
- Fryberger, S. and Dean, G., 1979. *Dune forms and wind regime*. A Study of Global Sand Seas. United States Geological Survey, Washington D.C., 429 pp.
- Gares, P. and Nordstrom, K., 1995. *A cyclic model of foredune blowout evolution for a leeward coast: Island Beach, New Jersey*. Annals of the Association of American Geographers, 85(1): 1-20.
- Hack, J., 1941. *Dunes of the western Navajo Country*. Geographical Review, 31(April): 240-264.

- Halsey, L. Catto, N. and Rutter, N. 1990. *Sedimentology and development of parabolic dunes, Grande Prairie dune field, Alberta*. Canadian Journal of Earth Science, 27: 1762-1778.
- Hesp, P., 1981. *The formation of shadow dunes*. Journal of Sedimentary Research, 51(1): 101-112.
- Hesp, P., 2002. *Foredunes and blowouts: initiation, geomorphology and dynamics*. Geomorphology, 48: 245-269.
- Hesp, P., and Hyde, R. 1996. *Flow dynamics and geomorphology of a trough blowout*. Sedimentology, 43: 505-526.
- Hogbom, I. 1923. *Ancient inland dunes of Northern and Middle Europe*. Geografiska Annaler, 5: 113-243
- Hugenholtz, C. and Wolfe, S., 2005. *Biogeomorphic model of dunefield activation and stabilization on the northern Great Plains*. Geomorphology, 70: 53-70.
- Hugenholtz, C. and Wolfe, S., 2006. *Morphodynamics and climate controls of two aeolian blowouts on the northern Great Plains, Canada*. Earth Surface Processes and Landforms, 31(May): 1540-1588.
- Inman, D., Ewing, G. and Corliss, J., 1966. *Coastal sand dunes of Guerrero Negro, Baja California, Mexico*. Geological Society of America Bulletin, 77(August): 787-803.
- Jennings, J. 1957. *On the orientation of parabolic or U-dunes*. Geographical Journal, 123(4): 474-801.
- Kadmon, R. and Hari.-Kari., R., 1999. *Studying long-term vegetation dynamics using digital processing of historical aerial photographs*. Remote Sensing of the Environment, 68: 164-177.
- Kar, A. 1990. *Megabarchanoids of the Thar: their environment, morphology and relationship with longitudinal dunes*. Geographical Journal, 156(1): 51-62.
- Kumler, M. 1969. *Plant succession on the sand dunes of the Oregon coast*. Ecology, 50(4): 695-705.
- Landsberg, S. 1956. *The orientation of dunes in Britian and Denmark in relation to wind*. Geographical Journal, 122(2): 176-190.
- Leatherman, S. 1979. *Barrier Islands from the Gulf of St. Lawrence to the Gulf of Mexico*. Accademic Press, New York, 325 pp.

- Lees, B. 2006. *Timing and formation of coastal dunes in Northeastern Australia*. Journal of Coastal Research, 22:78-89.
- Marin, L, Forman, S. Valdez, A. and Bunch, F. 2005. *Twentieth century dune migration at the Great Sand Dunes National Park and Preserve, Colorado, relation to drought variability*. Geomorphology, 70: 163-184.
- McKee, E. 1966. *Structures of dunes at White Sand National Monument, New Mexico (and a comparison with structures of dunes from other selected areas)*. Sedimentology, 7(1): 3-70.
- McKee, E. 1979. *Sedimentary structures in dunes. A Study of Global Sand Seas*. United States Geological Survey, Washington D.C., 429 pp.
- Melton, F. 1940. *A tentative classification of sand dunes its application to dune history in the southern High Plains*. Journal of Geology, 2(February-March): 113-161.
- Moore, L. 2000. *Shoreline mapping techniques*. Journal of Coastal Research, 16(1): 111-125.
- Moreno-Casasola, P. 1986. *Sand movement as a factor in the distribution of plant communities in a coastal dune system*. Vegetatio, 65: 67-77.
- Moreno-Casasola, P. and Espejel, I. 1986. *Classification and ordination of coastal sand dune vegetation along the Gulf and Caribbean Sea of Mexico*. Vegetatio, 66: 147-183.
- Morton, R., 1994. *Texas Barriers*. Geology of Holocene Barrier Island Systems. Springer-Verlag, Berlin, 464 pp.
- Muhs, D. and Wolfe, S. 1999. *Sand dunes of the northern Great Plains of Canada and the United States. Holocene Climate and Environmental Change in the Palliser Triangle: A Geoscientific Context for Evaluating the Impacts of Climate Change on the Southern Canadian Prairies*. Geological Survey of Canada, Montreal.
- National Climate Data Center. <http://www.ncdc.noaa.gov/oa/ncdc/html>
- Nordstrom, K, Psuty, N, and Carter, B, 1990. *Coastal Dune Form and Process*. John Wiley and Sons. Ltd, New York, 392 pp.
- Pearce, K. and Walker, I., 2005. *Frequency and magnitude biases in the 'Fryberger' model, with implications for characterizing geomorphically effective winds*. Geomorphology, 68: 39-56.

- Pye, K., 1982. *Morphological development of coastal dunes in a humid tropical environment, Cape Bedford and Cape Flattery, North Queensland*. Geografiska Annaler, 64(3/4): 213-227.
- Pye, K., 1983. *Formation and history of Queensland coastal dunes*. Zeitschrift Fur Geomorphologie, Supplement 45(May): 175-204.
- Pye, K., 1993. *Late Quaternary development of coastal parabolic megadune complexes in northeastern Australia*. International Association of Sedimentology, 16: 23-45.
- Pye, K., and Blott, S., 2006. *Coastal processes and morphological change in the Dunwich-Sizewell area, Suffolk, UK*. Journal of Coastal Research, 22(3): 453-474.
- Pye, K. and Tsoar, H., 1990. *Aeolian Sand and Sand Dunes*. Unwin Hyman Ltd, London, 396 pp.
- Robertson-Rintoul, M. 1990. A quantitative analysis of near-surface wind flow pattern over coastal parabolic dunes. *Coastal Dunes: Form and Process*. John Wiley & Sons. Ltd, New York, 392 pp.
- Semeniuk, V. Cresswell, I. and Wurm, P. 1989. *The Quindalup Dunes: the regional system, physical framework and vegetation habitats*. Journal of the Royal Society of Western Australia, 71(2 & 3): 23-48.
- Shepard, F. 1960. *Gulf Coast Barriers*. Recent sediments, northwest Gulf of Mexico. American Association of Petroleum Geologists, Tulsa, OK.
- Southern Regional Climate Center. <http://www.srcc.lsu.edu/southernClimate/atlas/>
- Story, R. 1982. *Notes on parabolic dunes, winds and vegetation in Northern Australia*. CSIRO Australian Division of Water and Land Resources, 43: 1-34.
- Thomas, D. and Tsoar, H., 1990. *The Geomorphic role of vegetation in desert dune systems*. Vegetation and Erosion: Processes and Environments. John Wiley & Sons, New York, 518 pp.
- Thompson, C. 1983. *Development and weathering of large parabolic dune systems along the subtropical coast of eastern Australia*. Zeitschrift Fur Geomorphologie, Supplement 45(May): 205-226.
- Texas Natural Resources Information System. <http://tnris.state.tx.us/>
- Texas Coastal Ocean Observation Network <http://lighthouse.tamucc.edu/TCOON/HomePage>
- Wasson, R.J., Rajaguru, S. N., Misra, V. N., Agrawal, D. P., Dhir, R. P., Singhvi, A. K. and Kameswara Rao, K., 1983. *Geomorphology, late Quaternary stratigraphy and*

- palaeoclimatology of the Thar dunefield*. Zeitschrift Fur Geomorphologie, Supplement 45(May): 117-151.
- Weise, B. and White, W. 1980. Padre Island National Seashore: A guide to the geology, natural environments, and history of a Texas barrier island. Bureau of Economic Geology; University of Texas at Austin, Austin, TX, 94 pp.
- Wolfe, S. and David, P., 1997. *Parabolic dunes: examples from the Great Sand Hills, southwestern Saskatchewan*. The Canadian Geographer, 41(2): 207-214.
- Wolfe, S. and Lemmen, D. 1999. *Monitoring of dune activity in the Great Sand Hills region, Saskatchewan. Holocene Climate and Environmental Change in the Palliser Triange: A Geoscientific Context for Evaluating the Impacts of Climate Change on the Southern Canadian Prairies*. Geological Survey of Canada, Montreal.
- Wright, L. and Short, A. 1984. *Morphodynamic variability of surf zones and beaches: a synthesis*. Marine Geology, 56: 93-119.

Appendix: Sand Rose Sediment Drift Potentials Tables

Bob Hall Pier 1996-2007 Total

Wind Directions	Wind classes		WF		WF		WF		WF		WF		WF		DP's
	5.6 to <=7	0.49	7 to <=8.7	1.71	8.7 to <=11.3	4.93	11.3 to <=14.3	12.66	14.3 to <=17.4	27.07	17.4 to <=35	145.02	35 to <=50	676.00	
CALM	0.00%	0.00%	0.00%	0.00%	0.00%	0.00%	0.00%	0.00%	0.00%	0.00%	0.00%	0.00%	0.00%	0.00%	0.00%
E	1.92%	0.93%	1.18%	2.01%	0.42%	2.06%	0.12%	1.48%	0.01%	0.23%	0.01%	0.91%	0.00%	0.00%	7.62%
ENE	1.13%	0.55%	0.81%	1.39%	0.45%	2.24%	0.11%	1.39%	0.01%	0.25%	0.01%	1.21%	0.00%	0.00%	7.02%
ESE	3.67%	1.79%	3.28%	5.61%	1.39%	6.84%	0.09%	1.17%	0.00%	0.11%	0.00%	0.60%	0.00%	0.00%	16.13%
N	1.07%	0.52%	1.32%	2.26%	1.29%	6.37%	0.49%	6.25%	0.07%	1.95%	0.00%	0.45%	0.00%	0.00%	17.81%
NE	1.08%	0.52%	0.93%	1.60%	0.73%	3.58%	0.19%	2.45%	0.03%	0.93%	0.01%	1.51%	0.00%	0.00%	10.60%
NNE	0.87%	0.42%	1.05%	1.79%	1.15%	5.65%	0.37%	4.71%	0.06%	1.75%	0.01%	0.76%	0.00%	0.00%	15.08%
NNW	0.66%	0.32%	0.72%	1.22%	0.78%	3.86%	0.23%	2.90%	0.03%	0.68%	0.00%	0.45%	0.00%	0.00%	9.43%
NW	0.31%	0.15%	0.44%	0.75%	0.41%	2.03%	0.12%	1.56%	0.02%	0.45%	0.00%	0.00%	0.00%	0.00%	4.94%
S	1.09%	0.53%	1.15%	1.97%	0.96%	4.73%	0.23%	2.89%	0.02%	0.45%	0.00%	0.00%	0.00%	0.00%	10.57%
SE	4.69%	2.28%	5.61%	9.60%	4.13%	20.35%	0.50%	6.31%	0.02%	0.59%	0.00%	0.60%	0.00%	0.00%	39.73%
SSE	2.70%	1.31%	3.31%	5.67%	3.04%	15.00%	0.65%	8.21%	0.05%	1.24%	0.01%	1.06%	0.00%	0.00%	32.49%
SSW	0.20%	0.10%	0.11%	0.19%	0.05%	0.23%	0.01%	0.08%	0.00%	0.00%	0.00%	0.00%	0.00%	0.00%	0.60%
SW	0.05%	0.02%	0.03%	0.05%	0.00%	0.01%	0.00%	0.00%	0.00%	0.00%	0.00%	0.00%	0.00%	0.00%	0.08%
W	0.04%	0.02%	0.04%	0.07%	0.02%	0.10%	0.01%	0.07%	0.00%	0.00%	0.00%	0.00%	0.00%	0.00%	0.26%
WNW	0.12%	0.06%	0.12%	0.21%	0.14%	0.67%	0.03%	0.36%	0.00%	0.03%	0.00%	0.15%	0.00%	0.00%	1.48%
WSW	0.03%	0.01%	0.01%	0.02%	0.01%	0.07%	0.01%	0.09%	0.00%	0.00%	0.00%	0.00%	0.00%	0.00%	0.20%
Totals	19.61%	9.54%	20.12%	34.41%	14.98%	73.81%	3.15%	39.91%	0.32%	8.66%	0.05%	7.71%	0.00%	0.00%	174.04%

Bob Hall Pier 1996-2007 Winter

Wind Directions	Wind classes		WF		WF		WF		WF		WF		WF		DP's
	5.6 to <=7	0.49	7 to <=8.7	1.71	8.7 to <=11.3	4.93	11.3 to <=14.3	12.66	14.3 to <=17.4	27.07	17.4 to <=35	145.02	35 to <=50	676.00	
E	0.85%	0.41%	0.40%	0.68%	0.13%	0.66%	0.05%	0.62%	0.00%	0.00%	0.00%	0.00%	0.00%	0.00%	2.38%
ENE	0.65%	0.31%	0.32%	0.54%	0.36%	1.78%	0.09%	1.18%	0.00%	0.00%	0.00%	0.00%	0.00%	0.00%	3.83%
ESE	1.77%	0.86%	1.07%	1.84%	0.21%	1.04%	0.00%	0.05%	0.00%	0.00%	0.00%	0.00%	0.00%	0.00%	3.79%
N	1.98%	0.96%	2.63%	4.50%	2.48%	12.23%	0.81%	10.25%	0.12%	3.19%	0.00%	0.59%	0.00%	0.00%	31.72%
NE	1.51%	0.73%	1.32%	2.26%	1.22%	5.99%	0.24%	3.09%	0.03%	0.88%	0.01%	1.77%	0.00%	0.00%	14.73%
NNE	1.57%	0.77%	1.89%	3.23%	2.26%	11.12%	0.66%	8.34%	0.07%	1.87%	0.00%	0.00%	0.00%	0.00%	25.34%
NNW	1.43%	0.69%	1.57%	2.69%	1.59%	7.84%	0.51%	6.44%	0.05%	1.32%	0.00%	0.00%	0.00%	0.00%	18.99%
NW	0.61%	0.30%	0.85%	1.46%	0.95%	4.67%	0.24%	3.04%	0.02%	0.55%	0.00%	0.00%	0.00%	0.00%	10.02%
S	0.99%	0.48%	0.95%	1.62%	0.69%	3.41%	0.23%	2.94%	0.03%	0.88%	0.00%	0.00%	0.00%	0.00%	9.33%
SE	3.48%	1.69%	2.55%	4.36%	1.02%	5.03%	0.09%	1.13%	0.00%	0.00%	0.00%	0.00%	0.00%	0.00%	12.22%
SSE	2.14%	1.04%	2.22%	3.80%	1.58%	7.80%	0.38%	4.79%	0.06%	1.54%	0.00%	0.00%	0.00%	0.00%	18.97%
SSW	0.22%	0.11%	0.11%	0.19%	0.06%	0.28%	0.00%	0.00%	0.00%	0.00%	0.00%	0.00%	0.00%	0.00%	0.58%
SW	0.02%	0.01%	0.01%	0.02%	0.00%	0.00%	0.00%	0.00%	0.00%	0.00%	0.00%	0.00%	0.00%	0.00%	0.03%
W	0.08%	0.04%	0.10%	0.17%	0.04%	0.20%	0.01%	0.15%	0.00%	0.00%	0.00%	0.00%	0.00%	0.00%	0.57%
WNW	0.23%	0.11%	0.23%	0.40%	0.24%	1.16%	0.04%	0.46%	0.00%	0.00%	0.00%	0.00%	0.00%	0.00%	2.14%
WSW	0.02%	0.01%	0.02%	0.03%	0.00%	0.00%	0.00%	0.00%	0.00%	0.00%	0.00%	0.00%	0.00%	0.00%	0.04%
Totals	17.56%	8.54%	16.26%	27.81%	12.83%	63.22%	3.36%	42.50%	0.38%	10.25%	0.02%	2.36%	0.00%	0.00%	154.67%

Bob Hall Pier 1996-2007 Spring

Wind Directions	Wind classes		WF		WF		WF		WF		WF		WF		DP's
	5.6 to <=7	0.49	7 to <=8.7	1.71	8.7 to <=11.3	4.93	11.3 to <=14.3	12.66	14.3 to <=17.4	27.07	17.4 to <=35	145.02	35 to <=50	676.00	
E	2.66%	1.29%	1.84%	3.15%	0.75%	3.69%	0.17%	2.14%	0.02%	0.67%	0.01%	1.19%	0.00%	0.00%	12.13%
ENE	1.45%	0.71%	1.17%	2.00%	0.74%	3.63%	0.14%	1.77%	0.02%	0.45%	0.01%	1.19%	0.00%	0.00%	9.74%
ESE	4.63%	2.25%	4.77%	8.16%	2.50%	12.32%	0.21%	2.66%	0.00%	0.11%	0.00%	0.00%	0.00%	0.00%	25.50%
N	0.64%	0.31%	0.81%	1.39%	0.94%	4.64%	0.36%	4.58%	0.09%	2.34%	0.00%	0.60%	0.00%	0.00%	13.87%
NE	1.20%	0.58%	1.07%	1.84%	0.77%	3.81%	0.24%	3.07%	0.05%	1.23%	0.01%	1.79%	0.00%	0.00%	12.32%
NNE	0.52%	0.25%	0.72%	1.23%	0.95%	4.68%	0.34%	4.27%	0.07%	1.78%	0.00%	0.60%	0.00%	0.00%	12.82%
NNW	0.39%	0.19%	0.49%	0.84%	0.63%	3.08%	0.23%	2.86%	0.02%	0.56%	0.01%	1.19%	0.00%	0.00%	8.72%
NW	0.27%	0.13%	0.37%	0.64%	0.32%	1.56%	0.13%	1.67%	0.04%	1.00%	0.00%	0.00%	0.00%	0.00%	5.00%
S	0.62%	0.30%	0.67%	1.14%	0.63%	3.12%	0.14%	1.72%	0.01%	0.33%	0.00%	0.00%	0.00%	0.00%	6.62%
SE	5.07%	2.47%	7.90%	13.51%	6.43%	31.68%	1.05%	13.28%	0.05%	1.34%	0.01%	1.19%	0.00%	0.00%	63.48%
SSE	2.34%	1.14%	3.23%	5.53%	3.28%	16.16%	0.85%	10.73%	0.09%	2.45%	0.02%	3.58%	0.00%	0.00%	39.59%
SSW	0.16%	0.08%	0.09%	0.15%	0.02%	0.10%	0.00%	0.05%	0.00%	0.00%	0.00%	0.00%	0.00%	0.00%	0.39%
SW	0.04%	0.02%	0.03%	0.05%	0.00%	0.00%	0.00%	0.00%	0.00%	0.00%	0.00%	0.00%	0.00%	0.00%	0.07%
W	0.05%	0.02%	0.02%	0.04%	0.01%	0.06%	0.00%	0.00%	0.00%	0.00%	0.00%	0.00%	0.00%	0.00%	0.12%
WNW	0.10%	0.05%	0.08%	0.13%	0.08%	0.41%	0.04%	0.52%	0.00%	0.11%	0.00%	0.60%	0.00%	0.00%	1.82%
WSW	0.01%	0.01%	0.00%	0.01%	0.00%	0.00%	0.00%	0.00%	0.00%	0.00%	0.00%	0.00%	0.00%	0.00%	0.01%
Totals	20.15%	9.80%	23.28%	39.82%	18.06%	88.95%	3.90%	49.33%	0.46%	12.37%	0.08%	11.94%	0.00%	2.87%	212.20%

Bob Hall Pier 1996-2007 Fall

Wind Directions	Wind classes		WF		WF		WF		WF		WF		WF		DP's
	5.6 to <=7	0.49	7 to <=8.7	1.71	8.7 to <=11.3	4.93	11.3 to <=14.3	12.66	14.3 to <=17.4	27.07	17.4 to <=35	145.02	35 to <=50	676.00	
E	2.05%	1.00%	1.25%	2.13%	0.46%	2.26%	0.15%	1.94%	0.01%	0.23%	0.00%	0.00%	0.00%	0.00%	7.56%
ENE	1.68%	0.82%	1.14%	1.96%	0.56%	2.76%	0.15%	1.88%	0.02%	0.46%	0.00%	0.00%	0.00%	0.00%	7.88%
ESE	3.00%	1.46%	2.59%	4.42%	0.84%	4.15%	0.09%	1.08%	0.00%	0.12%	0.00%	0.00%	0.00%	0.00%	11.22%
N	1.56%	0.76%	1.73%	2.97%	1.64%	8.09%	0.79%	10.01%	0.08%	2.19%	0.00%	0.62%	0.00%	0.00%	24.63%
NE	1.24%	0.60%	1.10%	1.88%	0.80%	3.94%	0.26%	3.23%	0.03%	0.81%	0.00%	0.62%	0.00%	0.00%	11.08%
NNE	1.21%	0.59%	1.39%	2.38%	1.27%	6.26%	0.46%	5.87%	0.11%	3.11%	0.01%	1.23%	0.00%	0.00%	19.44%
NNW	0.72%	0.35%	0.75%	1.28%	0.87%	4.27%	0.17%	2.15%	0.03%	0.81%	0.00%	0.00%	0.00%	0.00%	8.86%
NW	0.34%	0.17%	0.47%	0.80%	0.36%	1.78%	0.11%	1.45%	0.01%	0.23%	0.00%	0.00%	0.00%	0.00%	4.43%
S	0.87%	0.42%	0.96%	1.64%	0.97%	4.75%	0.37%	4.68%	0.01%	0.35%	0.00%	0.00%	0.00%	0.00%	11.85%
SE	3.68%	1.79%	3.73%	6.39%	1.88%	9.24%	0.24%	3.01%	0.00%	0.12%	0.00%	0.00%	0.00%	0.00%	20.54%
SSE	2.42%	1.18%	2.87%	4.91%	2.69%	13.26%	0.70%	8.83%	0.01%	0.35%	0.00%	0.00%	0.00%	2.87%	31.39%
SSW	0.17%	0.08%	0.14%	0.23%	0.06%	0.29%	0.01%	0.16%	0.00%	0.00%	0.00%	0.00%	0.00%	0.00%	0.77%
SW	0.09%	0.05%	0.06%	0.09%	0.00%	0.02%	0.00%	0.00%	0.00%	0.00%	0.00%	0.00%	0.00%	0.00%	0.16%
W	0.04%	0.02%	0.04%	0.07%	0.02%	0.08%	0.00%	0.05%	0.00%	0.00%	0.00%	0.00%	0.00%	0.00%	0.23%
WNW	0.11%	0.05%	0.16%	0.28%	0.21%	1.05%	0.03%	0.43%	0.00%	0.00%	0.00%	0.00%	0.00%	0.00%	1.81%
WSW	0.07%	0.03%	0.03%	0.04%	0.04%	0.21%	0.03%	0.32%	0.00%	0.00%	0.00%	0.00%	0.00%	0.00%	0.61%
Totals	19.25%	9.37%	18.40%	31.48%	12.67%	62.42%	3.56%	45.11%	0.32%	8.75%	0.02%	2.47%	0.00%	2.87%	162.46%

Bob Hall Pier 1996-2007 Survey

Wind Directions	Wind classes		WF		WF		WF		WF		WF		WF		DP's
	5.6 to <=7	0.49	7 to <=8.7	1.71	8.7 to <=11.3	4.93	11.3 to <=14.3	12.66	14.3 to <=17.4	27.07	17.4 to <=35	145.02	35 to <=50	676.00	
CALM	0.00%	0.00%	0.00%	0.00%	0.00%	0.00%	0.00%	0.00%	0.00%	0.00%	0.00%	0.00%	0.00%	0.00%	0.00%
E	1.19%	0.58%	0.61%	1.05%	0.07%	0.36%	0.02%	0.23%	0.00%	0.00%	0.00%	0.00%	0.00%	0.00%	2.21%
ENE	0.90%	0.44%	0.40%	0.68%	0.42%	2.05%	0.09%	1.14%	0.00%	0.00%	0.00%	0.00%	0.00%	0.00%	4.31%
ESE	3.21%	1.56%	1.93%	3.31%	0.34%	1.69%	0.02%	0.23%	0.00%	0.00%	0.00%	0.00%	0.00%	0.00%	6.79%
N	1.17%	0.57%	1.34%	2.29%	1.16%	5.69%	0.25%	3.20%	0.04%	0.98%	0.02%	2.62%	0.00%	0.00%	15.35%
NE	1.30%	0.63%	1.10%	1.88%	0.98%	4.80%	0.14%	1.83%	0.11%	2.93%	0.04%	5.24%	0.00%	0.00%	17.32%
NNE	1.32%	0.64%	1.54%	2.63%	1.81%	8.90%	0.52%	6.63%	0.07%	1.96%	0.00%	0.00%	0.00%	0.00%	20.75%
NNW	0.61%	0.30%	0.54%	0.93%	0.65%	3.20%	0.38%	4.80%	0.04%	0.98%	0.00%	0.00%	0.00%	0.00%	10.21%
NW	0.23%	0.11%	0.20%	0.34%	0.33%	1.60%	0.16%	2.06%	0.04%	0.98%	0.00%	0.00%	0.00%	0.00%	5.09%
S	1.19%	0.58%	1.23%	2.10%	1.63%	8.01%	0.45%	5.72%	0.02%	0.49%	0.00%	0.00%	0.00%	0.00%	16.89%
SE	4.71%	2.29%	5.63%	9.64%	3.07%	15.12%	0.34%	4.34%	0.00%	0.00%	0.00%	0.00%	0.00%	0.00%	31.40%
SSE	3.49%	1.70%	4.44%	7.60%	4.01%	19.75%	1.01%	12.80%	0.04%	0.98%	0.00%	0.00%	0.00%	0.00%	42.83%
SSW	0.18%	0.09%	0.18%	0.31%	0.14%	0.71%	0.02%	0.23%	0.00%	0.00%	0.00%	0.00%	0.00%	0.00%	1.34%
SW	0.09%	0.04%	0.04%	0.06%	0.00%	0.00%	0.00%	0.00%	0.00%	0.00%	0.00%	0.00%	0.00%	0.00%	0.11%
W	0.00%	0.00%	0.00%	0.00%	0.00%	0.00%	0.00%	0.00%	0.00%	0.00%	0.00%	0.00%	0.00%	0.00%	0.00%
WNW	0.02%	0.01%	0.04%	0.06%	0.02%	0.09%	0.02%	0.23%	0.00%	0.00%	0.00%	0.00%	0.00%	0.00%	0.39%
WSW	0.00%	0.00%	0.00%	0.00%	0.00%	0.00%	0.00%	0.00%	0.00%	0.00%	0.00%	0.00%	0.00%	0.00%	0.00%
Totals	19.63%	9.55%	19.22%	32.87%	14.61%	71.97%	3.43%	43.44%	0.34%	9.29%	0.05%	7.86%	0.00%	0.00%	174.97%

South Bird Island 1994-07 Total

Wind Directions	Wind classes		WF		WF		WF		WF		WF		WF		DP's
	5.6 to <=7	0.49	7 to <=8.7	1.71	8.7 to <=11.3	4.93	11.3 to <=14.3	12.66	14.3 to <=17.4	27.07	17.4 to <=35	145.02	35 to <=50	676.00	
E	1.54%	0.75%	0.72%	1.22%	0.21%	1.06%	0.31%	0.00%	0.03%	0.00%	0.60%	0.00%	0.00%	0.00%	3.96%
ENE	0.94%	0.46%	0.59%	1.01%	0.20%	1.01%	0.03%	0.36%	0.00%	0.08%	0.01%	1.04%	0.00%	0.00%	3.96%
ESE	3.25%	1.58%	2.44%	4.17%	0.72%	3.55%	0.02%	0.22%	0.00%	0.06%	0.00%	0.15%	0.00%	0.00%	9.73%
N	0.79%	0.38%	1.06%	1.80%	1.08%	5.32%	0.39%	4.92%	0.04%	1.19%	0.00%	0.45%	0.00%	0.00%	14.08%
NE	0.74%	0.36%	0.67%	1.15%	0.38%	1.87%	0.04%	0.55%	0.01%	0.36%	0.00%	0.60%	0.00%	0.00%	4.88%
NNE	1.07%	0.52%	1.11%	1.89%	1.10%	5.40%	0.49%	6.16%	0.05%	1.28%	0.01%	0.89%	0.00%	0.00%	16.15%
NNW	0.40%	0.20%	0.50%	0.85%	0.56%	2.75%	0.22%	2.83%	0.02%	0.64%	0.00%	0.00%	0.00%	0.00%	7.26%
NW	0.35%	0.17%	0.41%	0.70%	0.42%	2.09%	0.13%	1.64%	0.01%	0.28%	0.00%	0.00%	0.00%	0.00%	4.87%
S	0.63%	0.30%	0.40%	0.69%	0.16%	0.81%	0.02%	0.27%	0.00%	0.03%	0.00%	0.00%	0.00%	0.00%	2.11%
SE	5.28%	2.57%	5.16%	8.83%	3.11%	15.33%	0.23%	2.90%	0.01%	0.19%	0.00%	0.15%	0.00%	0.00%	29.98%
SSE	2.76%	1.34%	2.48%	4.25%	1.41%	6.97%	0.24%	3.01%	0.01%	0.36%	0.00%	0.45%	0.00%	0.00%	16.38%
SSW	0.18%	0.09%	0.08%	0.14%	0.02%	0.08%	0.00%	0.04%	0.00%	0.00%	0.00%	0.00%	0.00%	0.00%	0.34%
SW	0.04%	0.02%	0.02%	0.04%	0.00%	0.01%	0.00%	0.03%	0.00%	0.00%	0.00%	0.00%	0.00%	0.00%	0.09%
W	0.05%	0.02%	0.04%	0.07%	0.03%	0.15%	0.01%	0.10%	0.00%	0.00%	0.00%	0.00%	0.00%	0.00%	0.35%
WNW	0.17%	0.08%	0.18%	0.32%	0.15%	0.74%	0.06%	0.71%	0.01%	0.25%	0.00%	0.15%	0.00%	0.00%	2.25%
WSW	0.03%	0.02%	0.01%	0.02%	0.01%	0.07%	0.01%	0.10%	0.00%	0.00%	0.00%	0.00%	0.00%	0.00%	0.21%
Totals	18.23%	8.87%	15.88%	27.16%	9.58%	47.19%	1.91%	24.16%	0.18%	4.75%	0.03%	4.46%	0.00%	0.00%	116.60%

South Bird Island 1994-07 Winter

Wind Directions	Wind classes		WF		WF		WF		WF		WF		WF		DP's
	5.6 to <=7	0.49	7 to <=8.7	1.71	8.7 to <=11.3	4.93	11.3 to <=14.3	12.66	14.3 to <=17.4	27.07	17.4 to <=35	145.02	35 to <=50	676.00	
CALM	0.00%	0.00%	0.00%	0.00%	0.00%	0.00%	0.00%	0.00%	0.00%	0.00%	0.00%	0.00%	0.00%	0.00%	0.00%
E	0.46%	0.22%	0.08%	0.14%	0.03%	0.14%	0.01%	0.09%	0.00%	0.00%	0.00%	0.00%	0.00%	0.00%	0.60%
ENE	0.55%	0.27%	0.25%	0.42%	0.11%	0.52%	0.01%	0.09%	0.00%	0.00%	0.01%	1.06%	0.00%	0.00%	2.36%
ESE	1.18%	0.57%	0.45%	0.77%	0.08%	0.38%	0.00%	0.00%	0.00%	0.00%	0.00%	0.00%	0.00%	0.00%	1.72%
N	1.69%	0.82%	2.13%	3.64%	2.33%	11.47%	0.67%	8.52%	0.08%	2.27%	0.00%	0.00%	0.00%	0.00%	26.72%
NE	1.24%	0.60%	1.10%	1.88%	0.49%	2.42%	0.04%	0.46%	0.01%	0.20%	0.00%	0.53%	0.00%	0.00%	6.09%
NNE	1.89%	0.92%	2.05%	3.51%	2.03%	9.98%	0.82%	10.32%	0.06%	1.67%	0.00%	0.00%	0.00%	0.00%	26.41%
NNW	0.82%	0.40%	1.18%	2.02%	1.28%	6.31%	0.53%	6.73%	0.02%	0.59%	0.00%	0.00%	0.00%	0.00%	16.05%
NW	0.64%	0.31%	0.88%	1.50%	0.88%	4.36%	0.22%	2.81%	0.01%	0.20%	0.00%	0.00%	0.00%	0.00%	9.17%
S	0.62%	0.30%	0.40%	0.68%	0.21%	1.04%	0.04%	0.55%	0.00%	0.00%	0.00%	0.00%	0.00%	0.00%	2.58%
SE	3.29%	1.60%	2.68%	4.58%	1.29%	6.36%	0.03%	0.41%	0.00%	0.00%	0.00%	0.00%	0.00%	0.00%	12.96%
SSE	2.45%	1.19%	2.11%	3.62%	1.43%	7.03%	0.37%	4.65%	0.01%	0.20%	0.00%	0.00%	0.00%	0.00%	16.68%
SSW	0.20%	0.10%	0.08%	0.14%	0.02%	0.09%	0.00%	0.00%	0.00%	0.00%	0.00%	0.00%	0.00%	0.00%	0.33%
SW	0.05%	0.03%	0.01%	0.02%	0.00%	0.00%	0.00%	0.00%	0.00%	0.00%	0.00%	0.00%	0.00%	0.00%	0.05%
W	0.11%	0.05%	0.07%	0.12%	0.06%	0.30%	0.01%	0.09%	0.00%	0.00%	0.00%	0.00%	0.00%	0.00%	0.58%
WNW	0.37%	0.18%	0.40%	0.68%	0.27%	1.34%	0.12%	1.47%	0.01%	0.39%	0.00%	0.00%	0.00%	0.00%	4.08%
WSW	0.05%	0.02%	0.01%	0.01%	0.01%	0.04%	0.00%	0.00%	0.00%	0.00%	0.00%	0.00%	0.00%	0.00%	0.07%
Totals	15.61%	7.60%	13.89%	23.75%	10.51%	51.79%	2.86%	36.21%	0.20%	5.52%	0.01%	1.58%	0.00%	0.00%	126.44%

South Bird Island 1994-07 Spring

Wind Directions	Wind classes		WF		WF		WF		WF		WF		WF		DP's
	5.6 to <=7	0.49	7 to <=8.7	1.71	8.7 to <=11.3	4.93	11.3 to <=14.3	12.66	14.3 to <=17.4	27.07	17.4 to <=35	145.02	35 to <=50	676.00	
CALM	0.00%	0.00%	0.00%	0.00%	0.00%	0.00%	0.00%	0.00%	0.00%	0.00%	0.00%	0.00%	0.00%	0.00%	0.00%
E	2.34%	1.14%	1.34%	2.29%	0.43%	2.13%	0.06%	0.76%	0.00%	0.10%	0.00%	0.51%	0.00%	0.00%	6.92%
ENE	1.47%	0.71%	1.13%	1.93%	0.36%	1.77%	0.06%	0.71%	0.01%	0.29%	0.00%	0.00%	0.00%	0.00%	5.40%
ESE	4.72%	2.30%	4.20%	7.18%	1.32%	6.52%	0.03%	0.40%	0.00%	0.00%	0.00%	0.00%	0.00%	0.00%	16.39%
N	0.57%	0.28%	0.69%	1.19%	0.88%	4.33%	0.44%	5.57%	0.04%	1.14%	0.00%	0.51%	0.00%	0.00%	13.01%
NE	0.82%	0.40%	0.77%	1.31%	0.58%	2.88%	0.08%	0.98%	0.01%	0.38%	0.00%	0.51%	0.00%	0.00%	6.46%
NNE	0.90%	0.44%	0.92%	1.58%	1.02%	5.04%	0.46%	5.83%	0.04%	1.05%	0.01%	1.02%	0.00%	0.00%	14.96%
NNW	0.34%	0.17%	0.41%	0.70%	0.50%	2.44%	0.30%	3.83%	0.06%	1.71%	0.00%	0.00%	0.00%	0.00%	8.86%
NW	0.30%	0.15%	0.35%	0.60%	0.37%	1.80%	0.11%	1.38%	0.02%	0.48%	0.00%	0.00%	0.00%	0.00%	4.41%
S	0.42%	0.20%	0.28%	0.48%	0.09%	0.43%	0.02%	0.27%	0.00%	0.10%	0.00%	0.00%	0.00%	0.00%	1.47%
SE	7.12%	3.46%	7.86%	13.44%	5.38%	26.48%	0.57%	7.21%	0.01%	0.38%	0.00%	0.00%	0.00%	0.00%	50.98%
SSE	2.37%	1.16%	2.50%	4.28%	1.82%	8.96%	0.35%	4.45%	0.04%	0.95%	0.01%	1.53%	0.00%	0.00%	21.33%
SSW	0.11%	0.05%	0.09%	0.15%	0.01%	0.05%	0.00%	0.04%	0.00%	0.00%	0.00%	0.00%	0.00%	0.00%	0.30%
SW	0.02%	0.01%	0.01%	0.01%	0.00%	0.00%	0.00%	0.00%	0.00%	0.00%	0.00%	0.00%	0.00%	0.00%	0.02%
W	0.03%	0.02%	0.04%	0.06%	0.02%	0.09%	0.00%	0.04%	0.00%	0.00%	0.00%	0.00%	0.00%	0.00%	0.21%
WNW	0.14%	0.07%	0.16%	0.27%	0.09%	0.47%	0.02%	0.31%	0.01%	0.38%	0.00%	0.51%	0.00%	0.00%	2.01%
WSW	0.03%	0.01%	0.01%	0.02%	0.01%	0.07%	0.00%	0.00%	0.00%	0.00%	0.00%	0.00%	0.00%	0.00%	0.10%
Totals	21.71%	10.56%	20.74%	35.48%	12.88%	63.46%	2.51%	31.79%	0.26%	6.95%	0.03%	4.59%	0.00%	0.00%	152.83%

South Bird Island 1994-07 Summer

Wind Directions	Wind classes		WF		WF		WF		WF		WF		WF		DP's
	5.6 to <=7	0.49	7 to <=8.7	1.71	8.7 to <=11.3	4.93	11.3 to <=14.3	12.66	14.3 to <=17.4	27.07	17.4 to <=35	145.02	35 to <=50	676.00	
CALM	0.00%	0.00%	0.00%	0.00%	0.00%	0.00%	0.00%	0.00%	0.00%	0.00%	0.00%	0.00%	0.00%	0.00%	0.00%
E	2.34%	1.14%	1.07%	1.83%	0.21%	1.03%	0.01%	0.18%	0.00%	0.00%	0.01%	1.57%	0.00%	0.00%	5.75%
ENE	0.82%	0.40%	0.47%	0.80%	0.13%	0.64%	0.02%	0.23%	0.00%	0.00%	0.02%	2.62%	0.00%	0.00%	4.69%
ESE	5.53%	2.69%	4.11%	7.04%	1.22%	5.99%	0.03%	0.37%	0.01%	0.20%	0.00%	0.52%	0.00%	0.00%	16.80%
N	0.12%	0.06%	0.07%	0.12%	0.03%	0.14%	0.02%	0.23%	0.01%	0.20%	0.00%	0.00%	0.00%	0.00%	0.74%
NE	0.24%	0.12%	0.14%	0.25%	0.06%	0.32%	0.03%	0.37%	0.01%	0.39%	0.01%	1.05%	0.00%	0.00%	2.49%
NNE	0.24%	0.12%	0.10%	0.18%	0.06%	0.30%	0.01%	0.18%	0.01%	0.20%	0.01%	1.05%	0.00%	0.00%	2.02%
NNW	0.03%	0.02%	0.01%	0.02%	0.01%	0.04%	0.00%	0.00%	0.00%	0.00%	0.00%	0.00%	0.00%	0.00%	0.07%
NW	0.02%	0.01%	0.01%	0.01%	0.02%	0.09%	0.00%	0.00%	0.00%	0.00%	0.00%	0.00%	0.00%	0.00%	0.11%
S	0.92%	0.45%	0.47%	0.80%	0.11%	0.55%	0.01%	0.14%	0.00%	0.00%	0.00%	0.00%	0.00%	0.00%	1.94%
SE	7.96%	3.87%	7.84%	13.40%	4.40%	21.66%	0.19%	2.42%	0.01%	0.39%	0.00%	0.52%	0.00%	0.00%	42.27%
SSE	4.37%	2.13%	3.62%	6.18%	1.27%	6.27%	0.07%	0.91%	0.00%	0.10%	0.00%	0.00%	0.00%	0.00%	15.59%
SSW	0.21%	0.10%	0.09%	0.15%	0.01%	0.07%	0.01%	0.09%	0.00%	0.00%	0.00%	0.00%	0.00%	0.00%	0.41%
SW	0.03%	0.02%	0.03%	0.04%	0.00%	0.02%	0.00%	0.05%	0.00%	0.00%	0.00%	0.00%	0.00%	0.00%	0.12%
W	0.00%	0.00%	0.01%	0.01%	0.02%	0.11%	0.00%	0.05%	0.00%	0.00%	0.00%	0.00%	0.00%	0.00%	0.16%
WNW	0.03%	0.01%	0.03%	0.04%	0.02%	0.11%	0.00%	0.00%	0.00%	0.00%	0.00%	0.00%	0.00%	0.00%	0.16%
WSW	0.00%	0.00%	0.01%	0.01%	0.01%	0.04%	0.00%	0.00%	0.00%	0.00%	0.00%	0.00%	0.00%	0.00%	0.05%
Totals	22.85%	11.12%	18.06%	30.89%	7.59%	37.38%	0.41%	5.21%	0.05%	1.47%	0.05%	7.33%	0.00%	0.00%	93.38%

South Bird Island 1994-07 Fall

Wind Directions	Wind classes		WF		WF		WF		WF		WF		WF		DP's
	5.6 to <=7	0.49	7 to <=8.7	1.71	8.7 to <=11.3	4.93	11.3 to <=14.3	12.66	14.3 to <=17.4	27.07	17.4 to <=35	145.02	35 to <=50	676.00	
CALM	0.00%	0.00%	0.00%	0.00%	0.00%	0.00%	0.00%	0.00%	0.00%	0.00%	0.00%	0.00%	0.00%	0.00%	0.00%
E	1.47%	0.71%	0.45%	0.78%	0.19%	0.96%	0.03%	0.38%	0.00%	0.00%	0.00%	0.00%	0.00%	0.00%	2.83%
ENE	1.22%	0.59%	0.60%	1.03%	0.21%	1.01%	0.04%	0.47%	0.00%	0.00%	0.00%	0.00%	0.00%	0.00%	3.11%
ESE	1.95%	0.95%	0.87%	1.49%	0.15%	0.74%	0.00%	0.05%	0.00%	0.00%	0.00%	0.00%	0.00%	0.00%	3.22%
N	1.19%	0.58%	1.54%	2.63%	1.37%	6.75%	0.57%	7.25%	0.06%	1.62%	0.01%	1.09%	0.00%	0.00%	19.93%
NE	0.92%	0.45%	0.85%	1.46%	0.31%	1.53%	0.03%	0.43%	0.01%	0.30%	0.00%	0.00%	0.00%	0.00%	4.17%
NNE	1.56%	0.76%	1.57%	2.68%	1.55%	7.62%	0.67%	8.49%	0.07%	1.93%	0.01%	1.09%	0.00%	0.00%	22.56%
NNW	0.49%	0.24%	0.54%	0.92%	0.56%	2.77%	0.12%	1.52%	0.01%	0.30%	0.00%	0.00%	0.00%	0.00%	5.74%
NW	0.43%	0.21%	0.34%	0.59%	0.34%	1.66%	0.15%	1.94%	0.01%	0.30%	0.00%	0.00%	0.00%	0.00%	4.71%
S	0.55%	0.27%	0.49%	0.85%	0.26%	1.27%	0.01%	0.09%	0.00%	0.00%	0.00%	0.00%	0.00%	0.00%	2.48%
SE	3.26%	1.59%	2.39%	4.09%	1.17%	5.78%	0.09%	1.09%	0.00%	0.00%	0.00%	0.00%	0.00%	0.00%	12.55%
SSE	2.12%	1.03%	1.84%	3.15%	1.25%	6.14%	0.14%	1.80%	0.00%	0.00%	0.00%	0.00%	0.00%	0.00%	12.13%
SSW	0.20%	0.10%	0.06%	0.10%	0.01%	0.06%	0.00%	0.00%	0.00%	0.00%	0.00%	0.00%	0.00%	0.00%	0.25%
SW	0.07%	0.03%	0.03%	0.04%	0.00%	0.02%	0.00%	0.05%	0.00%	0.00%	0.00%	0.00%	0.00%	0.00%	0.14%
W	0.05%	0.03%	0.05%	0.08%	0.01%	0.07%	0.01%	0.19%	0.00%	0.00%	0.00%	0.00%	0.00%	0.00%	0.37%
WNW	0.11%	0.05%	0.12%	0.20%	0.21%	1.01%	0.08%	1.04%	0.01%	0.20%	0.00%	0.00%	0.00%	0.00%	2.51%
WSW	0.04%	0.02%	0.02%	0.04%	0.02%	0.11%	0.03%	0.38%	0.00%	0.00%	0.00%	0.00%	0.00%	0.00%	0.55%
Totals	15.63%	7.61%	11.77%	20.13%	7.62%	37.51%	1.99%	25.18%	0.17%	4.66%	0.01%	2.17%	0.00%	0.00%	97.25%

South Bird Island 1994-07 Survey

Wind Directions	Wind classes		WF		WF		WF		WF		WF		WF		DP's
	5.6 to <=7	0.49	7 to <=8.7	1.71	8.7 to <=11.3	4.93	11.3 to <=14.3	12.66	14.3 to <=17.4	27.07	17.4 to <=35	145.02	35 to <=50	676.00	
CALM	0.00%	0.00%	0.00%	0.00%	0.00%	0.00%	0.00%	0.00%	0.00%	0.00%	0.00%	0.00%	0.00%	0.00%	0.00%
E	1.44%	0.70%	0.41%	0.70%	0.02%	0.10%	0.02%	0.25%	0.00%	0.00%	0.00%	0.00%	0.00%	0.00%	1.74%
ENE	0.56%	0.27%	0.16%	0.27%	0.00%	0.00%	0.00%	0.00%	0.00%	0.00%	0.00%	0.00%	0.00%	0.00%	0.54%
ESE	3.14%	1.53%	1.65%	2.82%	0.50%	2.49%	0.02%	0.25%	0.00%	0.00%	0.00%	0.00%	0.00%	0.00%	7.08%
N	1.34%	0.65%	1.75%	2.99%	1.13%	5.55%	0.21%	2.70%	0.06%	1.58%	0.00%	0.00%	0.00%	0.00%	13.46%
NE	0.68%	0.33%	0.49%	0.83%	0.08%	0.38%	0.00%	0.00%	0.00%	0.00%	0.00%	0.00%	0.00%	0.00%	1.54%
NNE	1.28%	0.62%	1.71%	2.92%	1.61%	7.94%	0.41%	5.16%	0.04%	1.05%	0.00%	0.00%	0.00%	0.00%	17.69%
NNW	0.31%	0.15%	0.39%	0.66%	0.45%	2.20%	0.25%	3.19%	0.02%	0.53%	0.00%	0.00%	0.00%	0.00%	6.73%
NW	0.23%	0.11%	0.10%	0.17%	0.17%	0.86%	0.14%	1.72%	0.04%	1.05%	0.00%	0.00%	0.00%	0.00%	3.91%
S	0.54%	0.26%	0.45%	0.76%	0.25%	1.24%	0.00%	0.00%	0.00%	0.00%	0.00%	0.00%	0.00%	0.00%	2.27%
SE	5.38%	2.62%	3.55%	6.08%	1.79%	8.80%	0.06%	0.74%	0.00%	0.00%	0.00%	0.00%	0.00%	0.00%	18.22%
SSE	3.18%	1.55%	2.70%	4.62%	1.03%	5.07%	0.06%	0.74%	0.00%	0.00%	0.00%	0.00%	0.00%	0.00%	11.97%
SSW	0.10%	0.05%	0.06%	0.10%	0.00%	0.00%	0.00%	0.00%	0.00%	0.00%	0.00%	0.00%	0.00%	0.00%	0.15%
SW	0.00%	0.00%	0.00%	0.00%	0.00%	0.00%	0.00%	0.00%	0.00%	0.00%	0.00%	0.00%	0.00%	0.00%	0.00%
W	0.00%	0.00%	0.00%	0.00%	0.00%	0.00%	0.00%	0.00%	0.00%	0.00%	0.00%	0.00%	0.00%	0.00%	0.00%
WNW	0.10%	0.05%	0.04%	0.07%	0.00%	0.00%	0.00%	0.00%	0.02%	0.53%	0.00%	0.00%	0.00%	0.00%	0.64%
WSW	0.04%	0.02%	0.00%	0.00%	0.00%	0.00%	0.00%	0.00%	0.00%	0.00%	0.00%	0.00%	0.00%	0.00%	0.02%
Totals	18.32%	8.91%	13.43%	22.98%	7.03%	34.61%	1.16%	14.74%	0.17%	4.73%	0.00%	0.00%	0.00%	0.00%	85.97%

CCIA 1981-06 Total

Wind Directions	Wind classes		WF		WF		WF		WF		WF		WF		DP's
	5.6 to <=7	0.49	7 to <=8.7	1.71	8.7 to <=11.3	4.93	11.3 to <=14.3	12.66	14.3 to <=17.4	27.07	17.4 to <=35	145.02	35 to <=50	676.00	
CALM	0.00%	0.00%	0.00%	0.00%	0.00%	0.00%	0.00%	0.00%	0.00%	0.00%	0.00%	0.00%	0.00%	0.00%	0.00%
E	1.82%	0.89%	0.84%	1.44%	0.11%	0.55%	0.01%	0.13%	0.00%	0.04%	0.00%	0.00%	0.00%	0.00%	3.04%
ENE	0.58%	0.28%	0.35%	0.60%	0.06%	0.30%	0.00%	0.06%	0.00%	0.04%	0.00%	0.00%	0.00%	0.00%	1.28%
ESE	1.83%	0.89%	1.20%	2.06%	0.25%	1.23%	0.01%	0.15%	0.00%	0.01%	0.00%	0.00%	0.00%	0.00%	4.34%
N	1.61%	0.78%	1.29%	2.21%	0.47%	2.31%	0.06%	0.75%	0.00%	0.06%	0.00%	0.00%	0.00%	0.00%	6.11%
NE	1.02%	0.50%	0.66%	1.13%	0.18%	0.88%	0.02%	0.24%	0.00%	0.04%	0.00%	0.00%	0.00%	0.00%	2.77%
NNE	1.15%	0.56%	0.82%	1.41%	0.32%	1.58%	0.04%	0.47%	0.00%	0.07%	0.00%	0.00%	0.00%	0.00%	4.09%
NNW	0.64%	0.31%	0.56%	0.95%	0.24%	1.18%	0.03%	0.42%	0.00%	0.05%	0.00%	0.00%	0.00%	0.00%	2.90%
NW	0.31%	0.15%	0.27%	0.46%	0.15%	0.75%	0.04%	0.52%	0.01%	0.16%	0.00%	0.00%	0.00%	0.00%	2.04%
S	1.34%	0.65%	1.05%	1.80%	0.45%	2.24%	0.08%	0.96%	0.00%	0.10%	0.00%	0.07%	0.00%	0.00%	5.82%
SE	3.69%	1.79%	3.35%	5.73%	1.16%	5.69%	0.11%	1.42%	0.01%	0.15%	0.00%	0.00%	0.00%	0.00%	14.79%
SSE	3.18%	1.55%	3.16%	5.41%	1.47%	7.24%	0.25%	3.17%	0.02%	0.43%	0.00%	0.00%	0.00%	0.00%	17.79%
SSW	0.15%	0.07%	0.07%	0.13%	0.01%	0.07%	0.00%	0.02%	0.00%	0.00%	0.00%	0.00%	0.00%	0.00%	0.29%
SW	0.05%	0.03%	0.04%	0.04%	0.00%	0.02%	0.00%	0.00%	0.00%	0.00%	0.00%	0.00%	0.00%	0.00%	0.09%
W	0.06%	0.03%	0.03%	0.04%	0.01%	0.05%	0.00%	0.03%	0.00%	0.01%	0.00%	0.00%	0.00%	0.00%	0.17%
WNW	0.10%	0.05%	0.08%	0.14%	0.04%	0.20%	0.00%	0.06%	0.00%	0.04%	0.00%	0.00%	0.00%	0.00%	0.48%
WSW	0.03%	0.01%	0.01%	0.02%	0.00%	0.02%	0.00%	0.01%	0.00%	0.00%	0.00%	0.00%	0.00%	0.00%	0.05%
Total	17.54%	8.54%	13.77%	23.56%	4.93%	24.28%	0.67%	8.42%	0.04%	1.19%	0.00%	0.07%	0.00%	0.00%	66.06%

CCIA 1981-06 Winter

Wind Directions	Wind classes		WF		WF		WF		WF		WF		WF		DP's
	5.6 to <=7	0.49	7 to <=8.7	1.71	8.7 to <=11.3	4.93	11.3 to <=14.3	12.66	14.3 to <=17.4	27.07	17.4 to <=35	145.02	35 to <=50	676.00	
CALM	0.00%	0.00%	0.00%	0.00%	0.00%	0.00%	0.00%	0.00%	0.00%	0.00%	0.00%	0.00%	0.00%	0.00%	0.00%
E	1.00%	0.48%	0.41%	0.71%	0.03%	0.17%	0.00%	0.02%	0.00%	0.00%	0.00%	0.53%	0.00%	0.00%	1.91%
ENE	0.92%	0.45%	0.58%	0.99%	0.09%	0.45%	0.01%	0.07%	0.00%	0.05%	0.01%	0.79%	0.00%	0.00%	2.80%
ESE	0.57%	0.28%	0.30%	0.52%	0.08%	0.37%	0.01%	0.11%	0.00%	0.00%	0.00%	0.26%	0.00%	0.00%	1.55%
N	3.12%	1.52%	2.54%	4.34%	0.93%	4.58%	0.13%	1.63%	0.00%	0.05%	0.01%	1.84%	0.00%	0.00%	13.96%
NE	1.72%	0.84%	1.23%	2.11%	0.33%	1.65%	0.03%	0.44%	0.00%	0.05%	0.00%	0.53%	0.00%	0.00%	5.60%
NNE	1.91%	0.93%	1.53%	2.62%	0.59%	2.92%	0.07%	0.82%	0.01%	0.20%	0.00%	0.26%	0.00%	0.00%	7.75%
NNW	1.29%	0.63%	1.21%	2.07%	0.48%	2.38%	0.05%	0.62%	0.00%	0.00%	0.00%	0.53%	0.00%	0.00%	6.22%
NW	0.66%	0.32%	0.55%	0.94%	0.30%	1.45%	0.10%	1.21%	0.01%	0.39%	0.00%	0.00%	0.00%	0.00%	4.32%
S	1.19%	0.58%	1.26%	2.15%	0.72%	3.55%	0.16%	2.04%	0.01%	0.34%	0.01%	1.58%	0.00%	0.00%	10.23%
SE	1.66%	0.81%	1.54%	2.63%	0.65%	3.18%	0.12%	1.49%	0.00%	0.10%	0.01%	0.79%	0.00%	0.00%	9.00%
SSE	2.01%	0.98%	2.51%	4.30%	1.48%	7.27%	0.27%	3.37%	0.02%	0.44%	0.01%	1.58%	0.00%	0.00%	17.93%
SSW	0.19%	0.09%	0.13%	0.23%	0.04%	0.18%	0.01%	0.07%	0.00%	0.00%	0.00%	0.53%	0.00%	0.00%	1.09%
SW	0.09%	0.05%	0.03%	0.05%	0.01%	0.04%	0.00%	0.00%	0.00%	0.00%	0.00%	0.00%	0.00%	0.00%	0.13%
W	0.11%	0.05%	0.04%	0.07%	0.02%	0.08%	0.00%	0.02%	0.00%	0.00%	0.00%	0.00%	0.00%	0.00%	0.22%
WNW	0.19%	0.09%	0.17%	0.30%	0.08%	0.39%	0.01%	0.16%	0.01%	0.15%	0.00%	0.53%	0.00%	0.00%	1.62%
WSW	0.04%	0.02%	0.01%	0.02%	0.00%	0.02%	0.00%	0.00%	0.00%	0.00%	0.00%	0.00%	0.00%	0.00%	0.06%
Total	17.54%	8.11%	13.77%	23.56%	4.93%	28.69%	0.67%	12.08%	0.04%	1.76%	0.00%	9.71%	0.00%	0.00%	83.91%

CCIA 1981-06 Spring

Wind Directions	Wind classes		WF		WF		WF		WF		WF		WF		DP's
	5.6 to <=7	0.49	7 to <=8.7	1.71	8.7 to <=11.3	4.93	11.3 to <=14.3	12.66	14.3 to <=17.4	27.07	17.4 to <=35	145.02	35 to <=50	676.00	
CALM	0.00%	0.00%	0.00%	0.00%	0.00%	0.00%	0.00%	0.00%	0.00%	0.00%	0.00%	0.00%	0.00%	0.00%	0.00%
E	2.27%	1.10%	1.20%	2.06%	0.19%	0.96%	0.01%	0.16%	0.00%	0.00%	0.00%	0.00%	0.00%	0.00%	4.28%
ENE	0.57%	0.28%	0.35%	0.61%	0.07%	0.32%	0.01%	0.07%	0.00%	0.00%	0.00%	0.00%	0.00%	0.00%	1.28%
ESE	2.52%	1.23%	1.78%	3.04%	0.45%	2.20%	0.01%	0.13%	0.00%	0.05%	0.00%	0.00%	0.00%	0.00%	6.65%
N	1.28%	0.62%	1.09%	1.86%	0.43%	2.13%	0.05%	0.69%	0.00%	0.05%	0.00%	0.00%	0.00%	0.00%	5.36%
NE	0.91%	0.44%	0.62%	1.06%	0.17%	0.86%	0.02%	0.22%	0.00%	0.00%	0.00%	0.00%	0.00%	0.00%	2.59%
NNE	0.99%	0.48%	0.78%	1.33%	0.28%	1.38%	0.03%	0.38%	0.01%	0.14%	0.00%	0.00%	0.00%	0.00%	3.72%
NNW	0.49%	0.24%	0.46%	0.78%	0.29%	1.41%	0.06%	0.72%	0.01%	0.19%	0.00%	0.00%	0.00%	0.00%	3.33%
NW	0.29%	0.14%	0.29%	0.50%	0.16%	0.79%	0.05%	0.67%	0.01%	0.19%	0.00%	0.00%	0.00%	0.00%	2.29%
S	1.35%	0.66%	1.13%	1.93%	0.54%	2.68%	0.09%	1.12%	0.00%	0.10%	0.00%	0.07%	0.00%	0.00%	6.54%
SE	4.88%	2.37%	4.96%	8.48%	2.23%	10.98%	0.23%	2.91%	0.01%	0.19%	0.00%	0.00%	0.00%	0.00%	24.93%
SSE	4.20%	2.04%	4.72%	8.08%	2.74%	13.48%	0.50%	6.28%	0.03%	0.91%	0.00%	0.00%	0.00%	0.00%	30.79%
SSW	0.13%	0.06%	0.06%	0.10%	0.01%	0.06%	0.00%	0.00%	0.00%	0.00%	0.00%	0.00%	0.00%	0.00%	0.23%
SW	0.05%	0.03%	0.03%	0.05%	0.01%	0.03%	0.00%	0.00%	0.00%	0.00%	0.00%	0.00%	0.00%	0.00%	0.10%
W	0.07%	0.03%	0.03%	0.05%	0.01%	0.03%	0.01%	0.07%	0.00%	0.05%	0.00%	0.00%	0.00%	0.00%	0.23%
WNW	0.09%	0.04%	0.10%	0.16%	0.03%	0.16%	0.00%	0.04%	0.00%	0.00%	0.00%	0.00%	0.00%	0.00%	0.41%
WSW	0.04%	0.02%	0.02%	0.03%	0.01%	0.03%	0.00%	0.02%	0.00%	0.00%	0.00%	0.00%	0.00%	0.00%	0.10%
Total	17.54%	8.54%	13.77%	23.56%	4.93%	24.28%	0.67%	8.42%	0.04%	1.19%	0.00%	0.07%	0.00%	0.00%	92.82%

CCIA 1981-06 Summer

Wind Directions	Wind classes		WF		WF		WF		WF		WF		WF		DP's
	5.6 to <=7	0.49	7 to <=8.7	1.71	8.7 to <=11.3	4.93	11.3 to <=14.3	12.66	14.3 to <=17.4	27.07	17.4 to <=35	145.02	35 to <=50	676.00	
CALM	0.00%	0.00%	0.00%	0.00%	0.00%	0.00%	0.00%	0.00%	0.00%	0.00%	0.00%	0.00%	0.00%	0.00%	0.00%
E	1.91%	0.93%	0.84%	1.43%	0.12%	0.57%	0.01%	0.12%	0.01%	0.15%	0.00%	0.00%	0.00%	0.00%	3.19%
ENE	0.20%	0.10%	0.10%	0.17%	0.02%	0.08%	0.00%	0.05%	0.00%	0.05%	0.00%	0.00%	0.00%	0.00%	0.44%
ESE	2.68%	1.30%	1.88%	3.21%	0.34%	1.67%	0.01%	0.09%	0.00%	0.00%	0.00%	0.00%	0.00%	0.00%	6.28%
N	0.12%	0.06%	0.05%	0.08%	0.01%	0.05%	0.00%	0.02%	0.00%	0.00%	0.00%	0.00%	0.00%	0.00%	0.20%
NE	0.23%	0.11%	0.06%	0.11%	0.02%	0.11%	0.01%	0.07%	0.00%	0.00%	0.00%	0.00%	0.00%	0.00%	0.40%
NNE	0.14%	0.07%	0.04%	0.08%	0.01%	0.06%	0.00%	0.05%	0.00%	0.00%	0.00%	0.00%	0.00%	0.00%	0.25%
NNW	0.02%	0.01%	0.02%	0.03%	0.00%	0.01%	0.00%	0.00%	0.00%	0.00%	0.00%	0.00%	0.00%	0.00%	0.05%
NW	0.02%	0.01%	0.01%	0.01%	0.01%	0.03%	0.00%	0.02%	0.00%	0.00%	0.00%	0.00%	0.00%	0.00%	0.07%
S	1.64%	0.80%	0.89%	1.53%	0.12%	0.60%	0.00%	0.05%	0.00%	0.00%	0.00%	0.00%	0.00%	0.00%	2.97%
SE	5.67%	2.76%	4.87%	8.34%	1.14%	5.63%	0.04%	0.49%	0.00%	0.05%	0.00%	0.00%	0.00%	0.00%	17.26%
SSE	4.31%	2.10%	3.32%	5.68%	0.77%	3.80%	0.03%	0.37%	0.00%	0.00%	0.00%	0.00%	0.00%	0.00%	11.94%
SSW	0.14%	0.07%	0.03%	0.04%	0.00%	0.01%	0.00%	0.00%	0.00%	0.00%	0.00%	0.00%	0.00%	0.00%	0.12%
SW	0.03%	0.01%	0.01%	0.01%	0.01%	0.05%	0.00%	0.00%	0.00%	0.00%	0.00%	0.00%	0.00%	0.00%	0.07%
W	0.02%	0.01%	0.01%	0.02%	0.00%	0.02%	0.00%	0.00%	0.00%	0.00%	0.00%	0.00%	0.00%	0.00%	0.04%
WNW	0.02%	0.01%	0.01%	0.01%	0.01%	0.03%	0.00%	0.00%	0.00%	0.00%	0.00%	0.00%	0.00%	0.00%	0.05%
WSW	0.01%	0.00%	0.01%	0.01%	0.00%	0.02%	0.00%	0.00%	0.00%	0.00%	0.00%	0.00%	0.00%	0.00%	0.03%
Total	17.54%	8.54%	13.77%	23.56%	4.93%	24.28%	0.67%	8.42%	0.04%	1.19%	0.00%	0.00%	0.00%	0.00%	43.37%

CCIA 1981-06 Fall

Wind Directions	Wind classes		WF		WF		WF		WF		WF		WF		DP's
	5.6 to <=7	0.49	7 to <=8.7	1.71	8.7 to <=11.3	4.93	11.3 to <=14.3	12.66	14.3 to <=17.4	27.07	17.4 to <=35	145.02	35 to <=50	676.00	
CALM	0.00%	0.00%	0.00%	0.00%	0.00%	0.00%	0.00%	0.00%	0.00%	0.00%	0.00%	0.00%	0.00%	0.00%	0.00%
E	1.82%	0.89%	0.84%	1.44%	0.11%	0.55%	0.01%	0.13%	0.00%	0.04%	0.00%	0.00%	0.00%	0.00%	3.04%
ENE	0.58%	0.28%	0.35%	0.60%	0.06%	0.30%	0.00%	0.06%	0.00%	0.04%	0.00%	0.27%	0.00%	0.00%	1.54%
ESE	1.83%	0.89%	1.20%	2.06%	0.25%	1.23%	0.01%	0.15%	0.00%	0.01%	0.00%	0.00%	0.00%	0.00%	4.34%
N	1.61%	0.78%	1.29%	2.21%	0.47%	2.31%	0.06%	0.75%	0.00%	0.06%	0.00%	0.27%	0.00%	0.00%	6.38%
NE	1.02%	0.50%	0.66%	1.13%	0.18%	0.88%	0.02%	0.24%	0.00%	0.04%	0.00%	0.54%	0.00%	0.00%	3.31%
NNE	1.15%	0.56%	0.82%	1.41%	0.32%	1.58%	0.04%	0.47%	0.00%	0.07%	0.00%	0.27%	0.00%	0.00%	4.36%
NNW	0.64%	0.31%	0.56%	0.95%	0.24%	1.18%	0.03%	0.42%	0.00%	0.05%	0.00%	0.00%	0.00%	0.00%	2.90%
NW	0.31%	0.15%	0.27%	0.46%	0.15%	0.75%	0.04%	0.52%	0.01%	0.16%	0.00%	0.27%	0.00%	0.00%	2.31%
S	1.34%	0.65%	1.05%	1.80%	0.45%	2.24%	0.08%	0.96%	0.00%	0.10%	0.00%	0.27%	0.00%	0.00%	6.02%
SE	3.69%	1.79%	3.35%	5.73%	1.16%	5.69%	0.11%	1.42%	0.01%	0.15%	0.01%	1.07%	0.00%	0.00%	15.86%
SSE	3.18%	1.55%	3.16%	5.41%	1.47%	7.24%	0.25%	3.17%	0.02%	0.43%	0.01%	1.61%	0.00%	0.00%	19.40%
SSW	0.15%	0.07%	0.07%	0.13%	0.01%	0.07%	0.00%	0.02%	0.00%	0.00%	0.00%	0.00%	0.00%	0.00%	0.29%
SW	0.05%	0.03%	0.02%	0.04%	0.00%	0.02%	0.00%	0.00%	0.00%	0.00%	0.00%	0.00%	0.00%	0.00%	0.09%
W	0.06%	0.03%	0.03%	0.04%	0.01%	0.05%	0.00%	0.03%	0.00%	0.01%	0.00%	0.00%	0.00%	0.00%	0.17%
WNW	0.10%	0.05%	0.08%	0.14%	0.04%	0.20%	0.00%	0.06%	0.00%	0.04%	0.00%	0.00%	0.00%	0.00%	0.48%
WSW	0.03%	0.01%	0.01%	0.02%	0.00%	0.02%	0.00%	0.01%	0.00%	0.00%	0.00%	0.00%	0.00%	0.00%	0.05%
Total	17.54%	8.54%	13.77%	23.56%	4.93%	24.28%	0.67%	8.42%	0.04%	1.19%	0.00%	0.07%	0.00%	0.00%	70.54%

PAIS 1968-07 Total

Wind Directions	Wind classes		WF		WF		WF		WF		WF		WF		DP's
	5.6 to <=7	0.49	7 to <=8.7	1.71	8.7 to <=11.3	4.93	11.3 to <=14.3	12.66	14.3 to <=17.4	27.07	17.4 to <=35	145.02	35 to <=50	676.00	
CALM	0.00%	0.00%	0.00%	0.00%	0.00%	0.00%	0.00%	0.00%	0.00%	0.00%	0.00%	0.00%	0.00%	0.00%	0.00%
E	2.32%	1.13%	0.92%	1.58%	0.36%	1.79%	0.11%	1.41%	0.00%	0.00%	0.03%	4.05%	0.00%	0.00%	9.95%
ENE	0.00%	0.00%	0.00%	0.00%	0.00%	0.00%	0.00%	0.00%	0.00%	0.00%	0.00%	0.00%	0.00%	0.00%	0.00%
ESE	0.20%	0.10%	0.11%	0.19%	0.06%	0.27%	0.00%	0.00%	0.00%	0.00%	0.00%	0.00%	0.00%	0.00%	0.56%
N	2.96%	1.44%	1.67%	2.86%	1.70%	8.39%	0.39%	4.95%	0.11%	3.02%	0.08%	12.14%	0.00%	0.00%	32.80%
NE	1.28%	0.62%	0.59%	1.00%	0.47%	2.34%	0.14%	1.77%	0.03%	0.76%	0.06%	8.09%	0.00%	0.00%	14.58%
NNE	0.11%	0.05%	0.00%	0.00%	0.00%	0.00%	0.00%	0.00%	0.00%	0.00%	0.00%	0.00%	0.00%	0.00%	0.05%
NNW	0.00%	0.00%	0.03%	0.05%	0.03%	0.14%	0.00%	0.00%	0.00%	0.00%	0.00%	0.00%	0.00%	0.00%	0.19%
NW	0.78%	0.38%	0.45%	0.76%	0.75%	3.71%	0.14%	1.77%	0.06%	1.51%	0.00%	0.00%	0.00%	0.00%	8.13%
S	1.79%	0.87%	1.00%	1.72%	0.50%	2.47%	0.08%	1.06%	0.00%	0.00%	0.00%	0.00%	0.00%	0.00%	6.12%
SE	5.86%	2.85%	3.29%	5.63%	2.60%	12.79%	0.11%	1.41%	0.00%	0.00%	0.00%	0.00%	0.00%	0.00%	22.68%
SSE	0.06%	0.03%	0.06%	0.10%	0.06%	0.27%	0.00%	0.00%	0.00%	0.00%	0.00%	0.00%	0.00%	0.00%	0.40%
SSW	0.00%	0.00%	0.03%	0.05%	0.00%	0.00%	0.00%	0.00%	0.00%	0.00%	0.00%	0.00%	0.00%	0.00%	0.05%
SW	0.39%	0.19%	0.20%	0.33%	0.06%	0.27%	0.00%	0.00%	0.00%	0.00%	0.00%	0.00%	0.00%	0.00%	0.80%
W	0.47%	0.23%	0.22%	0.38%	0.20%	0.96%	0.03%	0.35%	0.00%	0.00%	0.00%	0.00%	0.00%	0.00%	1.93%
WNW	0.00%	0.00%	0.00%	0.00%	0.00%	0.00%	0.00%	0.00%	0.00%	0.00%	0.00%	0.00%	0.00%	0.00%	0.00%
WSW	0.00%	0.00%	0.00%	0.00%	0.00%	0.00%	0.00%	0.00%	0.00%	0.00%	0.00%	0.00%	0.00%	0.00%	0.00%
Totals	10.66%	5.19%	7.62%	13.04%	4.65%	22.92%	0.76%	9.56%	0.09%	2.43%	0.07%	9.76%	0.00%	0.00%	62.91%

PAIS 1968-07 Winter

Wind Directions	Wind classes		WF		WF		WF		WF		WF		WF		DP's
	5.6 to <=7	0.49	7 to <=8.7	1.71	8.7 to <=11.3	4.93	11.3 to <=14.3	12.66	14.3 to <=17.4	27.07	17.4 to <=35	145.02	35 to <=50	676.00	
CALM	0.00%	0.00%	0.00%	0.00%	0.00%	0.00%	0.00%	0.00%	0.00%	0.00%	0.00%	0.00%	0.00%	0.00%	0.00%
E	0.21%	0.10%	0.27%	0.47%	0.06%	0.30%	0.00%	0.00%	0.00%	0.00%	0.03%	4.41%	0.00%	0.00%	5.28%
ENE	0.00%	0.00%	0.00%	0.00%	0.00%	0.00%	0.00%	0.00%	0.00%	0.00%	0.00%	0.00%	0.00%	0.00%	0.00%
ESE	0.30%	0.15%	0.03%	0.05%	0.00%	0.00%	0.00%	0.00%	0.00%	0.00%	0.00%	0.00%	0.00%	0.00%	0.20%
N	3.53%	1.72%	2.49%	4.26%	1.82%	8.98%	0.49%	6.16%	0.06%	1.65%	0.06%	8.82%	0.00%	0.00%	31.58%
NE	1.06%	0.52%	0.70%	1.20%	0.43%	2.10%	0.12%	1.54%	0.00%	0.00%	0.06%	8.82%	0.00%	0.00%	14.16%
NNE	0.82%	0.40%	0.76%	1.30%	0.36%	1.80%	0.06%	0.77%	0.00%	0.00%	0.00%	0.00%	0.00%	0.00%	4.27%
NNW	0.88%	0.43%	0.88%	1.51%	0.55%	2.69%	0.12%	1.54%	0.00%	0.00%	0.00%	0.00%	0.00%	0.00%	6.17%
NW	0.91%	0.44%	0.70%	1.20%	0.79%	3.89%	0.09%	1.15%	0.03%	0.82%	0.00%	0.00%	0.00%	0.00%	7.51%
S	0.24%	0.12%	0.21%	0.36%	0.12%	0.60%	0.03%	0.38%	0.00%	0.00%	0.00%	0.00%	0.00%	0.00%	1.47%
SE	1.34%	0.65%	0.64%	1.09%	0.46%	2.25%	0.03%	0.38%	0.00%	0.00%	0.00%	0.00%	0.00%	0.00%	4.37%
SSE	0.40%	0.19%	0.18%	0.31%	0.12%	0.60%	0.03%	0.38%	0.00%	0.00%	0.03%	4.41%	0.00%	0.00%	5.90%
SSW	0.03%	0.01%	0.00%	0.00%	0.00%	0.00%	0.00%	0.00%	0.00%	0.00%	0.03%	4.41%	0.00%	0.00%	4.42%
SW	0.24%	0.12%	0.21%	0.36%	0.00%	0.00%	0.00%	0.00%	0.00%	0.00%	0.00%	0.00%	0.00%	0.00%	0.48%
W	0.24%	0.12%	0.09%	0.16%	0.18%	0.90%	0.00%	0.00%	0.00%	0.00%	0.00%	0.00%	0.00%	0.00%	1.17%
WNW	0.30%	0.15%	0.18%	0.31%	0.12%	0.60%	0.00%	0.00%	0.00%	0.00%	0.00%	0.00%	0.00%	0.00%	1.06%
WSW	0.00%	0.00%	0.00%	0.00%	0.00%	0.00%	0.00%	0.00%	0.00%	0.00%	0.00%	0.00%	0.00%	0.00%	0.00%
Totals	10.52%	5.12%	7.36%	12.58%	5.02%	24.70%	0.97%	12.31%	0.09%	2.47%	0.21%	30.85%	0.00%	0.00%	88.04%

PAIS 1968-07 Spring

Wind Directions	Wind classes		WF		WF		WF		WF		WF		WF		DP's
	5.6 to <=7	0.49	7 to <=8.7	1.71	8.7 to <=11.3	4.93	11.3 to <=14.3	12.66	14.3 to <=17.4	27.07	17.4 to <=35	145.02	35 to <=50	676.00	
CALM	0.00%	0.00%	0.00%	0.00%	0.00%	0.00%	0.00%	0.00%	0.00%	0.00%	0.00%	0.00%	0.00%	0.00%	0.00%
E	1.64%	0.80%	0.68%	1.17%	0.42%	2.05%	0.09%	1.13%	0.00%	0.00%	0.00%	0.00%	0.00%	0.00%	5.15%
ENE	0.15%	0.07%	0.06%	0.10%	0.03%	0.15%	0.00%	0.00%	0.00%	0.00%	0.00%	0.00%	0.00%	0.00%	0.32%
ESE	1.28%	0.62%	0.51%	0.87%	0.33%	1.61%	0.06%	0.75%	0.00%	0.00%	0.00%	0.00%	0.00%	0.00%	3.85%
N	1.07%	0.52%	1.10%	1.88%	1.10%	5.42%	0.09%	1.13%	0.06%	1.61%	0.03%	4.31%	0.00%	0.00%	14.88%
NE	0.57%	0.28%	0.68%	1.17%	0.24%	1.17%	0.03%	0.38%	0.00%	0.00%	0.00%	0.00%	0.00%	0.00%	2.99%
NNE	0.60%	0.29%	0.45%	0.76%	0.39%	1.91%	0.21%	2.64%	0.00%	0.00%	0.00%	0.00%	0.00%	0.00%	5.59%
NNW	0.27%	0.13%	0.51%	0.87%	0.39%	1.91%	0.09%	1.13%	0.00%	0.00%	0.00%	0.00%	0.00%	0.00%	4.03%
NW	0.36%	0.17%	0.27%	0.46%	0.39%	1.91%	0.06%	0.75%	0.03%	0.81%	0.00%	0.00%	0.00%	0.00%	4.10%
S	0.60%	0.29%	0.45%	0.76%	0.12%	0.59%	0.03%	0.38%	0.00%	0.00%	0.00%	0.00%	0.00%	0.00%	2.02%
SE	4.20%	2.04%	4.02%	6.87%	2.50%	12.31%	0.15%	1.88%	0.00%	0.00%	0.00%	0.00%	0.00%	0.00%	23.11%
SSE	1.10%	0.54%	0.95%	1.63%	0.51%	2.49%	0.00%	0.00%	0.00%	0.00%	0.00%	0.00%	0.00%	0.00%	4.66%
SSW	0.12%	0.06%	0.09%	0.15%	0.00%	0.00%	0.00%	0.00%	0.00%	0.00%	0.00%	0.00%	0.00%	0.00%	0.21%
SW	0.15%	0.07%	0.03%	0.05%	0.06%	0.29%	0.00%	0.00%	0.00%	0.00%	0.00%	0.00%	0.00%	0.00%	0.42%
W	0.33%	0.16%	0.21%	0.36%	0.03%	0.15%	0.03%	0.38%	0.00%	0.00%	0.00%	0.00%	0.00%	0.00%	1.04%
WNW	0.06%	0.03%	0.03%	0.05%	0.12%	0.59%	0.03%	0.38%	0.00%	0.00%	0.00%	0.00%	0.00%	0.00%	1.04%
WSW	0.00%	0.00%	0.00%	0.00%	0.00%	0.00%	0.00%	0.00%	0.00%	0.00%	0.00%	0.00%	0.00%	0.00%	0.00%
Totals	12.47%	6.07%	10.03%	17.15%	6.61%	32.54%	0.86%	10.92%	0.09%	2.42%	0.03%	4.31%	0.00%	0.00%	73.41%

PAIS 1968-07 Summer

Wind Directions	Wind classes WF		WF		WF		WF		WF		WF		WF		DP's
	5.6 to <=7	0.49	7 to <=8.7	1.71	8.7 to <=11.3	4.93	11.3 to <=14.3	12.66	14.3 to <=17.4	27.07	17.4 to <=35	145.02	35 to <=50	676.00	
CALM	0.00%	0.00%	0.00%	0.00%	0.00%	0.00%	0.00%	0.00%	0.00%	0.00%	0.00%	0.00%	0.00%	0.00%	0.00%
E	0.68%	0.33%	0.32%	0.55%	0.00%	0.00%	0.06%	0.75%	0.00%	0.00%	0.00%	0.00%	0.00%	0.00%	1.63%
ENE	0.06%	0.03%	0.03%	0.05%	0.00%	0.00%	0.00%	0.00%	0.00%	0.00%	0.00%	0.00%	0.00%	0.00%	0.08%
ESE	0.47%	0.23%	0.29%	0.50%	0.12%	0.58%	0.00%	0.00%	0.03%	0.80%	0.00%	0.00%	0.00%	0.00%	2.11%
N	0.15%	0.07%	0.12%	0.20%	0.03%	0.15%	0.00%	0.00%	0.00%	0.00%	0.00%	0.00%	0.00%	0.00%	0.42%
NE	0.18%	0.09%	0.12%	0.20%	0.06%	0.29%	0.03%	0.37%	0.00%	0.00%	0.00%	0.00%	0.00%	0.00%	0.95%
NNE	0.06%	0.03%	0.06%	0.10%	0.00%	0.00%	0.00%	0.00%	0.00%	0.00%	0.00%	0.00%	0.00%	0.00%	0.13%
NNW	0.00%	0.00%	0.03%	0.05%	0.00%	0.00%	0.00%	0.00%	0.00%	0.00%	0.00%	0.00%	0.00%	0.00%	0.05%
NW	0.03%	0.01%	0.00%	0.00%	0.00%	0.00%	0.03%	0.37%	0.00%	0.00%	0.00%	0.00%	0.00%	0.00%	0.39%
S	1.06%	0.52%	0.59%	1.01%	0.21%	1.02%	0.00%	0.00%	0.00%	0.00%	0.00%	0.00%	0.00%	0.00%	2.54%
SE	4.81%	2.34%	2.48%	4.24%	1.12%	5.52%	0.03%	0.37%	0.00%	0.00%	0.03%	4.28%	0.00%	0.00%	16.74%
SSE	1.42%	0.69%	1.06%	1.82%	0.38%	1.89%	0.06%	0.75%	0.06%	1.60%	0.00%	0.00%	0.00%	0.00%	6.73%
SSW	0.06%	0.03%	0.00%	0.00%	0.03%	0.15%	0.00%	0.00%	0.00%	0.00%	0.00%	0.00%	0.00%	0.00%	0.17%
SW	0.09%	0.04%	0.03%	0.05%	0.00%	0.00%	0.00%	0.00%	0.00%	0.00%	0.00%	0.00%	0.00%	0.00%	0.09%
W	0.06%	0.03%	0.03%	0.05%	0.03%	0.15%	0.00%	0.00%	0.00%	0.00%	0.00%	0.00%	0.00%	0.00%	0.22%
WNW	0.00%	0.00%	0.00%	0.00%	0.03%	0.15%	0.00%	0.00%	0.00%	0.00%	0.00%	0.00%	0.00%	0.00%	0.15%
WSW	0.03%	0.01%	0.00%	0.00%	0.00%	0.00%	0.00%	0.00%	0.00%	0.00%	0.00%	0.00%	0.00%	0.00%	0.01%
Totals	9.14%	4.45%	5.16%	8.83%	2.00%	9.87%	0.21%	2.61%	0.09%	2.39%	0.03%	4.28%	0.00%	0.00%	32.43%

PAIS 1968-07 Fall

Wind Directions	Wind classes WF		WF		WF		WF		WF		WF		WF		DP's
	5.6 to <=7	0.49	7 to <=8.7	1.71	8.7 to <=11.3	4.93	11.3 to <=14.3	12.66	14.3 to <=17.4	27.07	17.4 to <=35	145.02	35 to <=50	676.00	
CALM	0.00%	0.00%	0.00%	0.00%	0.00%	0.00%	0.00%	0.00%	0.00%	0.00%	0.00%	0.00%	0.00%	0.00%	0.00%
E	0.60%	0.29%	0.21%	0.36%	0.18%	0.89%	0.00%	0.00%	0.00%	0.00%	0.00%	0.00%	0.00%	0.00%	1.54%
ENE	0.27%	0.13%	0.15%	0.26%	0.03%	0.15%	0.00%	0.00%	0.00%	0.00%	0.00%	0.00%	0.00%	0.00%	0.54%
ESE	0.54%	0.26%	0.57%	0.98%	0.06%	0.30%	0.00%	0.00%	0.00%	0.00%	0.00%	0.00%	0.00%	0.00%	1.54%
N	1.87%	0.91%	1.84%	3.14%	1.59%	7.85%	0.39%	4.95%	0.00%	0.00%	0.03%	4.36%	0.00%	0.00%	21.21%
NE	0.90%	0.44%	0.30%	0.51%	0.33%	1.63%	0.06%	0.76%	0.03%	0.81%	0.00%	0.00%	0.00%	0.00%	4.16%
NNE	0.27%	0.13%	0.57%	0.98%	0.54%	2.67%	0.06%	0.76%	0.00%	0.00%	0.03%	4.36%	0.00%	0.00%	8.90%
NNW	0.57%	0.28%	0.75%	1.29%	0.39%	1.93%	0.09%	1.14%	0.03%	0.81%	0.00%	0.00%	0.00%	0.00%	5.45%
NW	0.54%	0.26%	0.36%	0.62%	0.45%	2.22%	0.15%	1.90%	0.00%	0.00%	0.00%	0.00%	0.00%	0.00%	5.01%
S	0.75%	0.37%	0.60%	1.03%	0.27%	1.33%	0.03%	0.38%	0.00%	0.00%	0.00%	0.00%	0.00%	0.00%	3.11%
SE	2.68%	1.30%	1.53%	2.62%	0.66%	3.26%	0.09%	1.14%	0.00%	0.00%	0.00%	0.00%	0.00%	0.00%	8.33%
SSE	1.08%	0.53%	0.90%	1.54%	0.24%	1.19%	0.09%	1.14%	0.03%	0.81%	0.00%	0.00%	0.00%	0.00%	5.21%
SSW	0.09%	0.04%	0.00%	0.00%	0.06%	0.30%	0.00%	0.00%	0.00%	0.00%	0.03%	4.36%	0.00%	0.00%	4.70%
SW	0.12%	0.06%	0.09%	0.15%	0.03%	0.15%	0.03%	0.38%	0.00%	0.00%	0.00%	0.00%	0.00%	0.00%	0.74%
W	0.18%	0.09%	0.03%	0.05%	0.06%	0.30%	0.00%	0.00%	0.00%	0.00%	0.00%	0.00%	0.00%	0.00%	0.44%
WNW	0.03%	0.01%	0.03%	0.05%	0.12%	0.59%	0.00%	0.00%	0.00%	0.00%	0.00%	0.00%	0.00%	0.00%	0.66%
WSW	0.03%	0.01%	0.00%	0.00%	0.00%	0.00%	0.00%	0.00%	0.00%	0.00%	0.00%	0.00%	0.00%	0.00%	0.01%
Totals	10.53%	5.12%	7.94%	13.59%	5.02%	24.75%	0.99%	12.57%	0.09%	2.44%	0.09%	13.09%	0.00%	0.00%	71.55%

PAIS 1968-07 Survey

Wind Directions	Wind classes		WF		WF		WF		WF		WF		WF		DP's
	5.6 to <=7	0.49	7 to <=8.7	1.71	8.7 to <=11.3	4.93	11.3 to <=14.3	12.66	14.3 to <=17.4	27.07	17.4 to <=35	145.02	35 to <=50	676.00	
CALM	0.00%	0.00%	0.00%	0.00%	0.00%	0.00%	0.00%	0.00%	0.00%	0.00%	0.00%	0.00%	0.00%	0.00%	0.00%
E	1.03%	0.50%	0.00%	0.00%	0.00%	0.00%	0.00%	0.00%	0.00%	0.00%	0.00%	0.00%	0.00%	0.00%	0.50%
ENE	0.00%	0.00%	0.00%	0.00%	0.00%	0.00%	0.00%	0.00%	0.00%	0.00%	0.00%	0.00%	0.00%	0.00%	0.00%
ESE	0.00%	0.00%	0.00%	0.00%	0.00%	0.00%	0.00%	0.00%	0.00%	0.00%	0.00%	0.00%	0.00%	0.00%	0.00%
N	1.03%	0.50%	2.05%	3.51%	0.51%	2.51%	0.00%	0.00%	0.00%	0.00%	0.00%	0.00%	0.00%	0.00%	6.52%
NE	0.51%	0.25%	0.00%	0.00%	0.51%	2.51%	0.00%	0.00%	0.00%	0.00%	0.00%	0.00%	0.00%	0.00%	2.76%
NNE	0.00%	0.00%	0.00%	0.00%	0.00%	0.00%	0.00%	0.00%	0.00%	0.00%	0.00%	0.00%	0.00%	0.00%	0.00%
NNW	0.00%	0.00%	0.00%	0.00%	0.00%	0.00%	0.00%	0.00%	0.00%	0.00%	0.00%	0.00%	0.00%	0.00%	0.00%
NW	0.51%	0.25%	0.00%	0.00%	0.00%	0.00%	0.00%	0.00%	0.00%	0.00%	0.00%	0.00%	0.00%	0.00%	0.25%
S	3.59%	1.75%	3.59%	6.14%	1.03%	5.07%	0.00%	0.00%	0.00%	0.00%	0.00%	0.00%	0.00%	0.00%	12.96%
SE	5.13%	2.50%	3.08%	5.27%	0.00%	0.00%	0.00%	0.00%	0.00%	0.00%	0.00%	0.00%	0.00%	0.00%	7.76%
SSE	0.00%	0.00%	0.51%	0.87%	0.00%	0.00%	0.00%	0.00%	0.00%	0.00%	0.00%	0.00%	0.00%	0.00%	0.87%
SSW	0.00%	0.00%	0.00%	0.00%	0.00%	0.00%	0.00%	0.00%	0.00%	0.00%	0.00%	0.00%	0.00%	0.00%	0.00%
SW	0.00%	0.00%	0.00%	0.00%	0.00%	0.00%	0.00%	0.00%	0.00%	0.00%	0.00%	0.00%	0.00%	0.00%	0.00%
W	0.00%	0.00%	0.00%	0.00%	0.00%	0.00%	0.00%	0.00%	0.00%	0.00%	0.00%	0.00%	0.00%	0.00%	0.00%
WNW	0.00%	0.00%	0.00%	0.00%	0.00%	0.00%	0.00%	0.00%	0.00%	0.00%	0.00%	0.00%	0.00%	0.00%	0.00%
WSW	0.00%	0.00%	0.00%	0.00%	0.00%	0.00%	0.00%	0.00%	0.00%	0.00%	0.00%	0.00%	0.00%	0.00%	0.00%
Totals	11.79%	5.74%	9.23%	15.79%	2.05%	10.10%	0.00%	0.00%	0.00%	0.00%	0.00%	0.00%	0.00%	0.00%	31.62%

Vita

Winston Aloysius Lujack McKenna was born on a warm night in Baton Rouge, Louisiana. He is the oldest of Jay and Andy McKenna's four children (Justin, Roberta, and Christopher). Winston's formative years were shared with the people of Annapolis, Maryland, where his love for the water was developed. After graduating from St. Mary's High School in Annapolis (1994), a brief stay was required at Roanoke College in Salem, Virginia. After two years at Roanoke College Winston finally came to his senses and transferred to the University of Hawai'i at Manoa, in Honolulu, Hawai'i. Winston's bachelor's degree in philosophy served him well while lifeguarding, but the desire to continue his education and the chance for monetary gain led Winston to graduate school in the Department of Geography and Anthropology at Louisiana State University. Winston's plans after graduation are to win the lottery, and buy a small island in the South Pacific, after going to work for a couple of years, of course.